

直接序列/分碼多工接取蜂巢式系統之  
功率控制機制效能分析

Performance Analysis for Power Control Schemes in  
DS/CDMA Cellular Systems

研究生：李界和

Student: Chieh-Ho Lee

指導教授：張仲儒 博士

Advisor: Dr. Chung-Ju Chang



博士論文

A Dissertation  
Submitted to Institute of Communication Engineering  
College of Electrical Engineering and Computer Science  
National Chiao Tung University  
in Partial fulfillment of the Requirements  
for the Degree of Doctor of Philosophy  
in  
Communication Engineering  
Hsinchu, Taiwan

2004 年 12 月

# 直接序列/分碼多工接取蜂巢式系統之 功率控制機制效能分析

研究生：李界和

指導教授：張仲儒

國立交通大學電信工程學系

## 摘要

對直接序列/分碼多工接取(DS/CDMA)蜂巢式系統的運作而言，功率控制是非常重要的  
一環。若沒有功率控制，系統容量將受到遠近效應的影響而變得很低，若有適當的功率控  
制，系統資源才得以公平地互享而展現系統應有的容量。在本論文中，我們將深入分析  
DS/CDMA 蜂巢式系統在功率控制機制的運行下，其系統容量的表現。

首先，我們分析了一種暫停式閉迴路功率控制(Truncated Closed-loop Power Control, TCPC)機制下的系統上鏈容量。該 TCPC 功率控制機制屬強度型(Strength-based)功率控制機制的一種。在 TCPC 機制下，當短程衰耗小於一預設遮斷準位(cutoff threshold)時，行動台暫停其傳輸作業；否則，控制行動台的發射功率以補償短程衰耗，使得在基地台處的接收功率盡量維持在一預設準位。我們成功地導出了下列各效能指標的公式：系統容量、平均系統傳輸量、行動台平均傳輸量、行動台消耗功率、及行動台傳輸延遲。數值結果顯示，所導出的公式具有相當的準確度，此外亦顯示這種 TCPC 功率控制機制可以達到比傳統的強度型功率控制機制更好的系統效能。另一方面，我們更進一步分析 TCPC 功率控制機制在考量有功率控制誤差的情形下的效能表現。所導出的公式可以相當準確地算出其系統容量。

接著，我們提出一種 AM-CF(Approximation Method by Characteristic Function)估算方法，用以估算 DS/CDMA 蜂巢式系統中干擾功率的機率分佈。干擾功率是分析 DS/CDMA 蜂巢式系統效能的重要因子。雖然一般所常用的高斯近似法可以很容易地套用到複雜的系統，但是高斯近似法被發現並不是很準確，造成所據以分析出來的系統容量都是過於樂觀的值。所提出的 AM-CF 估算方法可適用於考量了多路徑衰耗和具有功率控制的複雜環境，片元波形可以是方波形式或 sinc 形式。與模擬結果為參考標的，AM-CF 估算方法比傳統之高斯近似法有更好的估算準確度。

最後，我們提出一種分析方法，可成功地分析非理想之訊擾比型(SIR-based)功率控制機制的系統容量。透過對研究觀察所得的平均接收訊擾比獨特的性質，我們發現功率控制機制下的系統行為可以用一組線性聯立方程式表示之，並可據以解出每條上鏈的接收功率值。系統容量由接收功率值合理性的機率與平均位元錯誤率所定義並據以求得。只需該聯立方程式係數矩陣各子元素的一階級二階統計特性，並套用中央極限定理，我們成功地導出了系統容量的公式。結果顯示，分析結果與模擬結果非常接近，這顯示所提出的分析方式可以很準確地分析非理想之訊擾比型(SIR-based)功率控制機制的系統容量。

# Performance Analysis for Power Control Schemes in DS/CDMA Cellular Systems

Student: Chieh-Ho Lee

Advisor: Chung-Ju Chang

Institute of Communication Engineering  
National Chiao Tung University

## Abstract

Power control is an important system requirement for DS/CDMA (direct-sequence/code division multiple access) cellular systems. In the absence of power control the effect of near-far phenomena is dominant, and the system capacity is very low. On the other hand, when the power control exists, it allows users to share resources of the system equally between themselves. In this dissertation, the system capacity of a power controlled DS/CDMA cellular system is investigated.

Firstly, we investigate the system performance of a truncated closed-loop power control (TCPC) scheme for uplinks in DS/CDMA cellular systems over frequency-selective fading channels. The TCPC scheme adopts strength-based power control. In this scheme, a mobile station (MS) suspends its transmission when the short-term fading is less than a preset cutoff threshold; and otherwise, the MS transmits with power adapted to compensate for the short-term fading so that the received signal power level remains constant. Closed-form formulae are successfully derived for performance measures, such as system capacity, average system transmission rate, MS average transmission rate, MS power consumption, and MS suspension delay. Numerical results show that the analysis provides reasonable accuracy; and the TCPC scheme can substantially improve the system capacity, the average system transmission rate, and power saving over conventional closed-loop power control schemes. Moreover, the TCPC scheme under realistic considerations of power control error due to power control step size, power control

period, power control delay, and MS velocity is further investigated. A closed-form formula is obtained to effectively approximate the system capacity of the realistic TCPC scheme. A closed-form formula is obtained to effectively approximate the system capacity of the realistic TCPC scheme.

Next, an approximation method by characteristic function (AM-CF) method to approximate the distribution of interference in DS/CDMA cellular systems is proposed. The interference statistics is an important factor for analyzing the performance of a DS/CDMA cellular system. Although the most widely used method, the SGA (standard Gaussian approximation) method, is easy to use and applicable to a complicated circumstance, it is known that the SGA is not very accurate and leads to an optimistic analytical result of the system capacity. This method considers the effects of frequency-selective multipath fading; it also considers perfect power control and a rectangular/sinc chip waveform. The AM-CF method can yield results that fit the Monte Carlo simulation results more accurately than the conventional standard Gaussian approximation method.

Finally, a novel analytical method for analyzing the system capacity of an imperfect signal-to-interference ratio (SIR)-based power control scheme is proposed. Based on investigated properties of average received SIR, a set of linear equations is derived to obtain the average received power on each uplink. The system capacity is then obtained according to the feasibility of the average received powers and the corresponding average bit error rates. A closed-form solution for system capacity is successfully derived by employing the first and second order statistics of each element in the coefficient matrix and applying central limit theorem. Results show that the analytical results are consistent with the simulation results; this implies the novel analytical method is quite accurate.

# Acknowledgements

First of all, I would like to express my sincere gratitude to my advisor, Dr. Chung-Ju Chang, for his patient guidance and profound influence down the road to graduation.

Special thanks go my colleagues in the Broadband Network Lab. and all of my friends, for their genuine encouragement, kind help, and sweet memories.

Finally, I am deeply indebted to my wife and family for their love and supports. This dissertation is dedicated to my wife and children. Without their wholehearted care and full support, it is impossible for me to exploit the life in an unburdened way.



# Contents

Mandarin Abstract .....	i
English Abstract .....	iii
Acknowledgements .....	v
Contents .....	vi
List of Figures .....	viii
Chapter 1 Introduction.....	1
1.1 Motivation .....	1
1.2 Related Work .....	3
1.3 Dissertation Organization.....	9
Chapter 2 An Overview of the Power Control Techniques for DS/CDMA Cellular Systems .	11
2.1 Introduction .....	12
2.2 Cellular Systems.....	12
2.3 Power Control in DS/CDMA Cellular Systems .....	13
2.3.1 Uplink/Downlink Power Control .....	14
2.3.2 Centralized/Distributed Power Control .....	14
2.3.3 Open-loop/Closed-loop/Outer-loop Power Control .....	15
2.3.4 Strength-based/SIR-based/BER-based Power Control.....	18
2.3.5 Perfect/Imperfect Power Control.....	21
2.3.6 Power Control with Fixed Step Size/Adaptive Step Size.....	23
2.3.7 Truncated Power Control.....	24
2.3.8 Predictive Power Control .....	25
2.3.9 Combined Rate and Power Control.....	26
2.4 Concluding Remarks .....	28
Chapter 3 Performance Analysis of a Truncated Closed-Loop Power Control Scheme for DS/CDMA Cellular Systems .....	29
3.1 Introduction .....	30
3.2 System Model.....	32
3.2.1 Channel Model .....	32
3.2.2 Transmitter Model .....	34
3.2.3 Receiver Model .....	34
3.3 Performance Analysis.....	37
3.3.1 Ideal TCPC .....	38
3.3.2 Realistic TCPC .....	46

3.4 Numerical Results .....	50
3.5 Concluding Remarks .....	57
3.6 Notation List.....	57
Chapter 4 An Accurate Method for Approximating the Interference Statistics of DS/CDMA Cellular Systems with Power Control over Frequency-Selective Fading Channels	61
4.1 Introduction .....	62
4.2 System Model.....	62
4.3 The AM-CF Method .....	68
4.3.1 Approximating the Statistics of the Intra-cell Interference .....	68
4.3.2 Approximating the Statistics of the Other-cell Interference.....	70
4.3.3 Approximating the Statistics of MAI Interference .....	71
4.4 Results and Discussions .....	72
4.5 Notation List.....	75
Chapter 5 Capacity Analysis of an Imperfect SIR-based Power Control Scheme for Uplinks in DS/CDMA Cellular Systems .....	78
5.1 Introduction .....	79
5.2 System Model.....	81
5.3 Capacity Analysis .....	83
5.3.1 Properties of Ensemble Average Received SIR.....	83
5.3.2 Outage Probability .....	86
5.3.3 System Capacity .....	88
5.4 Numerical Results .....	90
5.5. Concluding Remarks .....	95
5.6 Notation List.....	96
Chapter 6 Conclusions and Future Works .....	98
Appendices .....	101
A. Proof the Equivalence Between the Event $\{Y>0\}$ and $\{\det(\mathbf{A})>0\}$ .....	101
B. Abbreviations and Acronyms.....	104
Bibliography .....	105
Vita .....	113



# List of Figures

Figure 3.1: Functional blocks of the realistic TCPC scheme .....	46
Figure 3.2: System capacity $C$ versus cutoff threshold $X_0$ .....	51
Figure 3.3: System capacity $C$ of various realistic power control schemes versus cutoff threshold $X_0$ .....	52
Figure 3.4: Average system transmission rate $\bar{\mathfrak{R}}$ versus cutoff threshold $X_0$ .....	53
Figure 3.5: MS average transmission rate $\bar{R}$ versus cutoff threshold $X_0$ .....	54
Figure 3.6: MS average transmission energy per bit $\bar{E}$ versus cutoff threshold $X_0$ .....	54
Figure 3.7: MS average suspension delay $\bar{D}$ versus cutoff threshold $X_0$ .....	55
Figure 3.8: System capacity versus MS velocity for power control delay .....	56
Figure 4.1: Comparison of cdf curves of interference signals .....	74
Figure 5.1: Ensemble average received SIR per bit $E(\Gamma_M)$ versus MS index $M$ in the system .....	91
Figure 5.2: Ensemble average received power $E(Q_M)$ versus MS index $M$ in the system .....	93
Figure 5.3: System capacity $C$ versus the target SIR threshold $\Gamma_{TH}$ .....	94
Figure 5.4: System capacity $C$ versus the target SIR threshold $\Gamma_{TH}$ for various $\zeta$ .....	95



# Chapter 1

## Introduction

---

### 1.1 Motivation

The wireless communications market has exploded in recent years. People love to and even have become used to have a mobile phone to communicate with others. The mobile phone is so convenient and can be used to promptly communicate with other people such that it has become an indispensable part of people's daily life. With more and more people joining into the mobile communication club, the technical progress of the mobile communication systems are driven by the market force. Among the technical issues, system capacity, service quality, and variety of communication services are the most important.

The fundamental problem of the wireless communication system is how to share the common wireless channels, e.g. a radio frequency band, by many mobile users in order to accommodate as many users as possible. Due to the very limited resource of the frequency spectrum allocation, the characteristics of the wireless channel and the requirement of the user mobility, it is indeed not an easy task to design the mobile communication systems to fulfill the ever-increasing demand.

In the evolution of mobile communications, mobile communication has evolved from the first-generation (1G) to the second-generation (2G) and is now evolving towards the second and a half-generation (2.5G), as well as the third-generation (3G), with the fourth-generation (4G) in the horizon. The 1G cellular mobile systems, such as the Nippon telephone and Telegraph (NTT)

system launched in 1979 in Japan, the Nordic Mobile Telephone (NMT) system in 1981 in Scandinavia, the Advanced Mobile Phone Service (AMPS) system in 1983 in United States, and the Total Access Communication System (TACS) in 1990 in United Kingdom, are all analog systems based on FDMA technique and mainly for voice facility. When look back to the history, the mobile communication is really successful service. The mobile market showed annual growth rate of 30~50 per cent, rising to nearly 20 million subscribers by 1990. The insufficiency of the 1G system capacity, as well as the problems with communication security, roaming, and transmission quality, together trigger the development of the second generation systems.

In the 2G cellular mobile systems, the Global Standard for Mobile Communications (GSM) system, based on TDMA technique, was deployed in 1992 in Europe. Also the Digital AMPS (D-AMPS, also known as IS-136), based on TDMA, launched in 1992 in North America. The Interim-Standard-95 (IS-95), based on narrow-band DS-SS, was commercially operated in 1998 in the United States, Hong Kong, Singapore, and Korea. On the other hand, the 2G system in Japan was Personal Digital Cellular (PDC), introduced in 1994. In order to improve audio quality, digital modulations are employed in 2G systems. Therefore, the 2G systems can also serve, but low bit-rate, data communications. The 2G systems offer higher spectrum efficiency, higher system capacity, better data services, and more advanced roaming than the 1G systems. The fraud prevention and encryption of user data has become standard feature. Speech service still dominates the airways, but the demand for the data services, such as short message, fax, etc, is growing rapidly.

The 2G systems have been very successful in many countries. However, there are still limitations in 2G systems in terms of system capacity, service quality and flexibility to accommodate various wideband services with different data rates. Specifically, in order to meet the growing demands of users for different kind of services, such as E-mail, Internet browsing, multimedia, data base access, etc., the system needs to have higher data rates up to 2Mbps and

more stringent Quality of Service (QoS) requirements. Therefore, third-generation (3G) systems are being developed to transcend the 2G systems.

3G cellular services, known as IMT-2000, will sustain higher data rates and open the door to many Internet style applications. The most important IMT-2000 proposals are the W-CDMA as the successor to GSM, cdma2000 as the successor to IS-95, and time-division synchronous CDMA (TD-SCDMA). In 3G systems, wideband CDMA has been chosen because theoretically it can provide higher capacity as compared to FDMA and TDMA schemes. However, in order to achieve this promised high capacity, good techniques are needed to overcome several wireless impairments. This is why significant research works are currently being devoted to improve the performance of DS/CDMA cellular systems, such as interference cancellation or multiuser detection, smart antennas, and power control, etc. Among those areas of researches, power control is the most crucial aspect since it plays an important role in a DS/CDMA cellular system.

Without power control schemes, the capacity of a DS/CDMA cellular system may be comparable with or even less than the capacity of FDMA or TDMA systems. Henceforth, in this dissertation, it is motivated to analyze the performance of the power control schemes in DS/CDMA cellular systems. The most important two kinds of power control schemes, the strength-based and SIR-based power control schemes, are considered, and more importantly, not only the ideal power control schemes but also the realistic, or say imperfect, power control schemes are investigated in the dissertation.

## 1.2 Related Work

The cellular system has evolved from the first-generation (1G) to the second-generation (2G), and is now evolving towards the second and a half-generation (2.5G), as well as the third-generation (3G), with the fourth-generation (4G) in the horizon. In order to provide service

to as many users as possible, the multiple access techniques adopted in each generation of the cellular systems also evolve from FDMA, TDMA, to CDMA. In 3G systems, wideband CDMA has been chosen because theoretically it can provide higher capacity as compared with FDMA and TDMA schemes. However, in order to achieve this promised high capacity, effective techniques are needed to overcome several wireless impairments. This is why significant research works are currently being devoted to improve the performance of DS/CDMA cellular systems, such as interference cancellation or multiuser detection, smart antennas, and power control, etc. Among those areas of research, power control is the most crucial aspect because it plays an important role in a DS/CDMA cellular system. Without good power control schemes, the capacity of a DS/CDMA system may be only comparable with or even less than the capacity of FDMA or TDMA systems.

The driving forces to use the spread spectrum or CDMA for terrestrial cellular systems are mainly the requirement to improve the system capacity. Many early researches focused on comparing the CDMA with the conventional TDMA and FDMA in order to understand the advantages of the CDMA. In 1985, A. J. Viterbi conducted a straightforward comparison of the capacity of CDMA to that of TDMA and FDMA for satellite applications and concluded that FDMA can achieve higher capacity than CDMA [1]. However, Gilhousen et al. [2] pointed out that in the mobile satellite environment, there are four major factors utilized by a CDMA system to render system capacity at least double that of FDMA and TDMA. These four major factors are: voice activity, spatial discrimination provided by multi-beam antenna, cross-polarization frequency reuse, and discrimination between multiple satellites providing co-coverage. The key point is that the CDMA capacity is only interference limited; unlike FDMA and TDMA whose capacities are basically bandwidth limited. Any reduction in interference in a CDMA system will convert directly and linearly into an increase in capacity [2]. Gilhousen et al. [3] further showed that the CDMA still exhibits its greatest advantage over TDMA and FDMA in terrestrial digital

cellular systems. The net improvement in capacity of CDMA over digital TDMA or FDMA is on the order of 4 to 6 and over the conventional analog FM/FDMA it is nearly a factor of 20.

It has been clear that power control is the single most important system requirement for CDMA, since only by control of each mobile's transmission power can resources be shared equitably among mobiles and capacity maximized [3]. Lot of literature can be found in the last decade having their focus on the power control issue. In [4], Aein investigated cochannel interference management in satellite systems. The important concept of carrier-to-interference (C/I) balancing, or equivalently the SIR balancing, was introduced by him wherein all users experience the same C/I level. And the problem is identified as an eigenvalue problem for positive matrices. Nettleton and Alavi further extend the results to spread spectrum cellular radio systems wherein the adjacent code channel interference becomes the dominant interference source, and show that C/I balancing substantially improves the system capacity [5], [6], [7].

In [8], Zander proposes an optimal centralized power control scheme to minimize the outage probability with the assumption that the knowledge of all the channel gains is obtainable and also studies the corresponding performance bound. Obviously, the centralized power control is not practical since it is impossible to know the gains in all the radio paths in the system. In view of this, the distributed power control that uses only the local obtainable information, e.g. the SIR ratio of the communicating link, is studied by lots of literature. In [9], Zander proposed a distributed C/I balancing scheme, named limited-information SRA-algorithm (LI-SRA). Although some performance gain is lost compared to the centralized power control in [8], the capacity gain on the order of 3-4 are still feasible as compared to fixed power control scheme. The LI-SRA scheme is found robust to measurement error and should be useful even if the C/I measurements were slow and less accurate.

In a DS/CDMA cellular system, many users can transmit messages simultaneously over the same radio channel, each using a specific spread-spectrum pseudo-noise (PN) code [10]. Within a

cell, the code channels in downlinks can be considered as mutually orthogonal because downlinks may exhibit synchronous CDMA transmission. However, these code channels in uplinks cannot be exactly mutually orthogonal for a set of asynchronous users, and thus mutual interference occurs among the uplinks. In such a case, a strong signal increases communication quality, and a weak signal may suffer from strong interference. This problem is referred to as the near-far effect and limits the CDMA system capacity [11]. Hence, power control is an essential issue in a DS/CDMA system.

Open-loop power control, that is, the average power control, is applied to compensate for the long-term channel fading such that the average received signal power level is constant and the near-far problem is solved [12]. Closed-loop power control, however, is typically used to mitigate the short-term channel fading so that an acceptable received signal quality can be attained for the uplink communication. Several closed-loop/open-loop power control schemes have been investigated, such as (i) the well-known perfect power control, within which MS transmission power is adjusted to the exact inverse of the short-term fading and thus the received signal power level remains constant. Such a method is also referred to as the channel inversion scheme [13], [14]; (ii) combined power/rate control proposed in [15], which is the same as the perfect power control except in that MS holds its transmission power at  $Q_0/X_0$  and adapts its transmission rate to  $S(t) \cdot R_0/X_0$  when  $S(t) < X_0$ , where  $Q_0$  is the desired received power level,  $X_0$  is a preset cutoff threshold,  $S(t)$  is the short-term fading at time  $t$ , and  $R_0$  is the data symbol rate; (iii) truncated average power control (TAPC) proposed in [16], which applies a truncated channel inversion scheme to conventional average power control. This truncated channel inversion scheme suspends transmission when the long-term channel fading falls below a cutoff threshold; otherwise it adaptively controls power according to the channel inversion scheme. By suspending transmission in this way, an improvement of system capacity was reported.

In studying a DS/CDMA cellular system, the interference statistics are essential to the

understanding of the system's dynamics. Approximating interference statistics has received a lot of attention. In the literature, the most widely used method is the SGA (standard Gaussian approximation) method. Although the SGA is easy to use and applicable to a complicated circumstance, e.g. the cellular system over the frequency-selective fading channel in [17], it is known that the SGA is not very accurate [18]. In order to improve accuracy, many other methods have been proposed, such as the improved Gaussian approximation (IGA) method [18], the simplified IGA method [19], and the characteristic function method [20]. These methods have better accuracy, however they are only applicable to the limited circumstance of a single cell system over the AWGN channel. Therefore, an approximation method that has better accuracy and can be applied to a complicated circumstance is still desirable. Therefore, the chapter 2 proposes an approximation method by characteristic function (AM-CF) to approximate the distribution of MAI (multiple access interference) signals in DS/CDMA cellular systems. The method considers the effects of a frequency-selective multipath fading channel; it also assumes perfect power control and a rectangular/sinc chip waveform. Using this method, the distribution of the MAI signals is more accurately approximated.

As above mentioned, [5], [6], [7] report that the SIR-balancing can improve the system capacity. However, the short-term fading effect is not considered in these works. In [12], [21], the short-term fading is considered in the system model, and the simulation results show that the SIR-based power control has the potential to achieve higher system capacity as compared the strength-based power control.

There were many works related to the strength-based power control scheme, such as the system capacity analysis, e.g. [3], the interference statistics, e.g. [22], the error probability, e.g. [17], etc. Nevertheless, the SIR-based power control is in fact more important, and the SIR-based power control system was reported as having the potential for higher system capacity [5], [6], [7], [21]. Actually, the SIR-based power control had been adopted in IMT-2000 systems as well as



IS-95 system. However, the corresponding analysis for the SIR-based power control is very complicated [21] and is found significantly different from that of the strength-based power control [23]. The reason is that the distribution of the received SIR, which is the key factor in conventional methods for analyzing the system capacity of power control schemes, e.g. [3], [24], is almost impossible to be derived for the SIR-based power control scheme because of the inherent interaction between the desired signal power and the interference power. Due to such a difficulty, few literature had successfully provided new analytical method for investigating the SIR-based power control scheme, e.g. [23], [25], [26], and most works make their study via simulation, e.g. [21], [27],[28], [29], for the SIR-based power control schemes.

Kim and Sung [23] proposed a methodology for analyzing the system capacity of the SIR-based power control scheme with consideration of the voice activity, the maximum received power, and the long-term fading. The analysis was extended to a multicode CDMA system and an overlaid multiband CDMA system in [25]. However, they did not take the multipath fading into account in the channel model. Kim and Adachi [26] further proposed a method to analytically evaluate the reverse link capacity of a CDMA system in a multipath fading environment. In [23], [25], and [26], by recursively calculating the statistics of both the received power of the uplink and the interference power to mimic their inherent interaction, the system capacity of an SIR-based power control scheme is numerically obtained. Note that, all of these analyses assume that the SIR-based power control is perfect such that the received SIR is kept at a preset level. However, in practical, the received SIR would be a random variable rather than a constant. It can be found that the analysis of the imperfect SIR-based power control scheme is further different from that of the ideal SIR-based power control scheme. There has been no analytical approach for analyzing the capacity of an imperfect SIR-based power control scheme. Therefore, in Chapter 5, we propose a novel analytical method by which the analysis of an imperfect power control scheme becomes mathematically tractable and the closed-form solutions for uplink capacity of

DS/CDMA cellular systems are successfully derived.

### 1.3 Dissertation Organization

In this introductory chapter we provide the synopsis of the thesis. This chapter presents the research motivation, paper survey, and thesis outline.

In Chapter 2, the evolution of the mobile systems is briefly reviewed. The importance of power control in the reverse link of a CDMA system is highlighted. Various kinds of the power control schemes in CDMA systems are described in this chapter. Among these power control schemes, the most important two schemes are the strength-based and the SIR-based power control schemes. The analysis of these two kinds of power control schemes is the scope of this dissertation.

In Chapter 3 we focus on the strength-based power control scheme. The system performance of a truncated closed-loop power control (TCPC) scheme for uplinks in DS/CDMA cellular systems over frequency-selective fading channels is conducted. It is shown that the TCPC scheme can achieve higher system capacity than the conventional strength-based power control scheme. We also successfully analyze an imperfect TCPC scheme (or called realistic TCPC scheme), i.e. TCPC scheme under realistic consideration of power control error due to power control step size, power control period, power control delay, and MS velocity. A closed-form formula is obtained to accurately approximate the system capacity of the imperfect TCPC scheme.

In Chapter 4 we turn to focus on one important factor, the interference statistics, in a strength-based power controlled DS/CDMA cellular system. The interference statistics of a DS/CDMA system are essential to the understanding of the system's dynamics. Although the conventional SGA (standard Gaussian approximation) method is easy to use and applicable to a complicated circumstance, e.g. the cellular system over the frequency-selective fading channel in

[17], it is known that the SGA is not very accurate [18]. In order to improve accuracy while still applicable to a complicated circumstance, we propose an approximation method by characteristic function (AM-CF) to approximate the distribution of the MAI (multiple access interference) signals in DS/CDMA cellular systems. The method considers the effect of a frequency-selective multipath fading channel; it also assumes perfect power control and a rectangular/sinc chip waveform. Using this method, the distribution of the MAI signals is more accurately approximated.

In Chapter 5 we focus on another important kind of power control scheme — the SIR-based power control scheme. In this chapter, we propose a novel analytical method to analyze the system capacity of an imperfect SIR-based power control scheme for uplinks in DS/CDMA cellular systems wherein the received SIR is a random variable. The system behavior can be described by a set of linear equations. A closed-form solution for the system capacity is successfully derived. And the derived formula needs only the first and second order statistics of each element in the coefficient matrix of the linear equation. Results show that the analytical and the simulation results are substantially matched together, which implies the novel analytical method is quite accurate.

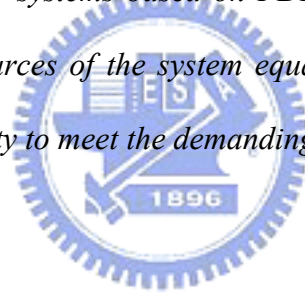
Finally, concluding remarks and future research topics are addressed in Chapter 6.

## Chapter 2

# An Overview of the Power Control Techniques for DS/CDMA Cellular Systems

---

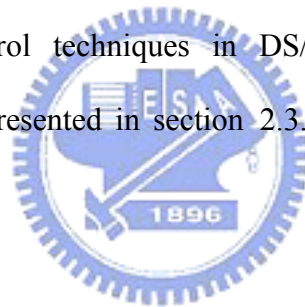
*Abstract—In this chapter, the cellular systems and various power control schemes are briefly reviewed. Power control is one of the most important factors for DS/CDMA cellular systems due to the near-far problem and the multipath fading. Without power control, the capacity of the DS/CDMA cellular system could become lower than that of cellular systems based on FDMA. A proper power control will make users to share resources of the system equally between themselves and thus enhance the system capacity to meet the demanding requirements.*



## 2.1 Introduction

Code Division Multiple Access (CDMA) has become the technology of choice for the third generation of cellular mobile systems because theoretically it can provide higher capacity compared with FDMA and TDMA schemes. However, in order to achieve the high capacity, techniques are needed to overcome several wireless impairments. One of the most important key aspects of CDMA is the power control. Many research works have been devoted to investigate the power control of DS/CDMA cellular systems and even design the power control algorithm to achieve an optimal performance. This chapter will briefly overview the relevant background related to this hot topic in DS/CDMA cellular systems.

The rest of this chapter is organized as follows. An overview of the cellular systems is given in section 2.2. The power control techniques in DS/CDMA cellular systems and their corresponding classifications are presented in section 2.3. Finally, the concluding remarks are given in section 2.4.



## 2.2 Cellular Systems

The 3G cellular services, known as IMT-2000, will sustain higher data rates and open the door to many Internet style applications. The most important IMT-2000 proposals are the W-CDMA as the successor to GSM, cdma2000 as the successor to IS-95, and time-division synchronous CDMA (TD-SCDMA). In 3G systems, wideband CDMA has been chosen because theoretically it can provide higher capacity compared with FDMA and TDMA schemes. However, in order to achieve this “promised” high capacity, good techniques are needed to overcome several wireless impairments. This is why significant research works are currently being devoted to improve the performance of DS/CDMA systems, such as interference cancellation or multiuser detection, smart antennas, and power control, etc. Among those areas of research, power control is the most crucial aspect because it plays an important role in a DS/CDMA cellular system.

Without good power control scheme, the capacity of a DS/CDMA system may be only comparable with or even less than the capacity of FDMA or TDMA systems. Henceforth, in this dissertation, it is motivated to analyze the performance of the power control schemes in DS/CDMA cellular systems.

## 2.3 Power Control in DS/CDMA Cellular Systems

The necessity for power control in FDMA/TDMA-based cellular networks stems from the requirement for co-channel interference management. This type of interference is caused by frequency reuse due to limited available frequency spectrum. By a proper power adjustment, the harmful effects of co-channel interference can be reduced. This allows a more “dense” reuse of resources and thus higher capacity.

The reason why the power control is the most important issue for a DS/CDMA cellular system is related to the unique feature of the CDMA system, MSs in the system are interfering with each other. In a DS/CDMA system, many users can transmit messages simultaneously over the same radio channel, each using a specific spread-spectrum pseudo-noise (PN) code [10]. Within a cell, the code channels in downlinks can be considered as mutually orthogonal because downlinks may exhibit synchronous CDMA transmission. However, these code channels in uplinks cannot be exactly mutually orthogonal for a set of asynchronous users, and thus mutual interference occurs among the uplinks. In such a case, a strong signal increases communication quality, and a weak signal may suffer from strong interference. This problem is referred to as the near-far effect and limits the CDMA system capacity [11]. Hence, well-designed power control is essential for proper functioning of the DS/CDMA cellular system. In the absence of power control the capacity of the DS/CDMA cellular system is very low, even lower than that of mobile systems based on FDMA or TDMA. Power control techniques in DS/CDMA systems can be classified in many different ways, which are described in-detail in the following subsections.

### 2.3.1 Uplink/Downlink Power Control

Power control schemes can be classified into two categories: uplink power control scheme, and downlink power control scheme. The uplink is also known as the reverse link, and the downlink is also known as the forward link. Uplink power control is found the single most important requirement for DS/CDMA systems due to the near-far problem [3]. Without uplink power control, i.e., each MS's transmission power is the same; the system capacity is found to be unacceptably low. In order to achieve the same average received signal power level, it is reported that a dynamic range of around 80dB while adapting MS's transmission power is required [3].

For the downlink link, there is no near-far problem since all signals are transmitted and hence vary together. In a single cell system, no downlink power control is required. However in a cellular system, interference from neighboring cell sites fades independently from the given cell site and thereby degrades performance. Thus it is necessary to apply power control in this case also, to reduce intercell interference. In this dissertation, we will focus on the uplink power control. And the contents in next coming sub-sections are all based on the uplink power control.

### 2.3.2 Centralized/Distributed Power Control

Power control schemes can be classified into two categories: centralized power control and distributed power control. A centralized power control is assumed to have all information about the gain of each link between any MS and any BS, and accordingly is capable of well controlling all the MSs' transmission power levels such that carrier-to-interference (CIR) balancing is met [31]. The concept of CIR-balancing is firstly introduced by Aein [4], in which all receivers experience the same CIR. As one can see, CIR-balancing implies fair resource usage among the users, therefore the outage probability is reduced and the system capacity is enhanced as compared CIR-unbalanced situation. The centralized power control for achieving CIR-balancing was identified as an eigenvalue problem for positive matrices for satellite systems [4],

FDMA/TDMA cellular systems [8], and DS/CDMA cellular systems [32]. The transmission power allocations are determined by the eigenvector corresponding to the minimum positive eigenvalue of the link-gain matrix. The study of the centralized power control reveals the optimal transmission power allocation to achieve CIR-balancing. However, to obtain the link-gain matrix need to know all of the link gains, which is obviously not practical.

The distributed power control is also known as decentralized power control. A decentralized power control scheme [9], [33], [34] adapts only one MS's power, and the algorithm depends only on local information, such as the measured SIR or the estimated gain of the channel from the specific MS to its serving BS. Due to depending only on local information, the distributed power control is more practical than the centralized one. However, the distributed power control would not perform better than the centralized one, e.g. in the aspect of convergence speed. Lee [35] proposed an algorithm to adapt each MS's power merely based on the local information, especially focused on the convergence issue of the power adaptation.

All the works studying either the centralized or distributed power control are also assumed rather ideal system model without considering the practical issues such as, (1) the power is practically adapted according to the periodically issued power control commands, (2) a power control command can only contain finite bits, (3) the existence of the power control command delay, (4) the short-term channel fading. Once these practical factors are further considered, the convergence of the distributed power control can become a very complex problem. The study of the centralized/distributed power control can indeed provide the first view to the power control scheme in a DS/CDMA cellular system without getting into the detail of practical issues.

### 2.3.3 Open-loop/Closed-loop/Outer-loop Power Control

From a viewpoint of realistic system, the power control techniques can be classified into three categories: open-loop power control, closed-loop power control, and outer-loop power



control.

The open-loop power control, also called average power control, is used to overcome the near-far and shadowing effects on the reverse link of a DS/CDMA cellular system. The open-loop power control is designed to ensure that the average received powers from all MSs in the same cell are equal to a preset level. By utilizing that the large-scale propagation loss is substantially reciprocal between uplink and downlink channels, the MS can compute the required transmission power based on the estimated channel gain on the downlink [3]. Such a task can be done by the MS itself without needing any feedback information from its serving BS, therefore this kind of power control is of an open-loop type. Due to the mechanism of the open-loop power control is so simple that only few literature, e.g. [36], [37], can be found.

Closed-loop power control aims at compensating for the received signal fluctuation due to short-term channel fading (or called multipath fading), which cannot be eliminated by the open-loop algorithm since the short-term channel fading can be very difference for the forward and reverse links. Usually, when talking about the closed-loop power control, it has implicitly assumed that the open-loop power control is a perfect one such that the near-far effect is perfected compensated. Due to the short-term fading is uncorrelated between uplink and downlink, the BS needs to measure some quality indicator, e.g. the received signal or the received SIR, and then sends a corresponding power control command back to the MS, so that the MS can adjust its transmission power accordingly. Obviously, this is a control mechanism in a closed-loop manner. Depending on what kind of quality indicator is measured at the BS, the closed-loop power control is further divided into three major classes. Please refer to section 2.3.4 for further detail.

Typical operation of a closed-loop power control is described as follows. The quality indicator, such as the received signal power, received SIR, or the bit error rate (BER) is estimated or measure at the BS for every power control period,  $T_p$ . In order to efficiently compensate for the short-term fading, the power control period should be shorter than the average fade duration of

the short-term fading. Then estimated quality indicator is compared with a preset target threshold. A finite-bit power control command is generated based on the difference between the estimated quality indicator and the target threshold and sent back to the MS via the downlink channel. The power control command is usually multiplexed with the downlink user data. The MS then extracts the power control command from the downlink data stream and adjust its transmission power by an amount of  $CMD * \Delta_p$  (dB) for the next power control period, where  $CMD$  denotes the power control command and  $\Delta_p$  is a preset step size in dB. Note that a delay is always introduced by such a control loop. This delay is called the power control loop delay. Due to lots of factors such as the power control period, finite-bit power control command, power control loop delay, etc., each MS's transmission power adaptation can never compensate the channel fading such that the corresponding quality indicator seen by the BS is always kept at the target threshold. In other words, the quality indicator seen by the BS would be a random variable. The quality indicator will have its mean around the target threshold. The difference between the estimated quality indicator and the target threshold is usually called power control error.

Note that closed-loop power control is only effective if and only if the validity of the power control command is good enough. A factor affects the validity of the power control command is the power control loop delay. A too-long power control loop delay will reduce the validity of the power control to reflect the current channel variation. Due to this fact, closed-loop power control is feasible in a terrestrial cellular environment, while not in a mobile satellite communications systems. Another factor is the speed of the multipath fading, or the MS mobility or velocity, which can also reduce the validity of the power control. The study of impact of the MS mobility on the system performance can be found in [38].

The outer-loop power control always cooperates with the SIR-based closed-loop power control, since for a typical strength-based power control, the target threshold is considered fixed and there is no corresponding outer-loop power control. The outer-loop power control is

employed to adapt the target SIR threshold used in the SIR-based power control such that the ultimate goal, the average BER, can be maintained at a certain level [39]. Note that, identical target SIR threshold for communication links does not imply identical BER performance. To speak more specifically, although identical target SIR threshold does imply that the received SIR at BS has its average around the same target SIR threshold, however, the variance of the received SIR is affected not only by the target SIR threshold but also by many other factors such as channel fading conditions, MS velocity, etc. Therefore, identical target SIR threshold can not guarantee identical distribution of the received SIR as well as identical average BER performance. In realistic system, different MSs may require different target SIR threshold and the outer-loop power control is needed to adaptively adjust the target SIR threshold in order to achieve the target BER performance for each uplink. The algorithm of updating target SIR threshold can be found in [40], [41], [42], [43]. To determine a proper target SIR threshold, the BS should be capable to estimate the average BER. The estimated average BER is then compared with a target BER, which might be difference for different type of communication services. If the estimated average BER is better than the target BER, the target SIR threshold is decreased; otherwise the target SIR threshold is increased. In fact, the outer-loop power control is a kind of BER-based power control.

#### 2.3.4 Strength-based/SIR-based/BER-based Power Control

According to what kind of quality indicator is measured to determine the power control command, the closed-loop power control can be classified into three categories: strength-based, SIR-based, and BER-based power control schemes.

In the strength-based power control scheme, the strength of the signal received by the BS from an MS is measured and compared with a preset target threshold. A one-bit power control command 'UP'/'DOWN' is periodically issued depending on whether the received signal power is lower/higher than the target threshold. In general, the power control command can be of more

than one bit, however in practical system the one-bit power control command is implemented due to its simplicity and light bandwidth requirement. For a typical strength-based power control scheme, the target threshold used in each BS is the same. Such a strength-based power control scheme will never diverge since the received power at the BS as well as the MS's transmission power will always converge. This is an advantage of the strength-based power control scheme. However, as can be easily found, the unification of the target threshold in the whole system is a negative factor to the system capacity. Typically, the central cells in the system will suffer from much interference than the boundary cells. Therefore the received SIR in the boundary cells will be unnecessary high and therefore the corresponding MSs will induce too much interference to the system. If these target thresholds that are unnecessary high can be somehow lowered down, the system capacity will be no doubt increased accordingly. There were many works related to the strength-based power control scheme, such the system capacity analysis [3], [44], the interference statistics [22], [45], the error probability analysis [17].

In a DS/CDMA cellular system, however, power control based on SIR is more suitable than that based on signal strength because the DS/CDMA cellular system is interference limited. It is shown in [21] that power control based on SIR appears to perform better than that based on the signal strength. Actually, the SIR-based power control had been adopted in IMT-2000 systems as well as IS-95 systems. In the SIR-based power control scheme the measured quality indicator is the received SIR. The operation of the SIR-based power control is basically the same as that of the strength-based power control, except for that the employed quality indicators are different. To speak more specifically, in the SIR-based power control scheme, the SIR received by the BS from an MS is measured and compared with a preset target SIR threshold. A one-bit power control command 'UP'/'DOWN' is periodically issued depending on whether the received SIR is lower/higher than the target SIR threshold. The MS adapts its transmission power based on power control command. It seems that the only difference between the strength-based and SIR-based

power control scheme is just the quality indicator. However, the characteristic of the SIR-based power control is very different from that of the strength-based power control. The corresponding theoretical analysis for the SIR-based power control becomes very complicated [21], and is found significantly different from that of the strength-based power control [23]. Due to such a difficulty, few literature had successfully provided theoretical methods for investigating the SIR-based power control scheme, e.g. [23], [25], [26], and most works made the study via simulation, e.g. [21], [27], [28], [29], for the SIR-based power control schemes.

In reality, the received SIR becomes dispersed with its mean around the target threshold. It can be found that the corresponding average BER becomes lower than that corresponds a SIR ideally fixed at the target threshold. Therefore the target SIR threshold for a realistic system should be set to a value higher than the  $\Gamma_0$ , where  $\Gamma_0$  is the SIR value for achieving the target BER performance. Moreover, the target threshold should become even higher, if the variance of the received SIR becomes larger. Adjusting the SIR target can be done by the outer-loop power control. How to set and adapt the target threshold is the key point of the SIR-based and can be found in lot of literature [40], [41], [42], [43], [46].

The major advantage of the SIR-based scheme is its better system performance on the system capacity. However, one of the side effects of the SIR-based schemes is the potential to get positive feedback to endanger the stability of the system when the number of active users exceeds the maximum system capacity. Positive feedback arises in a situation when one MS under instructions from the BS has to raise its transmission power, but the increase in its power also results in an increase in interference to other MSs so that these other MSs are then forced to also increase their power, etc. Once such a positive feedback situation occurs, it in fact implies that the overall interference has become too high and the system has become overloaded. The only way to dispel the positive feedback situation is to remove one or more MSs from the system. Once the overall interference is reduced, the system will leave from the overloaded state to a normal state,

wherein what occurs will be a negative feedback instead of the original positive feedback. When the SIR-based scheme operates at its normal state, the negative feedback will lead each MSs to use the transmission power as less as possible, which in turn reveals another advantage of the SIR-based power control scheme – power saving.

To avoid positive feedback effect, a strength-and-SIR-combined power control scheme is proposed in [47], [48]. In this scheme, SIR is used to control the target signal quality, while signal strength is used to control the interference level. For example when an MS's SIR is below the target threshold but its signal strength is already high enough, that MS cannot increase its transmission power. Moreover, power control should be also operated together with another technique, such as call admission control in order to prevent positive feedback [49], [50], [51] by assuming that the maximum system capacity is not exceeded.

In BER-based power control schemes, BER is defined as an average number of erroneous bits compared to the original sequence of bits. If the signal and average interference powers are constant, the BER will be a function of the received SIR, and in this case these two quality indicators are equivalent to each other. However, in reality the SIR is time-variant and thus the average SIR will not correspond to the average BER. Since the channel coding is implemented in every practical system, power control can be based on the average number of erroneous frames as well. Although the BER is a better quality indicator than the SIR, the accurate measurement of BER is not an easy job to do. Therefore the corresponding literature, e.g. [52], is few.

### 2.3.5 Perfect/Imperfect Power Control

According to characteristics of the quality indicator seen by the BS, power control schemes can be classified into: perfect power control and imperfect power control schemes. Since the quality indicator can be either the received signal power or the received SIR, the corresponding perfect power control schemes are referred as the perfect strength-based and perfect SIR-based

power control scheme, respectively. To speak more specifically, a perfect strength-based power control implies that the received signal power on each communication link is perfectly controlled to equal to the target threshold. In this case, each MS's transmission power will be a value proportional to the inverse of the short-term fading. On the other hand, a perfect SIR-based power control implies that the received SIR on each communication link is perfectly controlled to equal to the target SIR threshold. In this case, each MS's instantaneous transmission power can be calculated based on the analytical results derived by Zander [8] by letting short-term fading factors be included in the channel gain. Note that, since the global information is needed while calculating the MSs' transmission powers, a perfect SIR-based power control is a kind of centralized power control. Although such an ideal model is not practical, it makes the system analysis easy to be conducted. There is many analytical works can be found based on the perfect strength-based power control, while few are based on the perfect SIR-based power control, e.g. [23], [25], [26].



In an imperfect power control scheme, the quality indicator seen by the BS is modeled as a random variable. The difference between the quality indicator and the target threshold is called the power control error. In a strength-based power control, the power control error is the difference between the received signal and the target threshold and is usually modeled as a log-normal distributed random variable [53], [54], [55]. In a SIR-based power control, the power control error is the difference between the received SIR and the target threshold and seems can also be modeled as a log-normal distributed random variable. The mean of the quality indicator, in dB scale, can be well approximated by the target threshold, in dB scale [40]. However, how to model the corresponding variance is a big problem which is really hard to be derived, since the power control error is affected by too many factors such as power control step size, power control period, finite-bit power control command, power control loop delay, power control command error, and especially the MS's velocity. Some analytical results regarding to the distribution of

SIR can be found in [56], [57]. The imperfect power control is definitely more realistic than the perfect one. There are many works can be found, which are regarding e.g. system capacity [58], [59], [60], outage probability analysis [61].

### 2.3.6 Power Control with Fixed Step Size/Adaptive Step Size

According to strategies on the power adaptation step size, power control algorithms can be classified as follows: those where the power adaptation step size is fixed, and those where the power adaptation step size is made adaptive to the channel variation. Power control command in fixed step size scheme is a simple 1-bit command, which can only instruct the MS to increase or decrease the transmission power by a preset amount. Although with the cost of maybe worse performance due to the low adaptation resolution, the fixed step size scheme is easier to implement and is actually employed in the real systems like cdma2000. As can be seen, such a scenario is like a delta modulation.

Power control command in adaptive step size scheme is generally a multi-bit command. A specific example is the perfect strength-based power control, wherein an infinite-bit command would be needed to let MS's transmission power be adapted based on the actual difference between the received signal power and the target threshold. This is impractical since an infinite-bit command needs infinite communication bandwidth. In order to reduce the needed bandwidth for transmit the power control commands, the number of the power control command bits should be reduced to a certain amount. The difference between the estimated quality indicator and the target threshold is quantized according to a pulse code modulation (PCM) realization [62]. In such a case, the operation of a power control with adaptive step size acts like an adaptive delta-modulation algorithm.

The variable-step algorithm can be expected to have a good performance because the fading factor can be directly compensated during one power control interval with multiple power control



command bits. However in practice, this method is not efficient because it will require lot of downlink bandwidth to convey the power control commands to the respective MS. On the other hand, the fixed step size algorithm is also preferred due to the fact that it can reduce peak transmit power during deep fades. In a variable-step algorithm, the peak transmit power would be high to compensate for deep fades, and therefore may decrease the capacity due to excessive interference to other MSs. Due to this issue, the most existing schemes of closed-loop power control employ a fixed step algorithm, e.g. [24], [42], [50].

### 2.3.7 Truncated Power Control

Truncated power control is a kind of strength-based power control. The key point of a truncated power control is that the MS will suspend its transmission when the channel fading is less than a preset cutoff threshold; otherwise, the MS transmits with power adapted to compensate for the channel fading such that the received signal power level approaches to the target threshold. Conventional strength-based power control is a special case of the truncated power control by letting the cutoff threshold to be zero. Herein, the channel fading could mean the long-term fading, in this case the truncated power control is a truncated average power control [16] which is a kind of open-loop power control, or the short-term fading, in this case the truncated power control is a truncated closed-loop power control [63].

Since the DS/CDMA cellular system is an interference-limited system. Any way to reduce the overall interference in the system will equivalently increase the system capacity. This idea is proven true by the truncated power control [16], [63]. By suspending the transmission temporarily, or otherwise a high transmission power in order to compensate for the deep fading would occur and thus introduce high interference to others, the overall interference in the system can be reduced. A satisfactory capacity gain is reported and the corresponding analysis can be found in [63].

### 2.3.8 Predictive Power Control

The performance of a power control scheme is degraded by the power control loop delay. The following factors contribute to the total power control loop delay. First, quality indicator measurement at the BS takes time. Normally, the quality indicator measurement is performed during part of the power control period and hence, contributes to a one power control period delay. Once the quality indicator measurement is completed, it needs to be compared with the target threshold to generate the power control command. Although the processing time at the BS can be negligible, the power control command may not be transmitted on the next immediate time slot on the downlink channel, because it depends on the synchronization between the uplink and downlink channels. Therefore, the second contributor is the synchronization delay between uplink and downlink channel. The third contributor to the loop delay is the propagation time of the power control command from the BS to the MS.

In order to compensate for the power control loop delay, many predictive power control schemes are employed such that the generation of the power control command is based on the predicted quality indicator, rather than the present estimated quality indicator, and the target threshold. The problem of feedback delay has been identified in [64], [65], [66]. A technique to compensate for feedback delay is proposed in [67] using a time delay compensation method. In this method, the estimated SIR at the BS is adjusted according to the power control commands that have been sent by the BS but whose effect have not taken place at the MS. In [64] the problem of feedback delay is overcome by using a linear prediction filter at the BS to predict the future channel strength. The prediction filter utilizes the previous and present channel correlation to perform the prediction. The filter coefficients can be computed in several ways. In [66], a recursive least squares algorithm is used to compute the predictor coefficients. And [28] proposes a new scheme, which makes use of the current and past information of the MS to predict future power gain due to channel variation and RAKE combining.

Note that if the prediction performs good enough, the variance of the received quality indicator can be thereby reduced which will in turn increase system capacity. A perfect predictive power control is equivalent to a system with zero power control loop delay. Therefore, the performance of a system with zero power control loop delay acts as the upper bound of any kind of predictive power control.

### 2.3.9 Combined Rate and Power Control

Perfect power control can result in high intercell interference due to tracking of deep fades. This translates into large interference to other users, leading to a capacity reduction. Limiting the user transmission power will not solve this problem because this will suppress both the interference and the signal itself. One solution is to jointly adapt the transmission power and the transmission rate according to the channel variation, if the users can tolerate some delay in their transmission.

From the SIR formula, it can be found that not only the transmission power but also the processing gain can be utilized to combat the channel variation. To speak more specifically, when a low channel gain is encountered, to increase the transmission power or to increase the processing gain is equivalent to obtain an identical SIR value. From such an observation, another kind of power control scheme, combined rate and power control, is proposed [15], [68], [69]. The main idea of the combined rate and power control scheme is to limit the increase in transmission power by some fixed level and gets the extra gain required by reducing the transmission rate, which in turn increases the processing gain in a CDMA system. By limiting the transmission power, which translates into a reduction of interference to other MSs as compared with the strength-based power control, the system capacity is thereby increased.

Many control algorithms adapting both the transmission rate and power can be found. The adaptation of transmission rate was first studied in [70] for Rayleigh fading channel. In [15], a

combined power/rate control scheme is considered that limits the increase in power by some fixed value and gets the extra gain required by reducing the rate. In [68], two combined rate and power control schemes are proposed to reduce the average transmission power, while still maintain the same average data rate and BER. (1) Power and rate adaptation, the power and rate adaptation scheme which performs the rate adaptation when the transmission power exceeds a preset threshold and adapts otherwise the transmission power to ensure a fixed-rate transmission; (2) truncated rate adaptation, which suspends transmitting data when the channel gain is below a threshold and then otherwise adapts the rate with a constant power. In [71], a SIR-based soft power control is proposed which has an upper and a lower threshold, perform the rate adaptation with fixed transmission power as the received SIR falls between the lower and higher thresholds, otherwise perform the power adaptation with fixed transmission rate.

There are two main techniques to adapt the processing gain. One technique is the flexible multi-rate CDMA radio interface architecture with different chip rate, which controls the processing gain according to the channel variation [72]. The other technique is the multi-code CDMA, which controls the number of given spreading code according to the channel variation [73]. The former method needs a sophisticated synchronization technique, and the latter method needs high transmission power.

Due to the transmission rate is adapted in accordance with the channel variation, the transmission rate is no longer a constant level. Thus the combined rate and power control is suitable for these delay-insensitive services, like data and image service, and not suitable for these services like voice and video that require constant bit rate transmission. Another side effect is that the average transmission rate of the MS would become smaller as compared with that in the conventional strength-based power control. This can be easily solved by setting appropriate processing gain in advance. For the performance comparison, the system capacity is no longer a proper indicator. A fair indicator would be the average system transmission rate, which is defined

as the product of the system capacity and average transmission rate. It is found that the combined rate and power control can achieve higher average system transmission rate than the conventional strength-based power control.

## 2.4 Concluding Remarks

This chapter provides a fundamental overview of the DS/CDMA cellular systems, the power control techniques, and the classification of these power control techniques. As a basis of a multi-user system, the multiple access techniques adopted by the cellular systems has evolved from 1G's and 2G's FDMA, TDMA to 3G's wideband CDMA. The reason is that the wideband CDMA theoretically can provide higher capacity compared with FDMA and TDMA schemes. However, in order to achieve the high capacity, one of the crucial techniques is the power control. This chapter further reviews the various classifications of the power controls in a DS/CDMA system. The power control can be classified as uplink/downlink power control, centralized/distributed power control, open-loop/closed-loop/outer-loop power control, strength-based/SIR-based/BER-based power control, perfect/imperfect power control, power control with fixed step size/adaptive step size. Aiming to further improve system capacity, the truncated power control and the predictive power control are also introduced. From the viewpoints of the above power control classifications, what this dissertation focuses on is the uplink, distributed, closed-loop, either truncated strength-based or SIR-based, either perfect or imperfect power control scheme with fixed step size. In the following chapters, the performance of the truncated strength-based and the SIR-based power control schemes are analyzed, respectively. Also, the problem of distribution estimation of the multiple access interference in the strength-based power control is addressed in yet another chapter.

## Chapter 3

# Performance Analysis of a Truncated Closed-Loop Power Control Scheme for DS/CDMA Cellular Systems

---

*Abstract—This chapter analyzes the system performance of a truncated closed-loop power control (TCPC) scheme for uplinks in DS/CDMA cellular systems over frequency-selective fading channels. In this TCPC scheme, a mobile station (MS) suspends its transmission when the short-term fading is less than a preset cutoff threshold; and otherwise, the MS transmits with power adapted to compensate for the short-term fading so that the received signal power level remains constant. Closed-form formulae are successfully derived for performance measures, such as system capacity, average system transmission rate, MS average transmission rate, MS power consumption, and MS suspension delay. Numerical results show that the analysis provides reasonable accuracy; and the TCPC scheme can substantially improve the system capacity, the average system transmission rate, and power saving over conventional closed-loop power control schemes. Moreover, the TCPC scheme under realistic consideration of power control error due to power control step size, power control period, power control delay, and MS velocity is further investigated. A closed-form formula is obtained to accurately approximate the system capacity of the realistic TCPC scheme. A closed-form formula is obtained to accurately approximate the system capacity of the realistic TCPC scheme.*

### 3.1 Introduction

In a DS/CDMA system, many users can transmit messages simultaneously over the same radio channel, each using a specific spread-spectrum pseudo-noise (PN) code [10]. Within a cell, the code channels in downlinks can be considered as mutually orthogonal because downlinks may exhibit synchronous CDMA transmission. However, these code channels in uplinks cannot be exactly mutually orthogonal for a set of asynchronous users, and thus mutual interference occurs among the uplinks. In such a case, a strong signal increases communication quality, and a weak signal may suffer from strong interference. This problem is referred to as the near-far effect and limits the CDMA system capacity [11]. Hence, power control is an essential issue in a DS/CDMA system.

*Open-loop* power control, that is, the average power control, is applied to compensate for the long-term channel fading such that the average received signal power level is constant and the near-far problem is solved [12]. *Closed-loop* power control, however, is typically used to mitigate the short-term channel fading so that an acceptable received signal quality can be attained for the uplink communication. Several *closed-loop/open-loop* power control schemes have been investigated, such as: 1) the well-known perfect power control, within which MS transmission power is adjusted to the exact inverse of the short-term fading and thus the received signal power level remains constant. Such a method is also referred to as the channel inversion scheme [13], [14]; 2) combined power/rate control proposed in [15], which is the same as the perfect power control except in that MS holds its transmission power at  $Q_0/X_0$  and adapts its transmission rate to  $S(t) \cdot R_0/X_0$  when  $S(t) < X_0$ , where  $Q_0$  is the desired received power level,  $X_0$  is a preset cutoff threshold,  $S(t)$  is the short-term fading at time  $t$ , and  $R_0$  is the data symbol rate; 3) truncated average power control (TAPC) proposed in [16], which applies a truncated channel inversion scheme to conventional average power control. This truncated channel inversion scheme suspends transmission when the *long-term channel fading* falls below a cutoff threshold; otherwise it

adaptively controls power according to the channel inversion scheme. By suspending transmission in this way, an improvement of system capacity was reported.

In this chapter, we propose a truncated closed-loop power control (TCPC) scheme, which extends the TAPC scheme by considering the fast closed-loop power control, since mitigating the rapid variations of fading by power control mechanism had been adopted in 3G systems like cdma2000 and WCDMA. In the TCPC scheme, when the short-term fading satisfies  $S(t) < X_0$ , MS suspends transmission; otherwise, MS adaptively transmits power to compensate for the *short-term fading* so that the received signal power level is constant. This chapter analyzes the performance of the TCPC scheme for uplinks in DS/CDMA cellular systems over frequency-selective fading channels. It first analyzes an ideal TCPC scheme in which the transmission power is continuously and instantaneously adjusted. Based on the SIR formula over a medium-term period, closed-form formulae are successfully derived for system performance including system capacity, average system transmission rate, MS average transmission rate, MS power consumption, and MS suspension delay. The upper limit of the average system transmission rate of the TCPC scheme achieved in a multi-cell system is also obtained, and it is found the same as that of the perfect power control scheme in a single-cell system. Numerical results show that the analysis is quite accurate; and the TCPC scheme is more effective than the conventional closed-loop power control schemes such as perfect power control [13], [14], combined power/rate control [15], and truncated average power control [16]. This chapter further analyzes the realistic TCPC scheme that considers power control error due to power control step size, power control command delay, and MS velocity. A closed-form formula is also derived to accurately approximate the system capacity of the realistic TCPC scheme. Numerical results indicate that the power control error has a significant impact on the system capacities of the TCPC and conventional closed-loop power control schemes.

The rest of this chapter is structured as follows. Section 2.2 introduces the system model and



derives a formula of the received SIR per bit. Section 3.3 derives the performance measures of the TCPC scheme in both ideal and realistic cases. Section 3.4 presents numerical results as well as simulation results for validation. Comparisons between TCPC and other conventional schemes are also presented. Finally, Section 3.5 remarks conclusions.

## 3.2 System Model

### 3.2.1 Channel Model

Consider  $N_B$  cells in a CDMA cellular system of which the central cell is surrounded by other cells in a hexagonal-grid configuration. Each cell has a base station (BS) located at the center and has  $N_M$  MSs uniformly distributed in the system. Generally, the frequency-selective multipath channel of the uplink ( $m, b$ ), denoting the channel from an arbitrary MS  $m$  to an arbitrary BS  $b$ , is described by a time-variant impulse response

$$u_{mb}(\tau; t) = \sum_{p=1}^K \sqrt{\alpha_{mb,p}(t)} \cdot e^{-j\theta_{mb,p}(t)} \cdot \delta(\tau - pT_c), \quad (3.1)$$

where  $m \in \{1, 2, \dots, N_B \cdot N_M\}$  denotes the MS index,  $b \in \{1, 2, \dots, N_B\}$  denotes the BS index,  $u_{mb}(\tau; t)$  is the response of the uplink ( $m, b$ ) at time  $t$ , due to an impulse applied at time  $(t - \tau)$ ;  $T_c$  represents the chip duration;  $K$  is the number of resolvable paths; and the random variables  $\alpha_{mb,p}(t)$  and  $\theta_{mb,p}(t)$  are the power gain and the phase of the  $p$ th path at time  $t$ , respectively [10].

The power gain of the  $p$ th path can be divided into two parts [74],

$$\alpha_{mb,p}(t) = L_{mb}(t) \cdot S_{mb,p}(t), \quad (3.2)$$

where  $L_{mb}(t)$  and  $S_{mb,p}(t)$  represent long-term fading and short-term fading, respectively. The long-term fading is normally modeled as

$$L_{mb}(t) = |\mathbf{z}_m(t) - \mathbf{x}_b(t)|^{-\eta} \cdot 10^{x_{mb}(t)/10}, \quad (3.3)$$

where  $\mathbf{z}_m(t)$  and  $\mathbf{x}_b(t)$  are complex numbers that represent the locations of MS  $m$  and BS  $b$ ,

respectively,  $\eta$  is the propagation exponent that depends on the environment, and  $x_{mb}(t)$  is a zero-mean Gaussian random process with standard deviation  $\sigma_x$ . The short-term fading is widely modeled as Rayleigh fading and  $S_{mb,p}(t)$  is exponentially distributed, i.e.

$$f_{S_p}(x) = \frac{1}{\mu_{S_p}} e^{-\frac{x}{\mu_{S_p}}}, \quad 0 \leq x, \quad (3.4)$$

where  $f_{S_p}(\cdot)$  represents the pdf of  $S_{mb,p}(t)$ ,  $\mu_{S_p} = E(S_{mb,p})$ . For the convenience, the multipath intensity profile (MIP) [10] of each uplink is assumed to be identical and every signal path has the same average received power. Without loss of generality, the overall short-term fading effect

$$S_{mb}(t) \triangleq \sum_{p=1}^K S_{mb,p}(t), \quad (3.5)$$

given the optimal maximal ratio combining, is normalized to have unit mean. Thus, the pdf of  $S_{mb}(t)$ , denoted by  $f_S(\cdot)$ , is found to have a gamma distribution, which is given by

$$f_S(x) = f_{\gamma(K,K)}(x), \quad (3.6)$$

where  $f_{\gamma(p_1,p_2)}(x)$  denotes the gamma pdf with parameters  $(p_1, p_2)$

$$f_{\gamma(p_1,p_2)}(x) = \frac{p_2^{p_1} \cdot x^{p_1-1}}{\Gamma(p_1)} e^{-p_2 x}, \quad 0 \leq x. \quad (3.7)$$

Note that the cdf of a gamma RV  $\gamma_{(p_1,p_2)}$  with parameters  $(p_1,p_2)$  is given by

$$F_{\gamma(p_1,p_2)}(x) = \int_0^x \frac{p_2^{p_1} \cdot y^{p_1-1}}{\Gamma(p_1)} e^{-p_2 y} dy. \quad (3.8)$$

The corresponding mean and variance are respectively given by

$$E(\gamma_{(p_1,p_2)}) = \frac{p_1}{p_2}, \quad (3.9)$$

$$\text{var}(\gamma_{(p_1,p_2)}) = \frac{p_1}{p_2^2}. \quad (3.10)$$

### 3.2.2 Transmitter Model

If BPSK modulation is considered, the transmitted low-pass equivalent signal of MS  $m$  is given by

$$s_m(t) = \sqrt{P_m(t)} \cdot d_m(t - \tau_m) \cdot c_m(t - \tau_m) \cdot e^{-j\phi_m}, \quad 1 \leq m \leq N_B \cdot N_M, \quad (3.11)$$

where  $P_m(t)$  is MS transmission power at time  $t$ ;  $d_m(t)$  is the MS bipolar data stream;  $c_m(t)$  is the corresponding PN sequence whose chip waveform is rectangular;  $\tau_m$  is a value between zero and the data symbol duration  $T$  and indicates each MS independent symbol timing due to asynchronous transmission; and  $\phi_m$  is the random carrier phase. Under a transmission power control,  $P_m(t)$  can be conceptually divided into two parts as

$$P_m(t) = P_{O,m}(t) \cdot P_{C,m}(t), \quad (3.12)$$

where  $P_{O,m}(t)$  and  $P_{C,m}(t)$  are the transmission powers controlled by open-loop and closed-loop power control schemes, respectively. This chapter assumes perfect open-loop power control, hence for each MS  $m$  served by its home BS  $h$ , we have

$$P_{O,m}(t) = 1/L_{mh}(t). \quad (3.13)$$

### 3.2.3 Receiver Model

Here, we consider a medium-term period which is sufficiently long to make the short-term fadings be averaged out while the long-term fadings remain almost constant since MSs move only a little. Over the medium-term period, a SIR formula is derived and closed-form formulae of the performance measures are obtained accordingly. Also, the set of the long-term fading from any MS  $m$  to any BS  $b$  is referred to as a scenario and is represented as  $\{L_{mb}, \forall(m, b)\}$  from which its time index  $t$  is dropped. Based on the models of channel impulse response given in (3.1) and the MS transmitted signal given in (3.11), the total signal received at a specific BS  $H$  can be found to be

$$\begin{aligned}
r_H(t) &= \sum_{m=1}^{N_B \cdot N_M} S_m(t) \otimes u_{mH}(\tau; t) \\
&= \sum_{m=1}^{N_B \cdot N_M} \sum_{p=1}^K \sqrt{L_{mH} \cdot S_{mH,p}(t) \cdot P_m(t)} \cdot d_m(t - pT_c - \tau_m) \cdot c_m(t - pT_c - \tau_m) \cdot e^{-j(\theta_{mH,p}(t) + \phi_m)},
\end{aligned} \tag{3.14}$$

where the background noise is ignored since it is much smaller than the other-cell interference. Consider a RAKE receiver with an optimal maximal ratio combiner to take full advantage of the multipath diversity. Here, we assume slow fading such that  $S_{mb}(t)$ ,  $S_{mb,p}(t)$ ,  $P_m(t)$ , and  $\theta_{mb,p}(t)$  can be treated as constants  $S_{mb}[n]$ ,  $S_{mb,p}[n]$ ,  $P_m[n]$ , and  $\theta_{mb,p}[n]$ , respectively, for all possible  $m$ ,  $b$ , and  $p$ , during the  $n$ th data symbol period. That is,

$$\begin{cases} S_{mb}(t) \approx S_{mb}[n], \\ S_{mb,p}(t) \approx S_{mb,p}[n], \\ P_m(t) \approx P_m[n], \\ \theta_{mb,p}(t) \approx \theta_{mb,p}[n], \end{cases} \quad nT \leq t < (n+1)T, \forall (m, b, p). \tag{3.15}$$

The decision statistics,  $Z_M[n]$ , corresponding to a target MS  $M$  communicating with the specific BS  $H$  can be derived and divided into three parts

$$\begin{aligned}
Z_M[n] &\triangleq \text{Re} \left\{ \sum_{p=1}^K \int_{nT+pT_c+\tau_M}^{(n+1)T+pT_c+\tau_M} r_H(t) \cdot \left( \sqrt{S_{MH,p}(t)} \cdot c_M(t - pT_c - \tau_M) \cdot e^{-j(\theta_{MH,p}(t) + \phi_M)} \right)^* dt \right\} \\
&= r_M[n] + I_A[n] + I_S[n].
\end{aligned} \tag{3.16}$$

The first term  $r_M[n]$  is the desired signal part given by

$$r_M[n] = T \cdot d_M[n] \cdot S_{MH}[n] \cdot \sqrt{L_{MH} \cdot P_M[n]}. \tag{3.17}$$

The second term  $I_A[n]$  represents the multiple access and multipath interference from the other MSs and can be obtained by

$$I_A[n] = \sum_{p=1}^K \sqrt{S_{MH,p}[n]} \cdot \sum_{m=1, m \neq M}^{N_B \cdot N_M} \sum_{p'=1}^K \sqrt{L_{mH} \cdot S_{mH,p'}[n] \cdot P_m[n]} \cdot I_{M,p}^{(m,p')}[n], \tag{3.18}$$

where

$$I_{M,p}^{(m,p')}[n] = \int_{nT+pT_c+\tau_M}^{(n+1)T+pT_c+\tau_M} d_m(t-p'T_c-\tau_m) \cdot c_m(t-p'T_c-\tau_m) \cdot c_M(t-pT_c-\tau_M) \cdot \cos(\theta_{mH,p}[n] + \phi_m - \theta_{MH,p}[n] - \phi_M) dt. \quad (3.19)$$

Over the medium-term period, the long-term fading, which is the local mean of the channel gain, is treated as constant; the short-term fading is typically modeled as a stationary random process. Hence the channel gain, which is the product of the long-term and short-term fading, becomes a stationary random process. The transmission power under strength-based power control, which is generally a function of channel gain, will turn out also to be stationary. If both MS data streams and PN sequences are assumed to be stationary, then the interference signal  $I_A[n]$  in (3.18) will resemble a noise-like stationary random process, and its distribution can be approximated by a Gaussian one according to the central limit theorem. Notably,  $I_A[n]$  having a mean of zero and a variance is the mean of the interference signal power at the output of the RAKE receiver, given by

$$E(I_A^2[n]) = \frac{G \cdot T_c^2}{3} \cdot S_{MH}[n] \cdot \sum_{m=1, m \neq M}^{N_B \cdot N_M} L_{mH} \cdot E(S_{mH}[n] \cdot P_m[n]), \quad (3.20)$$

where

$$G \triangleq \frac{T}{T_c}, \quad (3.21)$$

is the processing gain [10], and  $E(\cdot)$  is the expectation function. The third term  $I_S[n]$  represents the multipath interference itself. Since  $N_B \cdot N_M \gg 1$ ,  $I_S[n]$  would be much smaller than  $I_A[n]$ , and the effect of  $I_S[n]$  is ignored in the following.

The SIR per bit during the  $n$ th data symbol period of MS  $M$  at the output of RAKE receiver, defined in [10, p.244] and denoted by  $\Gamma_M[n]$ , is given by

$$\Gamma_M[n] = \frac{r_M^2[n]}{2E(I_A^2[n])} = \frac{3}{2} \cdot \frac{G \cdot Q_M[n]}{I_I + I_O}, \quad (3.22)$$

where  $Q_M[n]$  is the instantaneously received signal power, and  $I_I$  and  $I_O$  represent the mean power of the intra-cell interference signals and the mean power of the other-cell interference signals, respectively. In general, the term  $Q_M[n]$  can be obtained by,

$$\begin{aligned} Q_M[n] &= P_M[n] \cdot S_{MH}[n] \cdot L_{MH} \\ &= (P_{C,M}[n] \cdot S_{MH}[n]) \cdot (P_{O,M}[n] \cdot L_{MH}). \end{aligned} \quad (3.23)$$

Assuming that  $\{P_{C,m}[k], \forall m\}$  are independently and identically distributed (iid) with a mean of  $E(P_{C,m}[n])$ , which, for clearer notation, is denoted by

$$\bar{P}_C \equiv E(P_{C,m}[n]), \quad \forall m. \quad (3.24)$$

The  $\{Q_m[n], \forall m\}$  are also iid random variables with a mean given by

$$\bar{Q} \equiv E(Q_m[n]), \quad \forall m. \quad (3.25)$$

From (3.20) and (3.22),  $I_I$  and  $I_O$  can be obtained by

$$I_I = (N_M - 1) \cdot \bar{Q}, \quad (3.26)$$

$$I_O = \bar{P}_C \cdot \sum_{h \neq H} \sum_{m \in MS^{(h)}} \frac{L_{mH}}{L_{mh}}, \quad (3.27)$$

where

$$MS^{(h)} = \{m \mid \text{MS } m \text{ is served by BS } h\}, \quad (3.28)$$

denoting the index set of the MSs served by the BS  $h$ .

### 3.3 Performance Analysis

In the TCPC scheme, MS adjusts its transmission power to compensate for the *short-term fading* when the *short-term fading* is above a preset cutoff threshold  $X_0$  and suspends its transmission, otherwise. Accordingly, considering an target uplink  $(M, H)$ ,

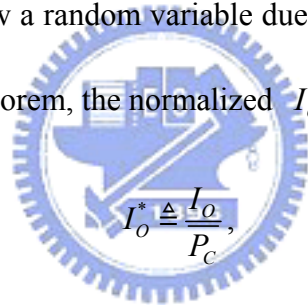
$$P_M[n] = \begin{cases} \frac{Q_0}{L_{MH}[n] \cdot S_{MH}[n]}, & \text{as } S_{MH}[n] \geq X_0, \\ 0, & \text{as } S_{MH}[n] < X_0, \end{cases} \quad (3.29)$$

where  $Q_0$  denotes the preset desired received power level. If the transmission power can be adjusted *continuously* and *immediately* as shown in (3.29), the scheme is referred to as an ideal TCPC.

### 3.3.1 Ideal TCPC

Conditional with on  $\{L_{mb}, \forall(m, b)\}$ , the SIR per bit in (3.22) given  $P_M[n] > 0$  is time constant over the medium-term period. The unconditioned SIR per bit is then obtained by considering all possible  $\{L_{mb}, \forall(m, b)\}$ . The formula of the unconditioned SIR per bit is the same as (3.22), but its denominator is now a random variable due to the randomness of  $\{L_{mb}, \forall(m, b)\}$ .

Again, applying the central limit theorem, the normalized  $I_O$ , represented as



$$I_O^* \triangleq \frac{I_O}{P_C}, \quad (3.30)$$

can be approximated by a Gaussian random variable  $\xi$  and expressed as

$$I_O^* \approx \xi(N_M \mu_O, N_M \sigma_O^2), \quad (3.31)$$

where  $\mu_O$  and  $\sigma_O^2$  are the mean and the variance of  $I_O^*$ , respectively when  $N_M = 1$ . The terms

$\mu_O$  and  $\sigma_O^2$  can be obtained by

$$\begin{cases} \mu_O = E\left(\sum_{h \neq H} I_h\right) = \sum_{h \neq H} E(I_h), \\ \sigma_O^2 = \text{var}\left(\sum_{h \neq H} I_h\right) = \sum_{h \neq H} \text{var}(I_h), \end{cases} \quad (3.32)$$

where

$$I_h \triangleq \left( \frac{L_{mH}}{L_{mh}} \middle| L_{mb} \leq L_{mh}, \forall b \right). \quad (3.33)$$

The  $I_h$  was analyzed by Zorzi [22], and its mean and variance can be numerically computed as

$$\begin{aligned} E(I_h) &= \lim_{y \rightarrow \infty} \left( y - \int_0^y \Pr(I_h \leq s) \cdot ds \right) \\ &= \left( y - \int_0^y \Pr(I_h \leq s) \cdot ds \right) \Big|_{y=1} + \lim_{\substack{y \rightarrow \infty \\ y \geq 1}} \left( y - \int_0^y \Pr(I_h \leq s) \cdot ds \right) \\ &= \left( 1 - \int_0^1 \Pr(I_h \leq s) \cdot ds \right) + \lim_{\substack{y \rightarrow \infty \\ y \geq 1}} \left( y - \int_0^y 1 \cdot ds \right) \\ &= 1 - \int_0^1 \Pr(I_h \leq s) \cdot ds, \end{aligned} \quad (3.34)$$

and

$$\begin{aligned} \text{var}(I_h) &= \lim_{y \rightarrow \infty} \left( y - 2 \int_0^y s \Pr(I_h \leq s) \cdot ds \right) - E^2(I_h) \\ &= \left( 1 - 2 \int_0^1 s \Pr(I_h \leq s) \cdot ds \right) - E^2(I_h), \end{aligned} \quad (3.35)$$

where

$$\begin{aligned} \Pr(I_h \leq s) &= \frac{\int \Pr(L_{mH}(\mathbf{z}) \leq sL_{mh}(\mathbf{z}), L_{mb}(\mathbf{z}) \leq L_{mh}(\mathbf{z}), \forall b) \cdot f_{\mathbf{z}_m}(\mathbf{z}) d\mathbf{z}}{\int \Pr(L_{mb}(\mathbf{z}) \leq L_{mh}(\mathbf{z}), \forall b) \cdot f_{\mathbf{z}_m}(\mathbf{z}) d\mathbf{z}} \\ &= \frac{\varphi(s)}{\varphi(1)}, \end{aligned} \quad (3.36)$$

notation  $L_{mh}(\mathbf{z})$  is used to denote the long-term fading of MS  $m$  whose location  $\mathbf{z}_m = \mathbf{z}$ ,  $f_X(\cdot)$

denotes the pdf of a random variable  $X$ , and

$$\begin{aligned} \varphi(s) &= \Pr(L_{mH}(\mathbf{z}) \leq sL_{mh}(\mathbf{z}), L_{mb}(\mathbf{z}) \leq L_{mh}(\mathbf{z}), \forall b) \\ &= \int f_{L_{mh}(\mathbf{z})}(y) \Pr(L_{mH}(\mathbf{z}) \leq sy) \prod_{b \neq h, H} \Pr(L_{mb}(\mathbf{z}) \leq y) dy. \end{aligned} \quad (3.37)$$

Considering an MS  $M$  in central cell  $H$ , the outage probability of the target uplink  $(M, H)$ ,

denoted by  $\Lambda_M$ , is defined as



$$\begin{aligned}
\Lambda_M &\triangleq \Pr(\Gamma_M[n] < \Gamma_0 | P_M[n] > 0) \\
&= \Pr\left(\frac{1.5G \cdot Q[n]}{(N_M - 1) \cdot \bar{Q} + \bar{P}_C \cdot I_O^*} < \Gamma_0\right),
\end{aligned} \tag{3.38}$$

where  $\Gamma_0$  is the minimum SIR per bit required to achieve a desired bit error rate at the output of the RAKE receiver. The outage probability given  $P_M[n] = 0$  is not considered, since no data is transmitted in that case. Notably, only the statistics relating to the central cell  $H$  are taken into account to avoid the corner effect. Using (3.22) and (3.31),  $\Lambda_M$  can be approximated by

$$\begin{aligned}
\Lambda_M &\approx \Pr\left(\frac{1.5G \cdot Q_0}{(N_M - 1) \cdot \bar{Q} + \bar{P}_C \cdot \xi(N_M \mu_O, N_M \sigma_O^2)} < \Gamma_0\right) \\
&= \Pr\left(\frac{1.5G \cdot Q_0 - \Gamma_0 (N_M - 1) \cdot \bar{Q}}{\Gamma_0 \bar{P}_C} < \xi(N_M \mu_O, N_M \sigma_O^2)\right) \\
&= 1 - F_\xi\left(\frac{1.5G \cdot Q_0 - \Gamma_0 (N_M - 1) \cdot \bar{Q}}{\Gamma_0 \cdot \bar{P}_C}, N_M \mu_O, N_M \sigma_O^2\right) \\
&= 1 - F_\xi\left(\frac{1.5G \cdot Q_0 - \Gamma_0 (N_M - 1) \cdot \bar{Q}}{\Gamma_0 \cdot \bar{P}_C} - N_M \mu_O, 0, N_M \sigma_O^2\right) \\
&= 1 - F_\xi\left(\frac{1.5G \cdot Q_0 - \Gamma_0 (N_M - 1) \cdot \bar{Q}}{\Gamma_0 \cdot \bar{P}_C \cdot \sqrt{N_M}} - \frac{N_M \mu_O}{\sqrt{N_M}}, 0, \sigma_O^2\right),
\end{aligned} \tag{3.39}$$

where  $F_\xi(\cdot, \mu_O, \sigma_O^2)$  indicates the cdf function of a Gaussian variable  $\xi$  with mean  $\mu_O$  and variance  $\sigma_O^2$ . The average transmission power  $\bar{P}_C$  controlled by the closed-loop power control can be obtained by

$$\bar{P}_C = \int_{x_0}^{\infty} \frac{Q_0}{y} f_s(y) dy. \tag{3.40}$$

For the case  $K=1$ ,

$$\begin{aligned}
\bar{P}_C &= \int_{x_0}^{\infty} \frac{Q_0}{y} f_{r(1,1)}(y) dy \\
&= \int_{x_0}^{\infty} \frac{Q_0}{y} \frac{1^1 \cdot y^{1-1}}{\Gamma(1)} e^{-y} dy
\end{aligned} \tag{3.41}$$

$$= Q_0 \cdot \int_{X_0}^{\infty} \frac{1}{y \cdot e^y} dy,$$

For  $K \geq 2$ ,

$$\begin{aligned} \overline{P}_C &= \int_{X_0}^{\infty} \frac{Q_0}{y} f_{\gamma(K,K)}(y) dy \\ &= \int_{X_0}^{\infty} \frac{Q_0}{y} \frac{K^K \cdot y^{K-1}}{\Gamma(K)} e^{-Ky} dy \\ &= Q_0 \int_{X_0}^{\infty} \frac{K^K \cdot y^{K-2}}{\Gamma(K)} e^{-Ky} dy \\ &= Q_0 \cdot \frac{K}{K-1} \int_{X_0}^{\infty} \frac{K^{K-1} \cdot y^{K-2}}{\Gamma(K-1)} e^{-Ky} dy \\ &= Q_0 \cdot \frac{K}{K-1} \cdot (1 - F_{\gamma(K-1,K)}(X_0)). \end{aligned} \quad (3.42)$$

The average received power  $\overline{Q}$  can be obtained by

$$\overline{Q} = \int_{X_0}^{\infty} Q_0 \cdot f_s(y) dy = Q_0 \cdot (1 - F_{\gamma(K,K)}(X_0)). \quad (3.43)$$

Five performance measures are investigated. The first measure is the system capacity  $C$  which is defined as the maximum number of users per cell that the system can support under the constraint that the outage probability of an arbitrary MS in central cell  $H$  is less than a preset outage threshold  $\Lambda_0$ . That is,

$$C \triangleq \left\lfloor \max_{N_M \in \mathbb{R}} \left\{ \arg \left[ (\Lambda_M < \Lambda_0) \Big|_{M \in MS^{(H)}} \right] \right\} \right\rfloor, \quad (3.44)$$

where the operator  $\lfloor \cdot \rfloor$  denotes the maximum integer below the argument. Substituting (3.39) into (3.44) yields  $C = \lfloor C^* \rfloor$  where  $C^*$  satisfies the following equation

$$F_{\xi} \left( \frac{1.5G \cdot Q_0 - \Gamma_0 \cdot (C^* - 1) \cdot \overline{Q}}{\Gamma_0 \cdot \overline{P}_C \cdot \sqrt{C^*}} - \frac{C^* \cdot \mu_O}{\sqrt{C^*}}, 0, \sigma_O^2 \right) = 1 - \Lambda_0. \quad (3.45)$$

$$\frac{1.5G \cdot Q_0 - \Gamma_0 \cdot (C^* - 1) \cdot \bar{Q}}{\Gamma_0 \cdot \bar{P}_C \cdot \sqrt{C^*}} - \frac{C^* \cdot \mu_0}{\sqrt{C^*}} = F_\xi^{-1}(1 - \Lambda_0, 0, \sigma_0^2). \quad (3.46)$$

Equation (3.46) is re-written in the form of  $\kappa_a \cdot C^* + \kappa_b \cdot \sqrt{C^*} - \kappa_c = 0$  where

$$\begin{cases} \kappa_a = \Gamma_0 \cdot (\bar{Q} + \bar{P}_C \cdot \mu_0), \\ \kappa_b = \Gamma_0 \cdot \bar{P}_C \cdot F_\xi^{-1}(1 - \Lambda_0, 0, \sigma_0^2), \\ \kappa_c = 1.5G \cdot Q_0 + \Gamma_0 \cdot \bar{Q}. \end{cases} \quad (3.47)$$

There are two solutions of  $\sqrt{C^*}$  given by

$$\sqrt{C^*} = \frac{-\kappa_b \pm \sqrt{\kappa_b^2 + 4\kappa_a \kappa_c}}{2\kappa_a}. \quad (3.48)$$

Note that  $\sqrt{C^*}$  should be always positive. Accordingly, the capacity  $C$  under the TCPC scheme is given by

$$C = \left[ \left( \frac{-\kappa_b + \sqrt{\kappa_b^2 + 4\kappa_a \kappa_c}}{2\kappa_a} \right)^2 \right] \left[ \left( \frac{-\kappa_b}{2\kappa_a} + \sqrt{\left( \frac{\kappa_b}{2\kappa_a} \right)^2 + \frac{\kappa_c}{\kappa_a}} \right)^2 \right]. \quad (3.49)$$

Notably, when  $X_0 = 0$ , the TCPC is reduced to the perfect power control and the above analyses remain applicable. On the other hand, when  $X_0 \rightarrow \infty$ , we have

$$\begin{aligned} \lim_{X_0 \rightarrow \infty} \frac{\kappa_b}{\kappa_a} &= \lim_{X_0 \rightarrow \infty} \frac{\Gamma_0 \cdot \bar{P}_C \cdot F_\xi^{-1}(1 - \Lambda_0, 0, \sigma_0^2)}{\Gamma_0 \cdot (\bar{Q} + \bar{P}_C \cdot \mu_0)} \\ &= F_\xi^{-1}(1 - \Lambda_0, 0, \sigma_0^2) \lim_{X_0 \rightarrow \infty} \frac{1}{\frac{\bar{Q}}{\bar{P}_C} + \mu_0} \\ &= \frac{F_\xi^{-1}(1 - \Lambda_0, 0, \sigma_0^2)}{\lim_{X_0 \rightarrow \infty} \left( \frac{\bar{Q}}{\bar{P}_C} \right) + \mu_0}, \end{aligned} \quad (3.50)$$

where

$$\begin{aligned}
\lim_{X_0 \rightarrow \infty} \left( \frac{\bar{Q}}{P_C} \right) &= \lim_{X_0 \rightarrow \infty} \frac{Q_0 \cdot (1 - F_{\gamma(K,K)}(X_0))}{Q_0 \cdot \frac{K}{K-1} \cdot (1 - F_{\gamma(K-1,K)}(X_0))} \\
&= \frac{K-1}{K} \lim_{X_0 \rightarrow \infty} \frac{\left. \frac{d(1 - F_{\gamma(K,K)}(x))}{dx} \right|_{x=X_0}}{\left. \frac{d(1 - F_{\gamma(K-1,K)}(x))}{dx} \right|_{x=X_0}} \\
&= \frac{K-1}{K} \lim_{X_0 \rightarrow \infty} \frac{f_{\gamma(K,K)}(X_0)}{f_{\gamma(K-1,K)}(X_0)} \\
&= \frac{K-1}{K} \lim_{X_0 \rightarrow \infty} \frac{\frac{K^K X_0^{K-1}}{\Gamma(K)} e^{-KX_0}}{\frac{K^{K-1} X_0^{K-2}}{\Gamma(K-1)} e^{-KX_0}} \\
&= \frac{K-1}{K} \lim_{X_0 \rightarrow \infty} \frac{K^K X_0^{K-1} \Gamma(K-1)}{K^{K-1} X_0^{K-2} \Gamma(K)} \\
&= \lim_{X_0 \rightarrow \infty} X_0 \\
&= \infty.
\end{aligned} \tag{3.51}$$

Therefore, we have



$$\lim_{X_0 \rightarrow \infty} \frac{\kappa_b}{\kappa_a} = 0. \tag{3.52}$$

On the other hand,

$$\begin{aligned}
\lim_{X_0 \rightarrow \infty} \frac{\kappa_c}{\kappa_a} &= \lim_{X_0 \rightarrow \infty} \frac{1.5G \cdot Q_0 + \Gamma_0 \cdot \bar{Q}}{\Gamma_0 \cdot (\bar{Q} + P_C \cdot \mu_O)} \\
&= \frac{1.5G \cdot Q_0 \cdot \left( \lim_{X_0 \rightarrow \infty} \frac{1}{Q} \right) + \Gamma_0}{\Gamma_0 \cdot \left( 1 + \mu_O \cdot \lim_{X_0 \rightarrow \infty} \frac{P_C}{Q} \right)},
\end{aligned} \tag{3.53}$$

where

$$\begin{aligned}
\lim_{X_0 \rightarrow \infty} \left( \frac{1}{Q} \right) &= \lim_{X_0 \rightarrow \infty} \frac{1}{Q_0 \cdot (1 - F_{\gamma(K,K)}(X_0))} \\
&= \infty.
\end{aligned} \tag{3.54}$$

By (3.51) and (3.54), we have

$$\lim_{X_0 \rightarrow \infty} \frac{\kappa_c}{\kappa_a} = \infty. \quad (3.55)$$

According to (3.49), (3.52) and (3.55), when  $X_0 \rightarrow \infty$ , the capacity becomes infinite, i.e.

$$\begin{aligned} \lim_{X_0 \rightarrow \infty} C &= \left[ \left( -\lim_{X_0 \rightarrow \infty} \frac{\kappa_b}{2\kappa_a} + \sqrt{\left( \lim_{X_0 \rightarrow \infty} \frac{\kappa_b}{2\kappa_a} \right)^2 + \lim_{X_0 \rightarrow \infty} \frac{\kappa_c}{\kappa_a}} \right)^2 \right] \\ &= \infty. \end{aligned} \quad (3.56)$$

The second measure is the MS average transmission rate  $\bar{R}$ . It is,

$$\bar{R} \triangleq \int_{X_0}^{\infty} R_0 \cdot f_S(y) dy = R_0 \cdot (1 - F_{\gamma(K,K)}(X_0)), \quad (3.57)$$

where  $R_0 = 1/T$  is the data symbol rate.

The third measure is the average system transmission rate  $\bar{\mathfrak{R}}$  which is defined as the average transmission rate multiplied by the system capacity. Thus  $\bar{\mathfrak{R}}$  is given by

$$\bar{\mathfrak{R}} \triangleq \bar{R} \cdot C \approx \left( -\frac{\kappa_b \cdot \sqrt{\bar{R}}}{2\kappa_a} + \sqrt{\left( \frac{\kappa_b \cdot \sqrt{\bar{R}}}{2\kappa_a} \right)^2 + \frac{\kappa_c \cdot \bar{R}}{\kappa_a}} \right)^2, \quad (3.58)$$

such that  $\bar{\mathfrak{R}}$  can be approximated as a monotonously increasing function of  $X_0$ . When  $X_0 = 0$ ,

(3.58) corresponds to the average system transmission rate of the perfect power control scheme

and is the lower limit of  $\bar{\mathfrak{R}}$ . By (3.57), it is obvious that

$$\begin{aligned} \lim_{X_0 \rightarrow \infty} \sqrt{\bar{R}} &= \lim_{X_0 \rightarrow \infty} \sqrt{R_0 \cdot (1 - F_{\gamma(K,K)}(X_0))} \\ &= \sqrt{R_0 \cdot (1 - \lim_{X_0 \rightarrow \infty} F_{\gamma(K,K)}(X_0))} \\ &= \sqrt{R_0 \cdot (1 - 1)} \\ &= 0. \end{aligned} \quad (3.59)$$

By (3.52) and (3.59), the factor  $(\kappa_b \cdot \bar{R}^{1/2} / \kappa_a)$  in (3.58) approaches to zero as  $X_0 \rightarrow \infty$ , i.e.

$$\lim_{X_0 \rightarrow \infty} \frac{\kappa_b \sqrt{\bar{R}}}{\kappa_a} = 0. \quad (3.60)$$

By (3.58) and (3.60), the upper limit of the average system transmission rate in a multi-cell system under TCPC is

$$\begin{aligned} \lim_{X_0 \rightarrow \infty} \bar{\mathfrak{R}} &= \left( -\lim_{X_0 \rightarrow \infty} \frac{\kappa_b \cdot \sqrt{\bar{R}}}{2\kappa_a} + \sqrt{\left( \lim_{X_0 \rightarrow \infty} \frac{\kappa_b \cdot \sqrt{\bar{R}}}{2\kappa_a} \right)^2 + \lim_{X_0 \rightarrow \infty} \frac{\kappa_c \cdot \bar{R}}{\kappa_a}} \right)^2 \\ &= \lim_{X_0 \rightarrow \infty} \frac{\kappa_c \cdot \bar{R}}{\kappa_a} \\ &= \lim_{X_0 \rightarrow \infty} \frac{R_0 \cdot (1.5G \cdot Q_0 + \Gamma_0 \cdot \bar{Q})}{Q_0 \cdot \Gamma_0 \cdot \left( 1 + \frac{\bar{P}_C}{\bar{Q}} \cdot \mu_0 \right)} \\ &= \frac{1.5G \cdot R_0}{\Gamma_0}, \end{aligned} \quad (3.61)$$

which is just the upper limit of the average system transmission rate in a single cell system under perfect power control.

The fourth measure is the MS average transmission energy per bit  $\bar{\mathcal{E}}$  which is defined as the average ratio of MS transmission power to its transmission rate when data is being transmitted.

$\bar{\mathcal{E}}$  is given by

$$\bar{\mathcal{E}} \triangleq E \left( \frac{P_M[n]}{R_M[n]} \middle| P_M[n] > 0 \right) = E \left( \frac{1}{L_{MH}} \right) \cdot \frac{\bar{P}_C}{\bar{R}}. \quad (3.62)$$

The last measure is the MS average suspension delay  $\bar{D}$ , which is defined as the expected duration of a suspension period. It is in fact the average fade duration defined as [75, p.189]

$$\bar{D}(r = \sqrt{X_0}) \triangleq \frac{\Pr(r \leq \sqrt{X_0})}{lcr(r = \sqrt{X_0})}, \quad (3.63)$$

where  $r \triangleq \sqrt{S_{MH}(t)}$  and  $lcr(r = \sqrt{X_0})$  is the level-crossing rate at a given strength level  $\sqrt{X_0}$ .

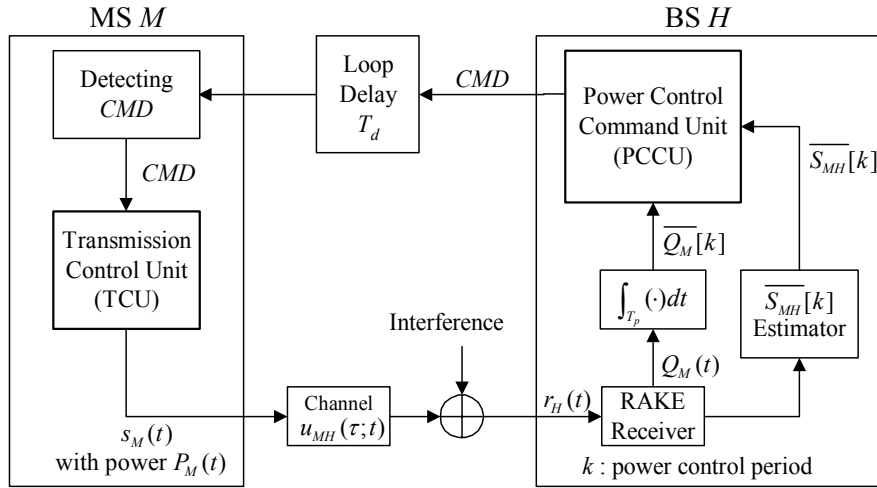


Figure 3.1: Functional blocks of the realistic TCPC scheme

Envelope  $r$  follows a Nakagami distribution since the overall short-term fading  $S_{MH}(t)$  follows a gamma distribution. Consequently, as in [76],  $lcr(\cdot)$  and  $\bar{D}(\cdot)$  are

$$lcr(r = \sqrt{X_0}) = f_m \cdot f_{\gamma(K,K)}(X_0) \sqrt{\frac{2\pi X_0}{K}}, \quad (3.64)$$

and

$$\bar{D}(r = \sqrt{X_0}) = \frac{F_{\gamma(K,K)}(X_0)}{f_m \cdot f_{\gamma(K,K)}(X_0)} \sqrt{\frac{K}{2\pi X_0}}, \quad (3.65)$$

where  $f_m$  is the maximal Doppler frequency.

### 3.3.2 Realistic TCPC

Considering that MS transmission power is adjusted discretely according to finite-bit power control commands and factors of power control error (PCE) due to step size for power adaptation  $\Delta_p$ , power control command loop delay  $T_d$ , MS velocity  $V$ , and power control period  $T_p$ , the TCPC scheme is referred to as a realistic TCPC scheme.

Figure 3.1 presents the functional blocks of the realistic TCPC scheme. The transmitted signal  $s_M(t)$  with power  $P_M(t)$  from MS  $M$  will pass through the channel  $u_{MH}(\tau;t)$  and suffer

interference from other MS transmissions. The received signal  $r_H(t)$  at the BS  $H$  is then fed into the optimal RAKE receiver to extract the averaged signal power  $\overline{Q}_M[k]$  over the  $k$ th power control period

$$\overline{Q}_M[k] = \frac{1}{T_p} \int_{kT_p}^{(k+1)T_p} Q(t) dt, \quad (3.66)$$

and estimate the average short-term channel fading  $\overline{S}_{MH}[k]$

$$\overline{S}_{MH}[k] = \frac{1}{T_p} \int_{kT_p}^{(k+1)T_p} S_{MH}(t) dt, \quad (3.67)$$

The BS  $H$  has a power control command unit (PCCU) to generate the power control command,  $CMD$ , periodically;

$$CMD = \begin{cases} +1, & \text{if } \overline{Q}_M[k] < Q_0, \overline{S}_{MH}[k] \geq X_0, \\ -1, & \text{if } \overline{Q}_M[k] \geq Q_0, \overline{S}_{MH}[k] \geq X_0, \\ 'suspend', & \text{if } \overline{S}_{MH}[k] < X_0. \end{cases} \quad (3.68)$$

The  $CMD$  is then transmitted through downlink channel to the destination MS. The MS has a transmission control unit (TCU) which adjusts  $P_M(t)$  according to the received  $CMD$ . It suspends the transmission temporarily if the received  $CMD$  is 'suspend'; and adapts its transmission power by an amount of  $CMD \cdot \Delta_p$  dB, otherwise.

In the realistic TCPC scheme, the received power is no longer a time constant. Conditional with  $Q_M[n] > 0$ , the power control error (PCE) is defined as

$$\psi \triangleq \frac{Q_M[n]}{Q_0}. \quad (3.69)$$

Thus, the outage probability  $\Lambda_M$  turns out to be the average of (3.38) over all possible PCE values.

Using (3.31),  $\Lambda_M$  can be approximated by



$$\begin{aligned}
\Lambda_M &\approx \int_0^\infty (1 - F_\xi(\frac{1.5G \cdot Q_0 \cdot y - \Gamma_0 \cdot (N_M - 1) \cdot \bar{Q}}{\Gamma_0 \cdot \bar{P}_C \cdot \sqrt{N_M}} - \frac{N_M \cdot \mu_0}{\sqrt{N_M}}), 0, \sigma_0^2)) \cdot f_\psi(y) dy \\
&= \int_0^\infty \int_y^\infty f_\xi(x; \mu_1, \sigma_1^2) dx \cdot f_\psi(y) dy \\
&= \int_0^\infty f_\xi(x; \mu_1, \sigma_1^2) F_\psi(x) dx,
\end{aligned} \tag{3.70}$$

where  $f_\xi(x; \mu_1, \sigma_1^2) = dF_\xi(x; \mu_1, \sigma_1^2) / dx$  is the Gaussian pdf function and

$$\mu_1 = \frac{\Gamma_0 (N_M - 1) \cdot \bar{Q} + \Gamma_0 \bar{P}_C N_M \mu_0}{1.5G \cdot Q_0}, \tag{3.71}$$

$$\sigma_1^2 = \left( \frac{\Gamma_0 \bar{P}_C}{1.5G \cdot Q_0} \right)^2 \cdot N_M \sigma_0^2. \tag{3.72}$$

As shown in (3.70),  $\Lambda_M$  equals an arithmetic average of  $F_\psi(x)$  with weighting function of  $f_\xi(x; \mu_1, \sigma_1^2)$ . Since  $f_\xi(x; \mu_1, \sigma_1^2)$  is a bell-shape like curve with peak at  $x=\mu_1$ ,  $\Lambda_M$  can be accurately approximated by

$$\Lambda_M \approx \int_0^\infty f_\xi(x; \mu_1, 0) F_\psi(x) dx = F_\psi(\mu_1). \tag{3.73}$$

Based on the system capacity definition given in (3.44), the system capacity can then be approximated by

$$C \approx \left\lceil \frac{1.5 \cdot F_\psi^{-1}(\Lambda_0) \cdot G / \Gamma_0 + \bar{Q} / Q_0}{\bar{P}_C \mu_0 / Q_0 + \bar{Q} / Q_0} \right\rceil. \tag{3.74}$$

From (3.74), it is found that the factor  $G/\Gamma_0$  is usually a number larger than other factors, thereby the PCE  $\psi$  plays an important role in affecting the system capacity  $C$ . The higher the dispersion degree of PCE is, the lower the factor  $F_\psi^{-1}(\Lambda_0)$  and the system capacity will be. Note that, merely the factor  $F_\psi^{-1}(\Lambda_0)$  is enough to estimate the system capacity, and the knowledge of the whole distribution of PCE  $\psi$  is not necessary. On the other hand, the factor  $\mu_0$  has nothing to do with closed-loop power control and is the same as that given in (3.32). The  $\bar{P}_C$  and  $\bar{Q}$  in the

realistic TCPC scheme depend on several factors including cutoff threshold  $X_0$ , step size  $\Delta_p$ , power control loop delay  $T_d$ , number  $K$  of resolvable paths, and MS velocity  $V$ . Hence, it is difficult to derive general formulae for  $\overline{P_C}$  and  $\overline{Q}$ . The simulation shows that the  $\overline{P_C}$  and  $\overline{Q}$  in the realistic TCPC scheme can be adequately approximated by the analytical results given in (3.40) and (3.43), respectively. Based on the above approximations and by assuming that the factor  $F_\psi^{-1}(\Lambda_0)$  is obtainable, the system capacity can be calculated.

Additionally, we assume that the average short-term channel fading  $\overline{S_{MH}[k]}$  is still Rayleigh distributed. Therefore, the performance measures  $\overline{R}$ ,  $\overline{E}$ , and  $\overline{D}$  have the same formulae given in (3.57), (3.62), and (3.65), respectively. Finally,  $\overline{\mathfrak{R}}$  is computed according to its definition. Notably, as  $X_0=0$ , the realistic TCPC becomes a realistic perfect power control and the above analyses remain applicable.

The realistic TCPC has an issue with how the transmitter can understand when  $\overline{S_{MH}[k]}$  turns out to be good after a bad period. Using the real TCPC applied to a WCDMA system [77] as an example. The WCDMA system has two types of uplink dedicated physical channels (DPCHs): the uplink dedicated physical data channel (DPDCH) and the uplink dedicated physical control channel (DPCCH). Each connection is allocated a DPCH including one DPCCH and several DPDCHs. The DPDCH is used to send user data, and its transmission is suspended when the received CMD is 'suspend'. The DPCCH is used to carry control information, including pilot symbols, power control command for downlink power control, and rate information of current uplink transmission, required by the BS; and the DPCCH is basically always on even when the DPDCH is suspended. Thus, whenever the transmission of DPDCH is suspended, the receiver can somehow monitor the DPCCH channel condition and generate the power control command according to (3.68).

Another issue is related to the MS velocity. By (3.65), for a mobile speed lower than 320

km/hr, the average fade duration can be found greater than or equal to one power control period, and the TCPC scheme is still workable. As the mobile speed increases, the appearance probability of 'suspend' command decreases and the TCPC scheme degrades toward the conventional closed-loop power control scheme.

### 3.4 Numerical Results

In the following examples, the DS/CDMA system has  $N_B=19$  cells; the propagation exponent  $\eta=3.5$ ; the shadowing effect  $\sigma_x=8$ ; the resolvable path number  $K=2$ ; the processing gain  $G=128$ ; the outage threshold  $\Lambda_0=1\%$ , and  $\Gamma_0=7$  dB to yield  $\text{BER} = 10^{-3}$  [3]. The Rayleigh fading random processes are generated according to Jake's model. Also, MS velocity = 80 km/hr; the step size of power adaptation  $\Delta_p=1$  dB; the power control period  $T_p=2/3$  ms; and the loop delay  $T_d=1 \cdot T_p$  are assumed for a realistic case. The antenna heights used with MS and BS are simply set to 0.003 and 0.01 times the BS radius, respectively, to prevent the occurrence of 'zero-distance' between an MS and a BS. The following figures show the numerical results of the performance of the ideal and realistic TCPC schemes, together with perfect power control [13], [14], combined power/rate control [15], and truncated average power control (TAPC) [16]. Simulation results are also provided to validate the theoretical analysis of the TCPC scheme. Notably, the performance of the perfect power control scheme is directly obtained from TCPC by setting  $X_0=0$ ; the cutoff thresholds for TAPC are applied such that the corresponding truncation probabilities are 10%.

For each scenario, the  $\{L_{mb}\}$  is randomly generated according to the channel model and the MS locations are uniformly distributed.  $I_O^* = I_O / \overline{P_C}$  can thus be calculated according to (3.27). Since TCPC is a type of strength-based power control, the distributions of  $Q_M[n]$  and PCE  $\psi$ , the average received power  $\overline{Q}$ , and the average MS transmission power  $\overline{P_C}$  are obtained by a

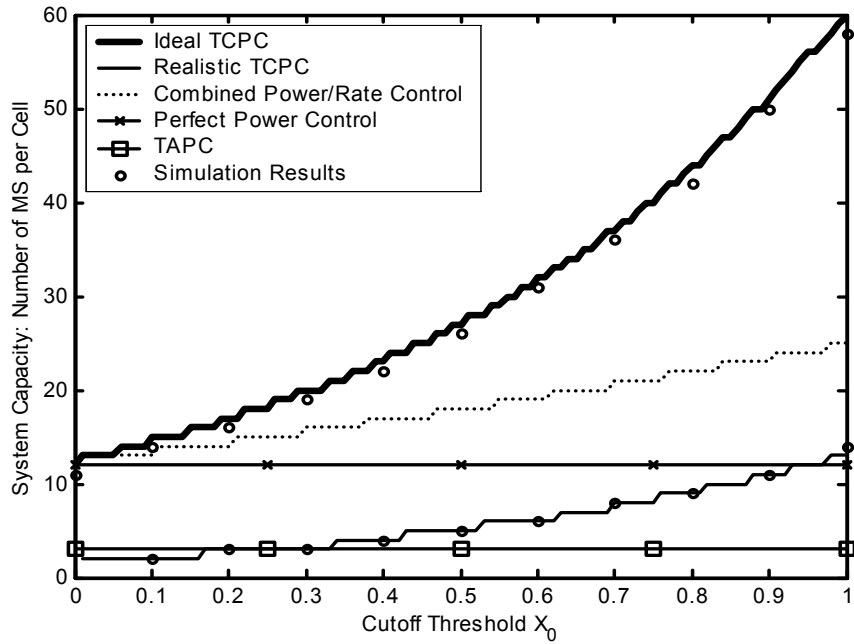


Figure 3.2: System capacity  $C$  versus cutoff threshold  $X_0$

bit-level single link simulation with 10,000 power control cycles. Based on the above factors, the outage probability can then be calculated. For each  $N_{M_s}$ , the overall outage probability is obtained by averaging the outage probability over 10,000 scenarios. Equivalently, the effect of MS movement on the outage probability is taken into account by considering many scenarios. The system capacity is then obtained. The other performance measures including  $\bar{R}$ ,  $\bar{E}$ , and  $\bar{D}$  are also obtained by a bit-level single link simulation. Finally,  $\bar{\mathcal{R}}$  is calculated.

Figure 3.2 plots the system capacity  $C$  versus the cutoff threshold  $X_0$ . It can be seen that the differences between analytical results and simulation results are small; this indicates that the theoretical analyses of the ideal and realistic TCPC schemes are quite accurate. Besides, it can be found that the ideal TCPC achieves the greatest system capacity over all the cutoff thresholds. This is mainly because TCPC suspends transmission as soon as the channel becomes bad, effectively reducing mutual interference. As  $X_0$  increases, the system capacity of the TCPC scheme rises at the cost of average transmission rate reduction and longer suspension delay, shown subsequently. TAPC has a low capacity because it suffers the short-term fading although it

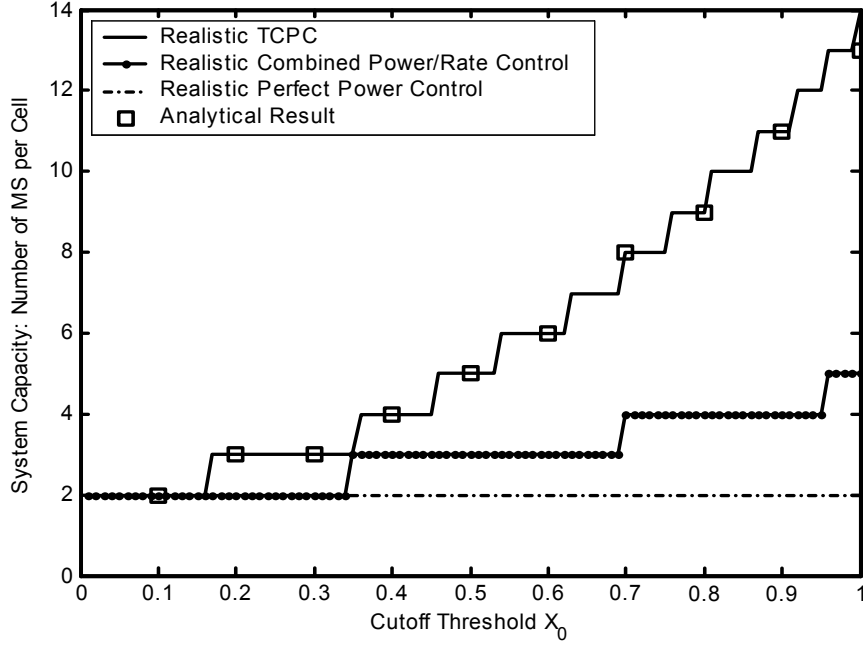


Figure 3.3: System capacity  $C$  of various realistic power control schemes versus cutoff threshold  $X_0$

employs a transmission suspension mechanism to reduce mutual interference. Considering the case of  $X_0=0.7$  for instance; the ideal TCPC can accommodate 37 MSs, while the combined power/rate control, the perfect power control, and the TAPC at the truncation probability of 10% can only accept 20, 12, and 3 MSs, respectively. Also, the realistic TCPC scheme yields a system capacity by 78~83% lower than that of the ideal TCPC scheme. This reveals that the PCE indeed has a great impact on the system capacity of the TCPC scheme.

Figure 3.3 further plots the system capacity  $C$  of various realistic power control schemes versus the cutoff threshold  $X_0$ . These simulation results show that the system capacity of each realistic power control scheme is tremendously reduced by the PCE, as compared with the results of the ideal power control schemes shown in Fig. 3.2. Also, the TCPC attains the greatest system capacity again in the realistic situations.

Figure 3.4 plots the average system transmission rate  $\bar{\mathfrak{R}}$  versus  $X_0$ , where  $\bar{\mathfrak{R}}$  is normalized by the default rate  $R_0$ . The ideal TCPC scheme is found to have the highest  $\bar{\mathfrak{R}}$  value.

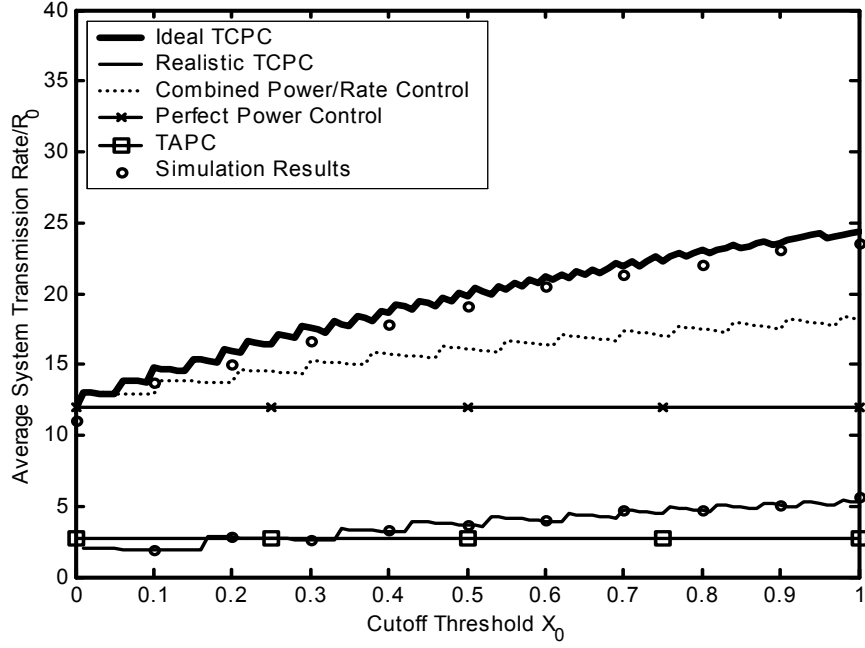


Figure 3.4: Average system transmission rate  $\bar{\mathfrak{R}}$  versus cutoff threshold  $X_0$

In the example with  $X_0=0.7$ , the ideal TCPC  $\bar{\mathfrak{R}}$  is 133% of that of the combined power/rate control scheme, 183% of that of the perfect power control scheme, and 815% of the TAPC scheme at the truncation probability of 10%. A larger  $X_0$  results in a higher  $\bar{\mathfrak{R}}$ . Notably,  $\bar{\mathfrak{R}}$  is a zigzag increasing function of  $X_0$ , not directly proportional to  $X_0$ . The stepwise constant capacity and the declining MS average transmission rate cause the zigzag curves of the TCPC and combined power/rate control schemes in the figure.

Figure 3.5 shows the MS average transmission rate  $\bar{R}$  versus  $X_0$ , where  $\bar{R}$  is also normalized by  $R_0$ . Of these power control schemes, TCPC has the lowest  $\bar{R}$  due to the transmission suspension, while TAPC  $\bar{R}/R_0$  is 0.9 since its suspension probability is considered to be 10%. The low  $\bar{R}$  value of the TCPC scheme is a side effect. However, TCPC maintains the greatest average system transmission rate as shown in Fig. 3.4. The side effect can be mitigated either by increasing the default rate  $R_0$  or assigning more than one code channel to an MS. Notably, the analytical curve of the realistic TCPC scheme coincides with that of the ideal TCPC

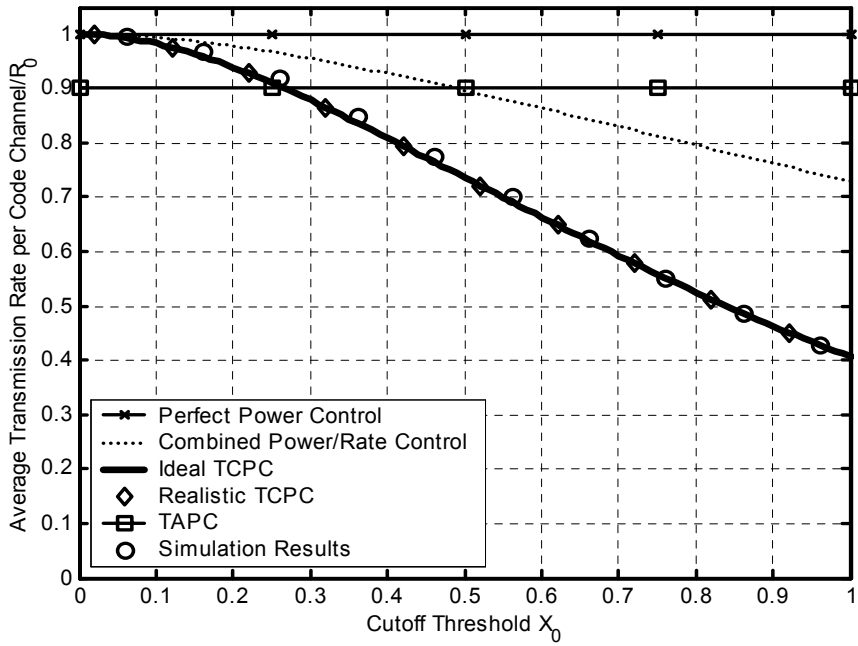


Figure 3.5: MS average transmission rate  $\bar{R}$  versus cutoff threshold  $X_0$

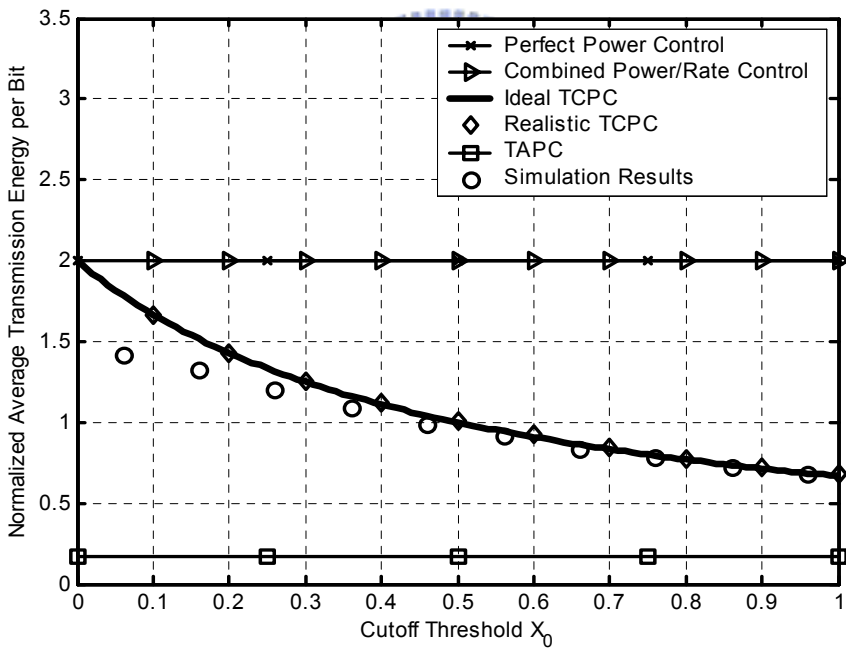


Figure 3.6: MS average transmission energy per bit  $\bar{E}$  versus cutoff threshold  $X_0$

scheme due to the assumption made in Section 3.3.2.

Figure 3.6 shows the MS average transmission energy per bit  $\bar{E}$  versus  $X_0$ , where  $\bar{E}$  is normalized by that of the perfect average power control scheme. It can be found that TAPC saves

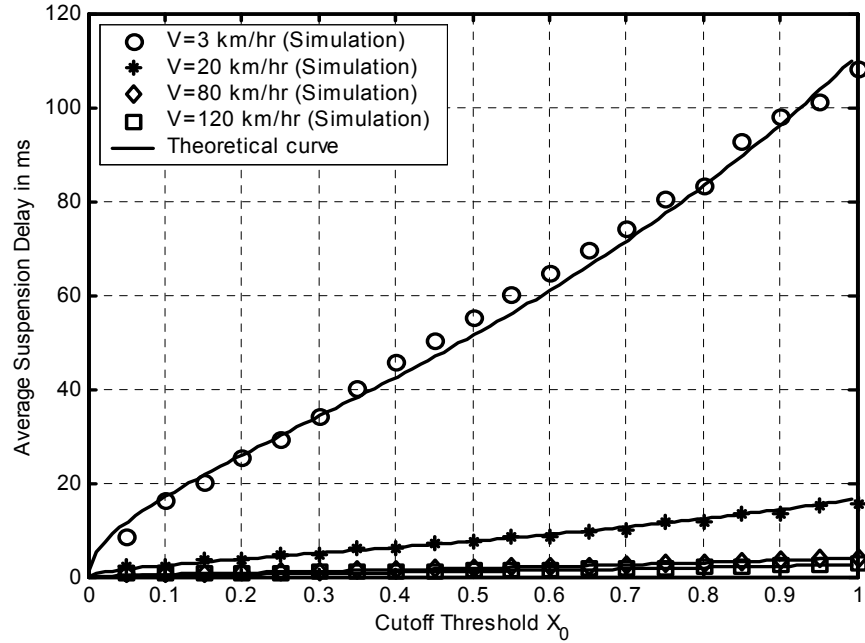


Figure 3.7: MS average suspension delay  $\bar{D}$  versus cutoff threshold  $X_0$

the power most, followed by TCPC. The reason is intuitive: both schemes apply the transmission suspension strategy. MS power consumption under perfect power control is highest since the MS uses high power to compensate for deep fading. One extreme case is  $K=1$ : the  $\bar{E}$  of the perfect power control scheme is theoretically infinite, which can be obtained by letting  $X_0 \rightarrow 0$  in (3.40), causing infinite interference and zero capacity. Also, the higher the  $X_0$  is, the more power the TCPC scheme can save. For  $X_0 \geq 0.4$ , it can be seen that the simulation results can be well approximated by the analytical results, which supports the using (3.62) as the analytical formula of  $\bar{E}$  for the realistic TCPC scheme in Section 3.3.2.

Figure 3.7 shows the MS average suspension delay  $\bar{D}$  of the realistic TCPC scheme versus  $X_0$  for  $V=\{3, 20, 80, 120\}$  km/hr. A larger  $X_0$  induces a longer suspension delay, which is undesired for real-time service. Such a suspension delay is another side effect of the TCPC scheme. However, once the delay requirement is stated, the upper limit of  $X_0$  for the best performance can be obtained. As shown in the figure,  $X_0$  should be less than 0.75 to guarantee



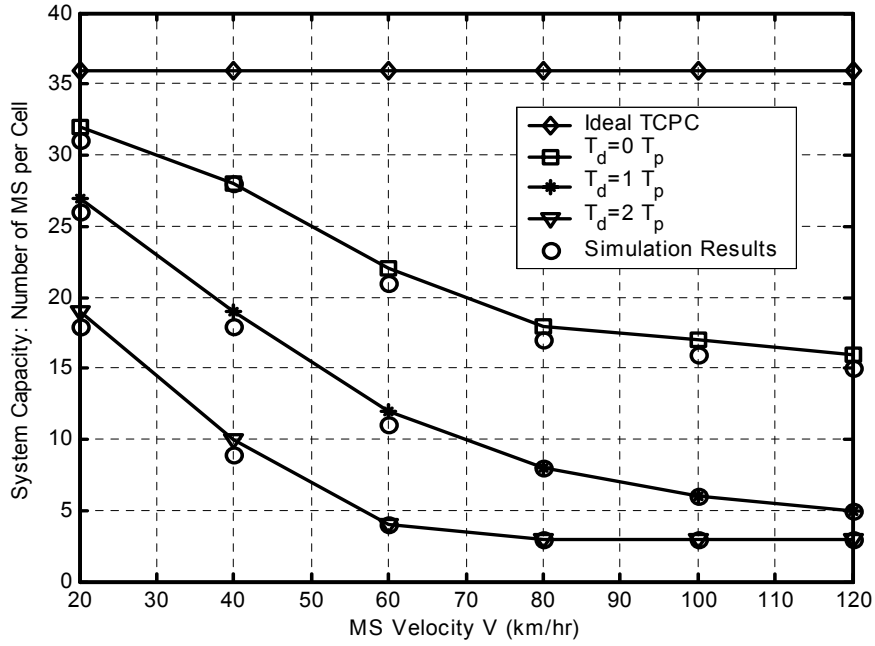


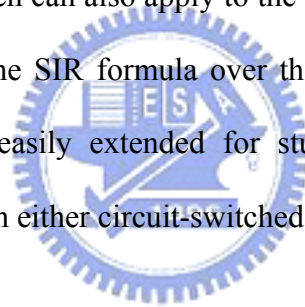
Figure 3.8: System capacity versus MS velocity for power control delay

that the suspension delay is less than 80 ms as the velocity is greater than 3 km/hr. The TAPC suspension delay would be much longer than that of the TCPC scheme, since the variation of long-term fading is much slower than that of short-term fading [74].

Figure 3.8 plots the system capacity of the realistic TCPC scheme versus the MS velocity  $V$  at cutoff threshold  $X_0=0.7$  and step size  $\Delta_p=1\text{dB}$  for power control delay  $T_d=0, 1 \cdot T_p, 2 \cdot T_p$ . It is found that the factor of MS velocity greatly affects system performance. For the case of  $T_d=1 \cdot T_p$ , the system capacity is 27 for  $V=20\text{km/hr}$ , which is 75% of the system capacity in ideal case. The capacity drops rapidly and becomes only 5 for  $V=120\text{km/hr}$ . The performance degradation is even worse for  $T_d=2 \cdot T_p$ . Though the case of  $T_d=0$  is practically impossible, its corresponding performance curve serves as an upper bound for the realistic TCPC scheme. The space between the performance curves for  $T_d=0$  and  $T_d=1 \cdot T_p$  means the performance gain that a power control scheme equipped with channel gain predictor to compensate the effect of power control command loop delay could have.

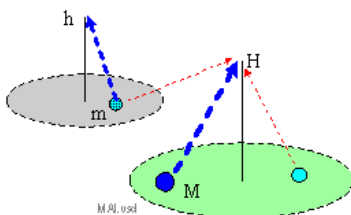
### 3.5 Concluding Remarks

The chapter analyzes the system performance of a truncated closed-loop power control (TCPC) scheme for uplinks in DS/CDMA cellular systems over frequency-selective fading channels. Based on the SIR formula over a medium-term period, closed-form formulae for five performance measures are successfully obtained, including system capacity, average system transmission rate, MS average transmission rate, MS average transmission energy per bit, and MS average suspension delay. This TCPC scheme is further analyzed under realistic conditions of power control error due to power control command loop delay, step size for power adaptation, and MS velocity. Simulation results are also provided to validate the theoretical analysis. Results show that the analysis is accurate and the TCPC scheme can greatly improve the system performance. The analytical approach can also apply to the conventional perfect power control by setting  $X_0=0$ . Notably, based on the SIR formula over the medium-term period, the analytical method presented herein can be easily extended for study of other type of strength-based closed-loop power control scheme in either circuit-switched or packet-switched CDMA systems.



### 3.6 Notation List

Notation	Description
$M$	Index of the target MS
$H$	Index of the BS that is the home BS of target MS $M$
$m$	Index of an arbitrary <u>m</u> obile station
$h$	Index of the BS that is the home BS of MS $m$
$b$	Index of an arbitrary BS $b$



Notation	Description
$c_m(t)$	PN spreading signal for MS $m$
$C$	System capacity defined in (3.44)
$C^*$	Refer to (3.45)
$CMD$	Power control command
$d_m(t)$	Data stream of MS $m$
$\bar{D}$	MS average suspension delay defined in (3.63)
$E(\cdot)$	Expectation function
$\bar{E}$	MS average transmission energy per bit defined in (3.62)

Notation	Description
$f_m$	Maximal Doppler frequency
$f_S(\cdot)$	Probability density function of $S_{mb}(t)$
$f_{S_p}(\cdot)$	Probability density function of $S_{mb,p}(t)$
$f_{\mathbf{z}_m}(\mathbf{z})$	Probability density function of $\mathbf{z}_m$ at location $\mathbf{z}$
$f_{\gamma(p_1,p_2)}(\cdot)$	Pdf of a two-parameter gamma random variable $\gamma$ with parameters $p_1$ and $p_2$
$F_{\gamma(p_1,p_2)}(\cdot)$	Cdf of a two-parameter gamma random variable $\gamma$ with parameters $p_1$ and $p_2$
$F_{\xi}(\cdot, \mu_o, \sigma_o^2)$	Cdf function of the Gaussian variable $\xi$ with mean $\mu_o$ and variance $\sigma_o^2$
$F_{\psi}(\cdot)$	Cdf of power control error $\psi$
$G$	Processing gain. $G \triangleq T/T_c$
$I_A[n]$	Multiple access and multipath interference (MAI) portion of $Z_M[n]$
$I_S[n]$	Multipath interference portion of $Z_M[n]$
$I_h$	$I_h \triangleq \left( \frac{L_{mH}}{L_{mh}} \mid L_{mb} \leq L_{mh}, \forall b \right)$
$I_t$	Mean power of the intra-cell interference signal that interferes the target uplink ( $M,H$ )
$I_o$	Mean power of the other-cell interference signal that interferes the target uplink ( $M,H$ )
$I_o^*$	Normalized $I_o$ , $I_o^* \triangleq I_o / \overline{P_c}$
$K$	Number of resolvable paths in each uplink channel
$k$	Index of power control period

Notation	Description
$lcr(r = \sqrt{X_0})$	Level-crossing rate at a given strength level $\sqrt{X_0}$
$L_{mb}(t)$	Long-term fading of the uplink ( $m,b$ ) at time $t$
$L_{mb}$	Long-term fading of the uplink ( $m,b$ ) which is approximately a constant during a medium-term period
$L_{MH}$	Long-term fading of the target uplink ( $M,H$ ) which is approximately a constant during a medium-term period
$\{L_{mb}, \forall(m,b)\}$	Scenario = $\{L_{mb} \mid \forall m,b\}$
$MS^{(h)}$	Set of the MSs that are served by BS $h$
$n$	Index of data symbol period
$N_B$	<u>N</u> umber of <u>b</u> ase stations in the cellular system. I.e. cell number
$N_M$	<u>N</u> umber of <u>m</u> obile stations in each cell of the cellular system
$p$	Index of resolvable path on an uplink
$P_m(t)$	Transmission power of MS $m$ at time $t$
$P_m[n]$	Transmission power of MS $m$ during $n$ th data symbol period
$P_M[n]$	Transmission power of target MS $M$ during $n$ th data symbol period
$P_{O,m}(t)$	A portion of the transmission power of MS $m$ at time $t$ , which is controlled by <u>o</u> pen-loop power control
$P_{O,m}[n]$	A portion of the transmission power of MS $m$ at $n$ th data symbol period, which is controlled by <u>o</u> pen-loop power control

Notation	Description
$P_{O,M}[n]$	A portion of the transmission power of target MS $M$ at $n$ th data symbol period, which is controlled by <u>o</u> pen-loop power control
$P_{C,m}(t)$	A portion of the transmission power of MS $m$ at time $t$ , which is controlled by <u>c</u> losed-loop power control
$P_{C,m}[n]$	A portion of the transmission power of MS $m$ at $n$ th data symbol period, which is controlled by <u>c</u> losed-loop power control
$P_{C,M}[n]$	A portion of the transmission power of target MS $M$ at $n$ th data symbol period, which is controlled by <u>c</u> losed-loop power control
$\overline{P_C}$	$= E(P_{C,m}[n])$
$Q_0$	Desired received power level
$Q_M[n]$	Received signal power at the $n$ th data symbol period of MS $M$
$\overline{Q}$	$= E(Q_M[n])$
	For TCPC scheme, $\overline{Q}$ is obtained by (3.43)
$\overline{Q_M}[k]$	Estimated average signal power at the $k$ th power control period of target MS $M$ in a realistic TCPC scheme
$r$	Envelope of $\sqrt{S_{MH}(t)}$ $r \triangleq \sqrt{S_{MH}(t)}$
$r_H(t)$	The total signal received at a specific BS $H$
$r_M[n]$	Desired signal portion of $Z_M[n]$
$R_0$	Data symbol <u>r</u> ate, $R_0 = 1/T$
$\overline{R}$	MS average transmission rate

Notation	Description
	defined in (3.57)
$\overline{\mathfrak{R}}$	Average system transmission rate defined in (3.58)
$s_m(t)$	Transmitted low-pass equivalent signal of MS $m$
$S(t)$	<u>S</u> hort-term fading at time $t$
$S_{mb,p}(t)$	Short-term fading of the $p$ th resolvable path of the uplink $(m,b)$ at time $t$
$S_{mb,p}[n]$	Short-term fading of the $p$ th resolvable path of the uplink $(m,b)$ during $n$ th data symbol period
$S_{mb}(t)$	Short-term fading of the uplink $(m,b)$ at time $t$ . $S_{mb}(t) \triangleq \sum_{p=1}^K S_{mb,p}(t)$
$S_{mb}[n]$	Short-term fading of the uplink $(m,b)$ during $n$ th data symbol period. $S_{mb}[n] \triangleq \sum_{p=1}^K S_{mb,p}[n]$
$S_{MH}[n]$	Short-term fading of the target uplink $(M,H)$ during $n$ th data symbol period.
$\overline{S_{MH}}[k]$	Estimated average short-term fading at the $k$ th power control period on the target uplink $(M,H)$ in a realistic TCPC scheme
$T$	Data symbol duration
$T_c$	Chip duration
$T_d$	Power control command loop delay
$T_p$	Power control period
uplink $(m,b)$	Uplink channel from an MS $m$ to a BS $b$
$u_{mb}(\tau;t)$	Time-variant impulse response of uplink $(m,b)$
$V$	MS velocity
$\text{var}(\cdot)$	Variance function

Notation	Description
$x_{mb}(t)$	A zero-mean Gaussian random process corresponding to the shadowing effect
$\mathbf{x}_b(t)$	A complex number that represents the location of BS $b$
$X_0$	Preset <b>cut</b> off threshold in TCPC scheme
$\mathbf{z}_m$	A complex number that represents the location of MS $m$
$Z_M[n]$	Decision statistics corresponding to an MS $M$ at $n$ th data symbol period

Notation	Description
$\xi$	A Gaussian random variable for approximating $I_O^*$
$\eta$	Propagation exponent
$\psi$	Power control error $\psi = Q_M[k]/Q_0$
$\mu_{S_p}$	$\mu_{S_p} = E(S_{mb,p})$
$\mu_1$	Quantity given by (3.71)
$\mu_O$	Mean of $I_O^*$ when $N_M = 1$
$\sigma_O^2$	Quantity given by (3.72)
$\sigma_1^2$	Variance of $I_O^*$ when $N_M = 1$
$\sigma_x$	Standard deviation of $x_{mb}(t)$
$\Lambda_M$	Outage probability of the target uplink ( $M,H$ ) defined in (3.38)

Notation	Description
$\Lambda_0$	Preset outage threshold
$\Gamma_0$	Minimum SIR per bit required to achieve a desired bit error rate
$\Gamma_M[n]$	SIR per bit during the $n$ th data symbol period of target MS $M$ at the output of RAKE receiver
$\Delta_p$	Step size for power adaptation
$\tau_m$	Transmission timing of MS $m$ due to asynchronous transmission among the MSs
$\phi_m$	Random carrier phase
$\delta(\tau)$	Impulse
$\varphi(s)$	Defined in (3.37)
$\alpha_{mb,p}(t)$	Power gain of the $p$ th resolvable path of the uplink ( $m,b$ ) at time $t$
$\theta_{mb,p}(t)$	Phase of the $p$ th resolvable path of the uplink ( $m,b$ ) at time $t$
$\theta_{mb,p}[n]$	Phase of the $p$ th resolvable path of the uplink ( $m,b$ ) during $n$ th data symbol period
$\kappa_a$	Quantity given in (3.47)
$\kappa_b$	Quantity given in (3.47)
$\kappa_c$	Quantity given in (3.47)

## Chapter 4

# An Accurate Method for Approximating the Interference Statistics of DS/CDMA Cellular Systems with Power Control over Frequency-Selective Fading Channels

---

*Abstract— This chapter proposes an approximation method by characteristic function (AM-CF) method to approximate the distribution of interference in DS/CDMA cellular systems. This method considers the effects of frequency-selective multipath fading; it also assumes perfect power control and a rectangular/sinc chip waveform. The AM-CF method can yield results that fit the Monte Carlo simulation results more accurately than the conventional standard Gaussian approximation method.*

## 4.1 Introduction

Interference statistics of a DS/CDMA (direct-sequence/code-division multiple-access) system are essential to the understanding of the system's dynamics. Approximating interference statistics has received a lot of attention. In the literature, the most widely used method is the SGA (standard Gaussian approximation) method. Although the SGA is easy to use and applicable to a complicated circumstance, e.g. the cellular system over the frequency-selective fading channel in [17], it is known that the SGA is not very accurate [18, p.1055]. In order to improve accuracy, many other methods have been proposed, such as the improved Gaussian approximation (IGA) method [18], the simplified IGA method [19], and the characteristic function method [20]. These methods have better accuracy, however they are only applicable to the limited circumstance of a single cell system over the AWGN channel. Therefore, an approximation method that has better accuracy and can be applied to a complicated circumstance is still desirable. This chapter proposes an approximation method by characteristic function (AM-CF) to approximate the distribution of MAI (multiple access interference) signals in DS/CDMA cellular systems. The method considers the effects of a frequency-selective multipath fading channel; it also assumes perfect power control and a rectangular/sinc chip waveform. Using this method, the distribution of the MAI signals is more accurately approximated.

## 4.2 System Model

The system under consideration is a DS/CDMA cellular system with  $N_B$  base stations (BSs) and  $N_M$  mobile stations (MSs) per cell, and with frequency-selective, slowly fading multipath channels. The power gain of each resolvable path  $p$  on an uplink from an arbitrary MS  $m$  to an arbitrary BS  $b$  is statistically divided into long-term fading  $L_{mb}$  and short-term fading  $S_{mb,p}$ ,

wherein  $m \in \{1, 2, \dots, N_B \cdot N_M\}$  denotes the MS index,  $b \in \{1, 2, \dots, N_B\}$  denotes the BS index, and  $p \in \{1, 2, \dots, K\}$  denotes the resolvable path index with  $K$  being the number of resolvable paths on an uplink. For simplicity,  $\{S_{mb,p}, \forall(m, b, p)\}$  are assumed to be Rayleigh fading that have an independently and identically distributed (iid) exponential pdf with mean  $1/K$  and variance  $1/K^2$ , i.e.

$$\begin{cases} E(S_{mb,p}) = \frac{1}{K}, \\ \text{var}(S_{mb,p}) = \frac{1}{K^2}, \end{cases} \quad \forall(m, b, p). \quad (4.1)$$

It is also assumed that binary phase-shift keying modulation and optimal RAKE receivers are employed. For a specific MS  $M$  communicating with its home BS  $H$ , the decision statistics  $Z_M[n]$  at the  $n$ -th data symbol (the symbol duration is  $T$ ), normalized with respect to  $T \cdot \sqrt{S_{MH}[n]}$ , is obtained in four parts [78] by

$$Z_M[n] = r_M[n] + I_A[n] + I_S[n] + z[n], \quad (4.2)$$

where  $S_{MH}[n] \triangleq \sum_{p=1}^K S_{MH,p}[n]$  is a unit-mean gamma random variable (RV) with variance  $1/K$ ,  $r_M[n]$  denotes the desired signal,  $I_A[n]$  represents the MAI interference consisting of the intra-cell interference and other-cell interference,  $I_S[n]$  is the multipath interference, and  $z[n]$  is the noise. Notably,  $I_S[n]$  and  $z[n]$  are usually negligible as compared to  $I_A[n]$  and will be ignored hereafter [17].

We consider a medium-term period over which the short-term fading varies while the long-term fading is constant. And the perfect strength-based power control is further assumed to be such that the transmission power of any one MS  $m$ ,  $1 \leq m \leq N_B \cdot N_M$ , is  $P_m[n] = Q_0 / (L_{mh} \cdot S_{mh}[n])$ , where  $h$  is the index of the BS communicating with MS  $m$ ,  $Q_0$  is the



common desired received power level in the system. The term  $r_M[n]$  is given by

$$\begin{aligned} r_M[n] &= d_M[n] \cdot \sqrt{P_M[n] \cdot L_{MH} \cdot S_{MH}[n]} \\ &= d_M[n] \cdot \sqrt{Q_0}, \end{aligned} \quad (4.3)$$

where  $d_M[n]$  represents the MS  $M$ 's data sequence that has values  $\{\pm 1\}$  with equal probability.

The term  $I_A[n]$  is obtained by

$$I[n] = \sum_{p=1}^K \sqrt{\frac{S_{MH,p}[n]}{S_{MH}[n]}} \sum_{m \neq M} \sum_{p'=1}^K \sqrt{P_m[n] \cdot L_{mH} \cdot S_{mH,p'}[n]} \cdot \alpha_{M,p}^{(m,p')}[n] \cdot \cos(\theta_{M,p}^{(m,p')}[n]), \quad (4.4)$$

where  $\alpha_{M,p}^{(m,p')}[n]$  and  $\theta_{M,p}^{(m,p')}[n]$  are RVs related to the spreading code cross-correlation and the phase difference of the signal paths, respectively. The term  $\alpha_{M,p}^{(m,p')}[n]$  is given by

$$\alpha_{M,p}^{(m,p')}[n] = \frac{1}{T} \int_{nT+(p+\tau_M)T_c}^{(n+1)T+(p+\tau_M)T_c} d_m(t - (p'+\tau_m)T_c) \cdot c_m(t - (p'+\tau_m)T_c) \cdot c_M(t - (p+\tau_M)T_c) dt, \quad (4.5)$$

where  $T_c$  is the chip duration,  $c_m(t)$  is MS  $m$ 's spreading signal, and  $\tau_m$  reflects the different timing due to asynchronous transmission and has a uniform distribution over  $[0,1)$ . For the case of random spreading codes with a rectangular chip waveform and an even processing gain  $G$ , it is known that  $E(\alpha_{M,p}^{(m,p')}[n]) = 0$  and  $\text{var}(\alpha_{M,p}^{(m,p')}[n]) = 2G/3$  [79]. On the other hand, the pdf of  $\alpha_{M,p}^{(m,p')}[n]$  equals to that of

$$\frac{\tau \sum_{i=1}^G d_m[i] \cdot c_m[i] \cdot c_M[i] + (1-\tau) \sum_{i=1}^G d_m[i] \cdot c_m[i] \cdot c_M[i+1]}{G}, \quad (4.6)$$

where  $\tau$  is a uniform RV over  $[0,1)$ , and  $c_m[i]$  is the random spreading code. It has the same pdf as that of a RV  $\alpha$  that is given by

$$\begin{aligned}\alpha &= \tau A + (1-\tau)B \\ &= B + \tau \cdot (A - B),\end{aligned}\tag{4.7}$$

where

$$\begin{cases} A = \frac{1}{G} \sum_{i=1}^G a_i, \\ B = \frac{1}{G} \sum_{i=1}^G b_i, \end{cases}\tag{4.8}$$

and  $\{a_i, b_i\}$  are iid RVs having values  $\{\pm 1\}$  with equal probability. It is not difficult to derive the probability functions of RVs  $A$  and  $B$  which are given by

$$\Pr(A = x) = \Pr(B = x) = f_b\left(\frac{(x+1)G}{2}; G\right), \quad x = -1, -1 + \frac{2}{G}, \dots, 1 - \frac{2}{G}, 1,\tag{4.9}$$

where



$$f_b(x; y) \triangleq \frac{C_x^y}{2^y},\tag{4.10}$$

denotes a binomial probability with binomial coefficient  $C_x^y$ . The cdf of RV  $\alpha$  is obtained by

$$\begin{aligned}\Pr(\alpha \leq x) &= \Pr(B + \tau \cdot (A - B) \leq x) \\ &= \sum_{j=-G/2}^{G/2} \Pr\left(\frac{2j}{G} + \tau \cdot (A - \frac{2j}{G}) \leq x\right) \Pr\left(B = \frac{2j}{G}\right) \\ &= \sum_{j=-G/2}^{G/2} \Pr\left(\tau \cdot (A - \frac{2j}{G}) \leq x - \frac{2j}{G}\right) \Pr\left(B = \frac{2j}{G}\right) \\ &= \sum_{j=-G/2}^{G/2} \sum_{k=-G/2}^{G/2} \Pr\left(\tau \cdot \left(\frac{2k}{G} - \frac{2j}{G}\right) \leq x - \frac{2j}{G}\right) \Pr\left(A = \frac{2k}{G}\right) \Pr\left(B = \frac{2j}{G}\right).\end{aligned}\tag{4.11}$$

For  $2(i-1)/G \leq x < 2i/G$ , the (4.11) becomes

$$\Pr(\alpha \leq x) \Big|_{\frac{2(i-1)}{G} \leq x < \frac{2i}{G}} = \sum_{j=-G/2}^{G/2} \sum_{k=-G/2}^{G/2} \Pr\left(\tau \cdot (k - j) \leq \frac{Gx}{2} - j\right) \Pr\left(A = \frac{2k}{G}\right) \Pr\left(B = \frac{2j}{G}\right)$$

$$\begin{aligned}
&= \sum_{j=-G/2}^{G/2} \sum_{k=-G/2}^{G/2} \Pr\left(\tau \cdot (k-j) \leq \frac{Gx}{2} - j\right) \Pr\left(A = \frac{2k}{G}\right) \Pr\left(B = \frac{2j}{G}\right) \\
&= \sum_{j=-G/2}^{i-1} \sum_{k=i}^{G/2} \Pr\left(\tau \leq \frac{Gx-2j}{2(k-j)}\right) \Pr\left(A = \frac{2k}{G}\right) \Pr\left(B = \frac{2j}{G}\right) \\
&\quad + \sum_{j=-G/2}^{i-1} \sum_{k=i}^{G/2} \Pr\left(A = \frac{2k}{G}\right) \Pr\left(B = \frac{2j}{G}\right) \\
&\quad + \sum_{j=i}^{G/2} \sum_{k=-G/2}^{i-1} \Pr\left(\tau \geq \frac{Gx-2j}{2(k-j)}\right) \Pr\left(A = \frac{2k}{G}\right) \Pr\left(B = \frac{2j}{G}\right) \\
&\quad + \sum_{j=i}^{G/2} \sum_{k=-G/2}^{i-1} \Pr\left(A = \frac{2k}{G}\right) \Pr\left(B = \frac{2j}{G}\right) \\
&= \sum_{j=-G/2}^{i-1} \sum_{k=i}^{G/2} \frac{Gx-2j}{2(k-j)} \Pr\left(A = \frac{2k}{G}\right) \Pr\left(B = \frac{2j}{G}\right) \\
&\quad + \sum_{j=-G/2}^{i-1} \sum_{k=i}^{G/2} \Pr\left(A = \frac{2k}{G}\right) \Pr\left(B = \frac{2j}{G}\right) \\
&\quad + \sum_{j=i}^{G/2} \sum_{k=-G/2}^{i-1} \left(1 - \frac{Gx-2j}{2(k-j)}\right) \Pr\left(A = \frac{2k}{G}\right) \Pr\left(B = \frac{2j}{G}\right) \\
&\quad + \sum_{j=i}^{G/2} \sum_{k=-G/2}^{i-1} \Pr\left(A = \frac{2k}{G}\right) \Pr\left(B = \frac{2j}{G}\right).
\end{aligned} \tag{4.12}$$

For  $2(i-1)/G < x < 2i/G$ , the corresponding pdf is given by

$$\begin{aligned}
f_\alpha(x) \Big|_{\frac{2(i-1)}{G} < x < \frac{2i}{G}} &= \frac{d \Pr(B + \tau \cdot (A - B) \leq x)}{dx} \Big|_{\frac{2(i-1)}{G} < x < \frac{2i}{G}} \\
&= \sum_{j=-G/2}^{i-1} \sum_{k=i}^{G/2} \frac{G}{2(k-j)} \Pr\left(A = \frac{2k}{G}\right) \Pr\left(B = \frac{2j}{G}\right) + \\
&\quad \sum_{j=i}^{G/2} \sum_{k=-G/2}^{i-1} \frac{-G}{2(k-j)} \Pr\left(A = \frac{2k}{G}\right) \Pr\left(B = \frac{2j}{G}\right) \\
&= \sum_{j=-G/2}^{i-1} \sum_{k=i}^{G/2} \frac{G \cdot f_b\left(k + \frac{G}{2}; G\right) f_b\left(j + \frac{G}{2}; G\right)}{2(k-j)} + \\
&\quad \sum_{j=i}^{G/2} \sum_{k=-G/2}^{i-1} \frac{G \cdot f_b\left(k + \frac{G}{2}; G\right) f_b\left(j + \frac{G}{2}; G\right)}{2(j-k)} \\
&= \sum_{j=-G/2}^{i-1} \sum_{k=i}^{G/2} \frac{G}{k-j} f_b\left(k + \frac{G}{2}; G\right) f_b\left(j + \frac{G}{2}; G\right).
\end{aligned} \tag{4.13}$$

Note, the cdf  $\Pr(\alpha \leq x)$  has discontinuous points at  $|x| = 2i/G, i = 0, 1, \dots, G/2$ . Therefore, the

corresponding pdf will have an impulse at these points. For  $|x|=2i/G, i=0,1,\dots,G/2$ , we have

$$\Pr\left(\tau\cdot\left(\frac{2k}{G}-\frac{2j}{G}\right)\leq x-\frac{2j}{G}\right)\Bigg|_{x=\frac{2i}{G}, i\in\mathbb{Z}} = \begin{cases} 1, & k=j=i, \\ \Pr\left(\tau\cdot\left(\frac{2k}{G}-\frac{2j}{G}\right)\leq \frac{2i}{G}-\frac{2j}{G}\right), & \text{otherwise.} \end{cases} \quad (4.14)$$

and

$$\lim_{x\rightarrow\left(\frac{2i}{G}\right)^-, i\in\mathbb{Z}} \Pr\left(\tau\cdot\left(\frac{2k}{G}-\frac{2j}{G}\right)\leq x-\frac{2j}{G}\right) = \begin{cases} 0, & k=j=i, \\ \Pr\left(\tau\cdot\left(\frac{2k}{G}-\frac{2j}{G}\right)\leq x-\frac{2j}{G}\right), & \text{otherwise.} \end{cases} \quad (4.15)$$

Based on (4.11), (4.14) and (4.15), the pdf  $f_\alpha(x)$  at  $|x|=2i/G, i=0,1,\dots,G/2$  is obtained by

$$\begin{aligned} f_\alpha(x)\Big|_{x=\frac{2i}{G}} &= \left( \Pr\left(\alpha \leq \frac{2i}{G}\right) - \lim_{x\rightarrow\left(\frac{2i}{G}\right)^-} \Pr(\alpha \leq x) \right) \cdot \delta(0) \\ &= \Pr\left(A \equiv \frac{2i}{G}\right) \Pr\left(B = \frac{2i}{G}\right) \cdot \delta(0) \\ &= f_b^2\left(i + \frac{G}{2}; G\right) \cdot \delta(0). \end{aligned} \quad (4.16)$$

From (4.13) and (4.16), the pdf  $f_\alpha(x)$  of  $\alpha_{M,p}^{(m,p)}[n]$  has a closed-form solution given by

$$f_\alpha(x) = \begin{cases} w_i \cdot \delta(0), & |x| = \frac{2i}{G}, \quad i \in \{0, 1, \dots, \frac{G}{2}\}, \\ v_i, & \frac{2(i-1)}{G} < |x| < \frac{2i}{G}, \quad i \in \{1, \dots, \frac{G}{2}\}, \end{cases} \quad (4.17)$$

where

$$w_i = f_b^2(n + G/2; G), \quad (4.18)$$

$$v_i = G \sum_{j=-G/2}^{i-1} \sum_{k=i}^{G/2} \frac{f_b(k + G/2; G) \cdot f_b(j + G/2; G)}{k - j}. \quad (4.19)$$

The term  $\theta_{M,p}^{(m,p)}[n]$  has a uniform distribution over  $[0,2\pi)$ , and therefore the  $\cos(\theta_{M,p}^{(m,p)}[n])$  is a zero-mean RV with variance 1/2, and its pdf, denoted by  $f_\varphi(x)$ , is given by

$$f_\varphi(x) = \frac{1}{\pi\sqrt{1-x^2}}, \quad |x| < 1. \quad (4.20)$$

### 4.3 The AM-CF Method

The distribution of the MAI signal in (4.4) is too complicated to be computed directly. We propose an AM-CF method to estimate the distribution of the MAI signal, which is composed of the intra-cell and other-cell interference signal. To help make things clearer, the time index  $k$  is neglected hereafter.

#### 4.3.1 Approximating the Statistics of the Intra-cell Interference

From (4.4), the intra-cell interference signal  $I_I$  is given by

$$I_I = \sum_{p=1}^K \sqrt{\frac{S_{MH,p}}{S_{MH}}} \sum_{m \in MS^{(H)}, m \neq M} \sum_{p'=1}^K \sqrt{\frac{Q_0 \cdot S_{mH,p'}}{S_{mH}}} \cdot \alpha_{M,p}^{(m,p')} \cdot \cos(\theta_{M,p}^{(m,p')}), \quad (4.21)$$

where  $MS^{(H)}$  denotes the index set of MSs communicating with BS  $H$ . Based on the statistics of  $\{\alpha_{M,p}^{(m,p')}\}$ ,  $\{\theta_{M,p}^{(m,p')}\}$ , and  $\{S_{mb,p}, \forall p, \forall (m,h) \neq (M,H)\}$ , the mean and variance of  $I_I$  can be obtained to be

$$\begin{cases} E(I_I) = 0, \\ \text{var}(I_I) = \frac{Q_0 \cdot (N_M - 1)}{3G}. \end{cases} \quad (4.22)$$

The terms within the summation in (4.21) are obviously not iid RVs, and it is very difficult to derive its pdf. The AM-CF method modifies the profile of  $\{S_{mb,p}, \forall (m,b,p)\}$  by removing

$\{S_{mb,p}, p = 2, \dots, K, \forall(m,b)\}$  and letting  $S_{mb,1} = \sum_{p=1}^K S_{mb,p}, \forall(m,b)$  and then treats terms within the summation in (4.21) as mutually independent RVs. By doing so, the overall characteristic function is obtained by simply multiplying the characteristic function of each term. As will be shown later, based on the AM-CF method, the pdf of  $I_I$  can be approximated without significant distortion by the pdf of  $I_I^*$  which is defined as

$$I_I^* \triangleq \sum_{i=1}^{N_M-1} \sqrt{Q_0} \cdot \alpha_i' \cdot \phi_i'. \quad (4.23)$$

The terms  $\{\alpha_i', \phi_i'\}$  are mutually independent RVs, and the pdfs of  $\alpha_i'$  and  $\phi_i'$  also have the forms given in (4.17) and (4.20), respectively. For the case of an even  $G$  and a rectangular chip waveform, the pdf of  $\chi_i' = \alpha_i' \cdot \phi_i'$  has a closed-form solution, denoted by  $f_{\chi'}(x)$ , given by

$$f_{\chi'}(x) = \int f_{\alpha'}(s) \cdot f_{\phi'}\left(\frac{x}{s}\right) \frac{1}{|s|} ds$$

$$= \begin{cases} w_0 \cdot \delta(x), & x = 0, \\ \frac{2v_i}{\pi} \log \frac{i + \sqrt{i^2 - G^2 \cdot x^2 / 4}}{G \cdot x / 2} + \sum_{j=i+1}^{G/2} \frac{2v_j}{\pi} \log \frac{j + \sqrt{j^2 - G^2 \cdot x^2 / 4}}{(j-1) + \sqrt{(j-1)^2 - G^2 \cdot x^2 / 4}} + \\ \sum_{j=i}^{G/2} \frac{w_j G}{\pi \sqrt{j^2 - (G \cdot x / 2)^2}}, & \frac{2(i-1)}{G} < |x| \leq \frac{2i}{G}, i \in \{1, 2, \dots, \frac{G}{2}\}. \end{cases} \quad (4.24)$$

The mean and variance of  $\chi_i'$  are zero and  $1/(3G)$ , respectively. Notably, the mean and variance of  $I_I^*$  are the same as the mean and variance of  $I_I$ , respectively. Since  $I_I^*$  is a sum of iid RVs, we have

$$F_{I_I^*}(\omega) = (F_{\chi'}(\sqrt{Q_0} \cdot \omega))^{N_M-1}, \quad (4.25)$$

where  $F_{\chi'}(\omega) = \mathcal{F}(f_{\chi'}(x))$  is the characteristic function of the pdf  $f_{\chi'}(x)$ , and  $\mathcal{F}(\cdot)$  represents the Fourier transform. Accordingly, the pdf of  $I_I^*$  is obtained by

$$f_{J_i^*}(x) = \mathcal{F}^{-1}(F_{J_i^*}(\omega)), \quad (4.26)$$

where  $\mathcal{F}^{-1}(\cdot)$  denotes the inverse Fourier transform.

### 4.3.2 Approximating the Statistics of the Other-cell Interference

From (4.4), the other-cell interference signal  $I_O$  is given by

$$I_O = \sum_{p=1}^K \sqrt{\frac{S_{MH,p}}{S_{MH}}} \cdot \sum_{h \neq H} \sum_{m \in MS^{(h)}} \sum_{p'=1}^K \sqrt{\frac{Q_0 \cdot L_{mH} \cdot S_{mH,p'}}{L_{mh} \cdot S_{mh}}} \cdot \alpha_{M,p}^{(m,p')} \cdot \cos(\theta_{M,p}^{(m,p')}). \quad (4.27)$$

The mean of  $I_O$  is zero and

$$\text{var}(I_O) = \sum_{h \neq H} \sum_{m \in MS^{(h)}} \frac{L_{mH}}{L_{mh}} \frac{K}{K-1} \frac{Q_0}{3G}. \quad (4.28)$$

By dividing the average other-cell interference power  $\text{var}(I_O)$ , from the  $N_B - 1$  cells, into  $N$  equal quantities, the AM-CF method estimates the pdf of  $I_O$  by the pdf of  $I_O^*$  which is defined

as

$$I_O^* \triangleq \sum_{i=1}^N \sqrt{Q_0 \cdot L'' \cdot \frac{S_{1,i}}{S_{2,i}}} \cdot \alpha_i'' \cdot \varphi_i''. \quad (4.29)$$

The parameter  $N$  is artificially introduced and  $L''$  is given by

$$L'' \triangleq \frac{1}{N} \sum_{h \neq H} \sum_{m \in MS^{(h)}} \frac{L_{mH}}{L_{mh}}, \quad (4.30)$$

so that the mean and variance of  $I_O^*$  equal to those of  $I_O$ . Once the  $N$  is chosen and assume  $\text{var}(I_O)$  is measurable, the term  $L''$  can be calculated according to its definition. By this way, the problem of measuring these quantities  $\{L_{mh}, L_{mH}\}$ , which is practically not easy to measure, is

bypassed. Another purpose of parameter  $N$  is to tune the distribution of  $I_O^*$ . The  $\{S_{1,i}, S_{2,i}\}$  are iid RVs with the same distributions as that of  $S_{MH}$ , and the pdf of  $\beta_i'' \triangleq \sqrt{S_{1,i}/S_{2,i}}$ , denoted by  $f_\beta(x)$ , is obtained by

$$f_\beta(x) = \int f_S(s \cdot x^2) \cdot f_S(s) \cdot 2s \cdot x \cdot ds = 2 \frac{\Gamma(2K) \cdot x^{2K-1}}{\Gamma^2(K) \cdot (1+x^2)^{2K}}, \quad (4.31)$$

where  $f_S(x)$  denotes the pdf of  $S_{MH}$ . The pdfs of  $\alpha_i''$  and  $\varphi_i''$  also have the form given by (4.17) and (4.20), respectively, and the pdf of  $\chi_i'' \triangleq \alpha_i'' \cdot \varphi_i''$  is the same as the  $f_\chi(x)$  given by (4.24). Consequently, the pdf of  $\psi_i = \beta_i'' \cdot \chi_i''$  has an identical pdf, denoted by  $f_\psi(x)$ , which is obtained by

$$f_\psi(x) = \int_{-1}^{+1} f_\chi(s) \cdot f_\beta(x \cdot s^{-1}) \cdot |s|^{-1} ds. \quad (4.32)$$

Since  $I_O^*$  is a sum of iid RVs,  $\sqrt{Q_0 \cdot L''} \cdot \psi_i$ , we have

$$F_{I_O^*}(\omega) = (F_\psi(\sqrt{Q_0 \cdot L''} \cdot \omega))^N, \quad (4.33)$$

where  $F_\psi(\omega)$  represents the characteristic function of the pdf  $f_\psi(x)$ .

### 4.3.3 Approximating the Statistics of MAI Interference

Since the intra-cell and other-cell interference signals are independent under a strength-based power control, the pdf of the MAI signal  $I$  can be approximated by

$$f_I(x) = \mathcal{F}^{-1}((F_\chi(\sqrt{Q_0} \cdot \omega))^{N_M-1} \cdot (F_\psi(\sqrt{Q_0 \cdot L''} \cdot \omega))^N). \quad (4.34)$$



Note that the BER is obtained by  $BER = \Pr(I < -\sqrt{Q_0})$ .

## 4.4 Results and Discussions

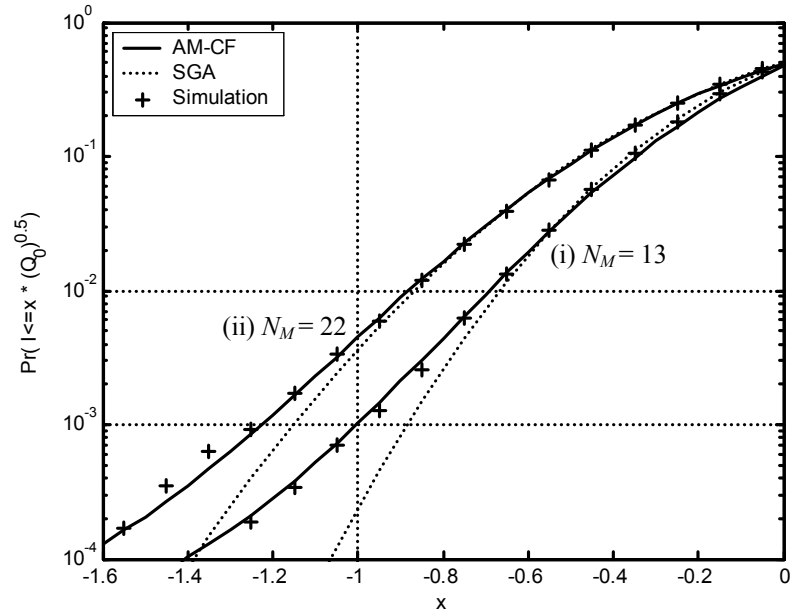
Figure 4.1(a) shows the cdf curves of MAI signals within the central cell using AM-CF and SGA methods, also the Monte Carlo simulation results based on (4.4), (4.5), and (4.20) with  $10^6$  samples are presented. The model of the long-term fading is the same as that in [78] with the propagation loss of 3.5 and the log-normal shadow fading standard deviation of 8dB; each MS chooses its serving BS based on measured pilot power [78]; and system parameters of  $(N_B, G, K)$  are chosen to be (19, 128, 2), respectively. The MS number  $N_M$  is 13 (22) and the parameter  $N$  is chosen as 20 (34) for case (i) (case (ii)) where the corresponding BER is around  $10^{-3}$  ( $5 \cdot 10^{-2}$ ). It is found that with proper  $N$ , AM-CF curves fit the simulation results better than SGA curves. For example, in case (i), BER based on the AM-CF method deviates from the simulation result by 4%, while BER based on the SGA method deviates by as high as 73%. The reason why the SGA does not work well is highly related to power control. Under a perfect strength-based power control, the MS's transmission power level might become pretty high due to a deep fade, which will induce a high other-cell interference power to others and therefore a shallow falloff of the pdf of  $I_o$ . In the proposed AM-CF method, as can be seen in (4.29),  $I_o^*$  contains the factor  $1/S_{2,i}$  which reflects the power control effect and thus the AM-CF can perform better than the SGA. Also notice that the AM-CF method seems not very sensitive to the value of parameter  $N$ .

Figure 4.1(b) shows results of the situation that is the same as those in Fig. 1(a) except that the chip waveform is changed to a sinc one. The MS number  $N_M$  is 45 (75) and the parameter  $N$  is chosen as 80 (130) for case (i) (case (ii)). For the situation of non-rectangular chip waveform, there is no closed-form for statistics of intra-cell and other-cell interferences. However, the Eqs. (4.23) and (4.29) in AM-CF method remain the same and the factor  $\alpha_{M,p}^{(m,p)}$  can be numerically

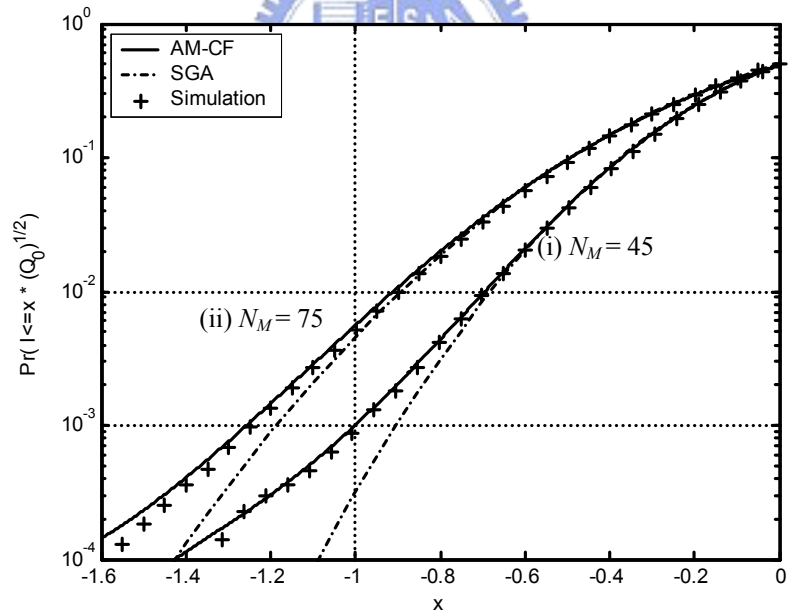
calculated according to (4.5). Results show that the AM-CF curves still fit the simulation results better than SGA curves. For example, in case (i), BER based on the AM-CF method deviates from the simulation result by 8%, while BER based on the SGA method deviates by as high as 64%. Also, the system attains a dramatic gain in system capacity by using sinc waveform. It is because the sinc waveform is the optimal one that can minimize the interference and improve the system capacity [80].

It can be believed that the rationale of the AM-CF method is applicable to more realistic conditions, such as short-term fadings with non-equal average power, power control error, power control period, power control step, power control command delay, MS velocity, etc. However further systematic work is needed to study these extensions of the AM-CF method. Moreover, the determination of the parameter  $N$  is still an issue that needs further study.





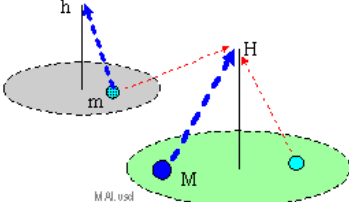
(a) Rectangular chip waveform



(b) Sinc chip waveform

Figure 4.1: Comparison of cdf curves of interference signals

## 4.5 Notation List

Notation	Description	Notation	Description
$m$	Index of an arbitrary <u>m</u> obile station	$f_\varphi(x)$	Pdf of $\cos(\theta_{M,p}^{(m,p)}[n])$
$h$	Index of the BS that is the home BS of MS $m$	$f_{\chi'}(x)$	Pdf of $\chi'_i$
$b$	Index of an arbitrary BS	$f_S(x)$	Pdf of $S_{MH}$
$M$	Index of a specific MS	$f_\beta(x)$	Pdf of $\beta_i''$
$H$	Index of the BS communicating with the specific MS $M$	$f_\psi(x)$	Pdf of $\psi_i$
		$\mathcal{F}(\cdot)$	Fourier transform
		$\mathcal{F}^{-1}(\cdot)$	Inverse Fourier transform
		$F_\chi(\omega)$	Characteristic function of $f_{\chi'}(x)$
		$F_\psi(\omega)$	Characteristic function of $f_\psi(x)$
$a_i$	RV having values $\{\pm 1\}$ with equal probability	$G$	Processing gain
$A$	Discrete RV defined in (4.8)	$G \triangleq T/T_c$	
$b_i$	RV having values $\{\pm 1\}$ with equal probability	$I_A[n]$	Multiple access and multipath interference (MAI) portion of $Z_M[n]$
$B$	Discrete RV defined in (4.8)	$I_S[n]$	Multipath interference portion of $Z_M[n]$
$c_m(t)$	PN spreading signal for MS $m$	$I_I$	Intra-cell interference signal
$c_m[i]$	PN spreading code of MS $m$	$I_I^*$	RV used to approximate the pdf of $I_I$
$C_x^y$	Binomial coefficient	$I_O$	Other-cell interference signal
$d_M[n]$	Data sequence of MS $m$	$I_O^*$	RV used to approximate the pdf of $I_O$
$E(\cdot)$	Expectation function	$K$	Number of resolvable paths in each uplink channel
$F_\xi(\cdot, \mu_O, \sigma_O^2)$	Cdf function of the Gaussian variable $\xi$ with mean $\mu_O$ and variance $\sigma_O^2$	$L''$	Quantity defined in (4.30)
$f_\alpha(x)$	Pdf of $\alpha_{M,p}^{(m,p)}[n]$	$L_{mb}$	Long-term fading of the
$f_b(x; y)$	Binomial probability		

Notation	Description
	uplink from MS $m$ to BS $b$
$L_{MH}$	Long-term fading of the uplink from a specific MS $M$ to its home BS $H$
$MS^{(h)}$	Index set of the MSs that are served by BS $h$
$n$	Index of data symbol period
$N_B$	<u>N</u> umber of <u>b</u> ase stations in the cellular system. I.e. cell number
$N_M$	<u>N</u> umber of <u>m</u> obile stations in each cell of the cellular system
$p$	Index of the resolvable path on an uplink
$P_m[n]$	Transmission power of MS $m$ during $n$ th data symbol period
$P_M[n]$	Transmission power of specific MS $M$ during $n$ th data symbol period
$Q_0$	Desired received power level
$r_M[n]$	Desired signal portion of $Z_M[n]$
$S_{mb,p}$	Short-term fading of the $p$ th resolvable path of the uplink from MS $m$ to BS $b$
$S_{mh}[n]$	Short-term fading of the uplink from an arbitrary MS $m$ to its home BS $h$ during $n$ th data symbol period
$S_{MH}[n]$	Short-term fading of the uplink from a specific MS $M$ to its home BS $H$ during $n$ th data symbol period
$S_{MH}$	$S_{MH}[n]$ after the index $n$ being dropped
$S_{1,i}$	RV having same distribution as that of $S_{MH}$

Notation	Description
$L_{MH}$	Long-term fading of the uplink from a specific MS $M$ to its home BS $H$
$MS^{(h)}$	Index set of the MSs that are served by BS $h$
$n$	Index of data symbol period
$N_B$	<u>N</u> umber of <u>b</u> ase stations in the cellular system. I.e. cell number
$N_M$	<u>N</u> umber of <u>m</u> obile stations in each cell of the cellular system
$p$	Index of the resolvable path on an uplink
$P_m[n]$	Transmission power of MS $m$ during $n$ th data symbol period
$P_M[n]$	Transmission power of specific MS $M$ during $n$ th data symbol period
$Q_0$	Desired received power level
$r_M[n]$	Desired signal portion of $Z_M[n]$
$S_{mb,p}$	Short-term fading of the $p$ th resolvable path of the uplink from MS $m$ to BS $b$
$S_{mh}[n]$	Short-term fading of the uplink from an arbitrary MS $m$ to its home BS $h$ during $n$ th data symbol period
$S_{MH}[n]$	Short-term fading of the uplink from a specific MS $M$ to its home BS $H$ during $n$ th data symbol period
$S_{MH}$	$S_{MH}[n]$ after the index $n$ being dropped
$S_{1,i}$	RV having same distribution as that of $S_{MH}$

Notation	Description	Notation	Description
$S_{2,i}$	RV having same distribution as that of $S_{MH}$	$\alpha_i''$	RV having a form given in (4.17)
$T$	Symbol duration	$\alpha_{M,p}^{(m,p')}[n]$	RV related to the spreading code cross-correlation between the resolvable path $p$ in the uplink from MS $M$ to BS $H$ and the resolvable path $p'$ in the uplink from MS $m$ to BS $H$
$T_c$	Chip duration	$\beta_i''$	$\beta_i'' \triangleq \sqrt{S_{1,i} / S_{2,i}}$
$v_i$	Quantity defined in (4.19)	$\varphi_i'$	RV having a form given in (4.20)
$\text{var}(\cdot)$	Variance function	$\varphi_i''$	RV having a form given in (4.20)
$w_i$	Quantity defined in (4.18)	$\chi_i'$	RV defined as $\chi_i' = \alpha_i' \cdot \varphi_i'$
$Z_M[n]$	Decision statistics corresponding to a specific MS $M$ at $n$ th data symbol period	$\chi_i''$	RV defined as $\chi_i'' \triangleq \alpha_i'' \cdot \varphi_i''$
$z[n]$	Noise	$\psi_i$	RV defined as $\psi_i = \beta_i'' \cdot \chi_i''$
$\xi$	A Gaussian random variable for approximating $I_O^*$	$\theta_{M,p}^{(m,p')}[n]$	RV related to the phase difference between the resolvable path $p$ in the uplink from MS $M$ to BS $H$ and the resolvable path $p'$ in the uplink from MS $m$ to BS $H$
$\tau_m$	Transmission timing of MS $m$ due to asynchronous transmission among the MSs		
$\tau$	Uniform RV over $[0,1)$		
$\mu_O$	Mean of $I_O^*$ when $N_M = 1$		
$\sigma_O^2$	Variance of $I_O^*$ when $N_M = 1$		
$\alpha$	RV defined in (4.7)		
$\alpha_i'$	RV having a form given in (4.17)		

## Chapter 5

# Capacity Analysis of an Imperfect SIR-based Power Control Scheme for Uplinks in DS/CDMA Cellular Systems

---

*Abstract—The chapter proposes a novel method to analyze the system capacity of an imperfect signal-to-interference ratio (SIR)-based power control scheme for uplinks in direct sequence/code division multiple access (DS/CDMA) cellular systems. Not ideally fixed at a preset level, the received SIR in the imperfect SIR-based power control scheme is a random variable affected by many practical factors such as power control loop delay and mobile velocity. Based on investigated properties of ensemble average received SIR per bit, a set of linear equations is derived to obtain the ensemble average received power on each uplink. The system capacity is then obtained according to the feasibility of the ensemble average received power vector and the ensemble average bit error rate. A closed-form solution for system capacity is approximately derived, which employs the first and second order statistics of each element in the coefficient matrix, by applying central limit theorem. Results show that numerical results are substantially matched with simulation results; this implies the novel analytical method is quite accurate.*

## 5.1 Introduction

In a DS/CDMA system, many users transmit messages simultaneously over the same radio channel, each using a specific spread-spectrum pseudo-noise (PN) code [10]. Within a cell, the code channels in downlinks can be considered as mutually orthogonal because downlinks exhibit synchronous CDMA transmission. However, these code channels in uplinks cannot be mutually orthogonal exactly for asynchronous mobile users, and thus mutual interference occurs. In such a case, a strong signal will have good communication quality, while a weak signal may suffer from strong interference. This problem is referred to as the near-far effect and limits the CDMA system capacity [11]. Therefore, power control is an important issue affecting the system capacity in uplinks of DS/CDMA cellular systems.

Power control schemes studied in the literature can be mainly classified into two categories: the strength-based power control [45] and the SIR-based power control [21], [27]. There were many works related to the strength-based power control scheme, such as the system capacity analysis, e.g. [3], the interference statistics, e.g. [22], the error probability, e.g. [17], etc. Nevertheless, the SIR-based power control is in fact more important. Ariyavisitakul [21] once indicated that the SIR-based power control system has the potential for higher system capacity. Actually, the SIR-based power control had been adopted in IMT-2000 systems as well as IS-95 system. However, the corresponding theoretical analysis for the SIR-based power control is very complicated [21] and is found significantly different from that of the strength-based power control [23]. Due to difficulty, few literature had successfully provided theoretical methods for investigating the SIR-based power control scheme, e.g. [23], [25], [26], and most works made the study via simulation, e.g. [21], [27], [28], [29], for the SIR-based power control schemes.

Kim and Sung [23] proposed a methodology for analyzing the system capacity of the SIR-based power control scheme with consideration of the voice activity, the maximum received




power, and the long-term fading. The analysis was extended to a multicode CDMA system and an overlaid multiband CDMA system in [25]. However, they did not take the multipath fading into account in the channel model. Kim and Adachi [26] further proposed a method to analytically evaluate the reverse link capacity of a CDMA system in a multipath fading environment. In [23], [25], and [26], by recursively calculating the statistics of both the received power on the uplink and the interference power to mimic their inherent interaction, the system capacity of an SIR-based power control scheme is numerically obtained. Note that, all of these analyses assume that the SIR-based power control is perfect such that the received SIR is kept at a preset level. However, in practical, the received SIR would be a random variable rather than a constant. It can be found that the analysis of the imperfect SIR-based power control scheme is further different from that of the ideal SIR-based power control scheme. There has never been any analytical approach for analyzing the capacity of an imperfect SIR-based power control scheme.

The chapter proposes a novel method to analyze the system capacity of an imperfect SIR-based power control scheme for uplinks of DS/CDMA cellular systems. The received SIR here considered is not ideally fixed at a preset level [40] but affected by many practical factors such as power control period, power control step size, power control loop delay, mobile velocity, and short-term fading characteristics. The proposed analytical method firstly investigates two properties of the ensemble average received SIR: the ensemble average received SIR per bit is approximately uncorrelated with the interference power; and the interference power from an interfering MS is approximately proportional to the interfering MS's received power at its home BS. Based on these two properties, a set of linear equations is derived to obtain the ensemble average received power on each uplink. A formula for the system capacity, based on the outage probability, is obtained in which the distribution of the determinant of the coefficient matrix of the linear equations is required. The outage probability is defined according to the feasibility of the ensemble average received power vector and the ensemble average bit error rate. A

closed-form solution for the system capacity is derived with the assumptions that the elements of the coefficient matrix are mutual uncorrelated random variables and then the employment of the central limit theorem. It merely requires the first and second order statistics of each element in the coefficient matrix. Simulations are conducted to validate the analysis. Results show that the numerical results and the simulation results are substantially matched, which implies the novel analytical method is quite accurate.

The rest of this chapter is structured as follows. Section 5.2 introduces the system model and the imperfect SIR-based power control scheme. Section 5.3 derives the system capacity of an imperfect SIR-based power control scheme. A closed-form solution is also obtained. Section 5.4 presents numerical results, together with simulation results for validation. Finally, Section 5.5 gives the concluding remarks.

## 5.2 System Model



The DS/CDMA cellular system under consideration is with  $N_B$  base stations (BSs) and  $N_M$  mobile stations (MSs) per cell, and with frequency-selective, slowly fading multipath channels. The power gain  $g_{mb,p}$  of each resolvable path  $p$  on a link from an arbitrary MS  $m$  to an arbitrary BS  $b$  is statistically divided into long-term fading  $L_{mb}$  and short-term fading  $S_{mb,p}$ , wherein  $m \in \{1, 2, \dots, N_B \cdot N_M\}$  denotes the MS index,  $b \in \{1, 2, \dots, N_B\}$  denotes the BS index, and  $p \in \{1, 2, \dots, K\}$  denotes the resolvable path index with  $K$  being the number of resolvable paths on an uplink. For simplicity,  $\{S_{mb,p}, \forall(m, b, p)\}$  are assumed to be in Rayleigh distribution that have an independently and identically distributed (iid) exponential probability density function (pdf) with mean  $1/K$  and variance  $1/K^2$ , where  $K$  is the number of resolvable paths in the uplink. It is also assumed that the binary phase-shift keying modulation and optimal RAKE receivers are employed. We consider a medium-term period [63] over which the long-term fading is treated as

constant while the short-term fading varies. For a specific MS  $M$  communicating with its home BS  $H$ , the instantaneous SIR per bit at the  $n$ -th data symbol, denoted by  $\Gamma_M[n]$ , is given by [3]

$$\Gamma_M[n] = \frac{G \cdot Q_M[n]}{\zeta \cdot I_M[n] + N_0}, \quad (5.1)$$

where  $G$  is the processing gain, the term  $Q_M[n]$  denotes the received signal power of MS  $M$  at the BS  $H$ ,  $\zeta$  is a factor depending on the PN chip waveform and the cross-correlation property of the PN codes [45], the term  $I_M[n]$  denotes the interference power, and  $N_0$  is the background noise contained in the total spread bandwidth. The  $Q_M[n]$  can be obtained by

$$Q_M[n] = P_M[n] \cdot L_{MH} \cdot S_{MH}[n], \quad (5.2)$$

where  $P_M[n]$  is the transmission power of the MS  $M$  at the  $n$ -th data symbol, and  $S_{MH}[n] \triangleq \sum_{p=1}^K S_{MH,p}[n]$  is a unit-mean gamma RV with variance  $1/K$ . The  $I_M[n]$  contains the intra-cell interference power and inter-cell interference power given by

$$\begin{aligned} I_M[n] &= \sum_{m \neq M} P_m[n] \cdot L_{mH} \cdot S_{mH}[n] \\ &= \sum_{\substack{m \neq M \\ m \in MS^{(H)}}} P_m[n] \cdot L_{mH} \cdot S_{mH}[n] + \sum_{h \neq H} \sum_{m \in MS^{(h)}} P_m[n] \cdot L_{mH} \cdot S_{mH}[n], \end{aligned} \quad (5.3)$$

where  $MS^{(h)}$  denotes the index set of those MSs communicating with BS  $h$ .

The mechanism of the imperfect SIR-based power control for uplinks in the DS/CDMA cellular system is described as follows. Consider an specific MS  $M$  communicating with its home BS  $H$ . The BS measures the SIR per bit for each data symbol, denoted by  $\Gamma_M[n]$ , and computes an average value, denoted by  $\overline{\Gamma}_M$ , by averaging  $\Gamma_M[n]$  over a power control period  $T_p$ . A one-bit power control command  $CMD$  is generated periodically by comparing  $\overline{\Gamma}_M$  with a preset target SIR threshold  $\Gamma_{TH}$ . If  $\overline{\Gamma}_M < \Gamma_{TH}$ ,  $CMD$  will be +1; otherwise,  $CMD$  will be -1. The power

control command  $CMD$  is then transmitted through the downlink channel to the destination MS. After a power control command loop delay  $T_d$ , the MS  $M$  receives the command  $CMD$  and adapts its transmission power by an amount of  $CMD \cdot \Delta_p$  dB, wherein  $\Delta_p$  is the power control step size. Noticeably, the  $\Gamma_M[n]$  is obviously no longer a time constant in such an imperfect SIR-based power control scheme. Since the long-term fading is regarded as constant during a medium-term period, the channel gain, which is the product of the short-term fading and long-term fading, would be a stationary random process. Thus it is reasonable to assume that each MS's transmission power  $P_M[n]$ , the corresponding received power  $Q_M[n]$ , the interference power  $I_M[n]$ , and the SIR per bit  $\Gamma_M[n]$ , are all stationary random processes under the imperfect SIR-based power control scheme during the medium-term period. The mean and variance of the  $\Gamma_M[n]$  can be obtained by [53]

$$\begin{cases} E(\Gamma_M[n]) = \exp(\kappa \cdot E(\tilde{\Gamma}_M[n]) + 0.5 \cdot \kappa^2 \cdot \text{var}(\tilde{\Gamma}_M[n])) \\ \quad = \Gamma_{TH} \cdot \exp(0.5 \cdot \kappa^2 \cdot \text{var}(\tilde{\Gamma}_M[n])), \\ \text{var}(\Gamma_M[n]) = E^2(\Gamma_M[n]) \cdot (\exp(\kappa^2 \cdot \text{var}(\tilde{\Gamma}_M[n])) - 1), \end{cases} \quad (5.4)$$

where  $\kappa \triangleq \ln(10)/10$ ,  $\tilde{\Gamma}_M[n] \triangleq 10 \cdot \log_{10}(\Gamma_M[n])$ , and  $E(\tilde{\Gamma}_M[n])$  can be approximated by  $10 \cdot \log_{10}(\Gamma_{TH})$  [40].

## 5.3 Capacity Analysis

In the following analysis, the index of the  $n$ -th data symbol,  $n$ , is neglected in order to have simple presentation.

### 5.3.1 Properties of Ensemble Average Received SIR

*Property 1:* The ensemble average SIR per bit of MS  $M$ ,  $E(\Gamma_M)$ , received at its home BS

in the imperfect SIR-based power control scheme can be well approximated by

$$E(\Gamma_M) \cong \frac{G \cdot E(Q_M)}{\zeta \cdot E(I_M) + N_0}, \quad \forall M \in \{1, 2, \dots, N_B \cdot N_M\}, \quad (5.5)$$

where  $E(\cdot)$  denotes the ensemble average operator and is performed with respect to the data symbol index  $n$ .

*Note:* Eq. (4.2) can be rewritten as

$$\Gamma_M \cdot (\zeta \cdot I_M + N_0) = G \cdot Q_M. \quad (5.6)$$

Recall that the goal of a SIR-based power control is to adjust the MS's transmission power such that the  $\Gamma_M$  approaches to a preset target SIR threshold  $\Gamma_{TH}$  as close as possible. If the  $\Gamma_M$  is exactly equal to  $\Gamma_{TH}$ , it would be obvious that  $\Gamma_M$  is statistically independent of the term  $(\zeta \cdot I_M + N_0)$ . Thus (5.5) can be obtained derived by taking statistical expectation of both sides of (5.6). In an imperfect SIR-based power control scheme, although the  $\Gamma_M$  is not exactly  $\Gamma_{TH}$ , it is still reasonable to assume that the  $\Gamma_M$  is uncorrelated with the term  $(\zeta \cdot I_M + N_0)$ . Therefore, (5.5) is obtained. ■

As will be shown in the Section 5.4, this assumption given in *Property I* seems quite acceptable. Based on the *Property I*, we have the following lemma.

*Lemma I:* If  $E(\Gamma_M) = E(\Gamma_N)$ ,  $\forall M, N \in MS^{(H)}$ ,  $H \in \{1, 2, \dots, N_B\}$ , then the ensemble average received power levels of MSs  $M$  and  $N$ ,  $E(Q_M) = E(Q_N)$ , equal to a common level, denoted by  $Y_H$ . That is,

$$E(Q_M) = E(Q_N) \equiv Y_H, \quad \forall M, N \in MS^{(H)}, H \in \{1, 2, \dots, N_B\}. \quad (5.7)$$

*Proof:* From  $E(\Gamma_M) = E(\Gamma_N)$  and (5.5),  $E(Q_M) = k \cdot E(Q_N)$  can be yielded, where  $k$  is a

time constant. Substituting this result back into  $E(\Gamma_M) = E(\Gamma_N)$ , one will then find that the solution is  $k = 1$ , which just implies  $E(Q_M) = E(Q_N)$ . Since this is true for any  $M, N \in MS^{(H)}$ , thus we have (5.7). ■

The phenomenon described in *Lemma I* complies with intuition. For an imperfect SIR-based power control scheme, it can be found that communication links in the same cell interfere with one another, the long-term fadings are typically compensated, and the characteristics of short-term fadings are identical to each other. From a symmetric viewpoint it seems reasonable that the ensemble average received power on one uplink will be the same as that on another uplink.

*Property II:* The correlation between the transmission power of an MS  $m$  communicating with its home BS  $h$ ,  $P_m$ , and the channel gain of the interference link from MS  $m$  to BS  $H$ ,  $g_{mH}$ , exists in a manner that the ensemble average interference power to BS  $H$ ,  $E(P_m \cdot g_{mH})$ , is proportional to the ensemble average received power  $E(Q_m)$  of the MS  $m$  at its home BS  $h$  and the long term fading factor ( $L_{mH} / L_{mh}$ ). It is given by

$$E(P_m \cdot g_{mH}) = \beta \cdot E(Q_m) \cdot \frac{L_{mH}}{L_{mh}}, \quad \forall m \in MS^{(h)}, h \neq H, \quad (5.8)$$

where  $g_{mH} \triangleq \sum_{p=1}^K g_{mH,p}$  and  $\beta$  is a constant.

*Note:* In the steady state, a constant  $\beta_1$  would exist such that  $E(P_m \cdot g_{mH}) = \beta_1 \cdot E(P_m) \cdot E(g_{mH})$ . In the SIR-based power control, MS's transmission power would also depend on the channel gains of the interference links; hence the constant  $\beta_1$  should be any positive number except 1. Since the long-term fadings are time constant and are assumed to be exactly compensated by power control, another constant  $\beta_2$  would exist such that

$E(P_m) = \beta_2 \cdot E(Q_m) / L_{mh}$ , where  $\beta_2$  is a constant related to those practical factors mentioned before. From the channel model, we have  $E(g_{mH}) = L_{mH}$ . Therefore (5.8) is obtained with  $\beta = \beta_1 \cdot \beta_2$ . ■

In general,  $\beta$  may be different for different indexes  $(m, h)$ . However, for simplicity, the value of  $\beta$  is here assumed to be a constant independent of  $m$  and  $h$ . As can be seen from simulation results, this assumption seems quite acceptable.

### 5.3.2 Outage Probability

Based on the *Properties I and II* and *Lemma I*, the ensemble average SIR per bit  $E(\Gamma_M)$  can be obtained by

$$E(\Gamma_M) = \frac{G \cdot Y_H}{\zeta \cdot \left( (N_M - 1) \cdot Y_H + \sum_{h \neq H} \sum_{m \in MS^{(h)}} \beta \cdot Y_h \cdot \frac{L_{mH}}{L_{mh}} \right) + N_0}, \quad (5.9)$$

where  $N_M$  is the number of MS in each cell. Considering  $E(\Gamma_M) = \Gamma_0$ ,  $\forall M \in MS^{(H)}$ ,  $H \in \{1, 2, \dots, N_B\}$ , where  $\Gamma_0$  denotes the common ensemble average SIR per bit, one will obtain  $N_B$  linear equations with  $N_B$  unknowns,  $Y_1, Y_2, \dots, Y_{N_B}$ , given by

$$G \cdot Y_H = \zeta \cdot \Gamma_0 \cdot (N_M - 1) \cdot Y_H + \zeta \cdot \Gamma_0 \cdot \sum_{h \neq H} \sum_{m \in MS^{(h)}} \beta \cdot Y_h \cdot \frac{L_{mH}}{L_{mh}} + \Gamma_0 \cdot N_0, \quad H = 1, 2, \dots, N_B. \quad (5.10)$$

Rewriting the above linear equations in a matrix form, we have

$$\mathbf{A}\mathbf{Y} = \mathbf{N}, \quad (5.11)$$

where  $\mathbf{Y} = [Y_1, Y_2, \dots, Y_{N_B}]_{(N_B \times 1)}$  is the ensemble average received power vector,  $\mathbf{N} = [n_0]_{(N_B \times 1)}$  with  $n_0 = (\Gamma_0 \cdot N_0) / (G - \zeta \cdot \Gamma_0 \cdot (N_M - 1))$ , and  $\mathbf{A} = [a_{bh}]_{(N_B \times N_B)}$  is the coefficient matrix with

$$a_{bh} = \begin{cases} 1, & b = h, \\ -\frac{\zeta \cdot \Gamma_0 \cdot \beta \sum_{m \in MS^{(h)}} \frac{L_{mb}}{L_{mh}}}{G - \zeta \cdot \Gamma_0 \cdot (N_M - 1)}, & b \neq h. \end{cases} \quad (5.12)$$

Usually the coefficient matrix  $\mathbf{A}$  is nonsingular, and the ensemble average received power vector  $\mathbf{Y}$  can thus be obtained by  $\mathbf{Y} = \mathbf{A}^{-1}\mathbf{N}$ . If the solution  $\mathbf{Y}$  in (5.12) contains all-positive elements (i.e.,  $\mathbf{Y} > 0$ ),  $\mathbf{Y}$  is called feasible, denoting that the system is not overloaded; otherwise, the system is heavily overloaded and some communication links should be suspended or terminated temporarily.

For simplicity, it is assumed that the received SIR per bit on each uplink has an identical pdf, denoted by  $f_\Gamma(\cdot)$ . Thus the ensemble average bit error rate (BER), denoted by  $P_e$ , can be yielded as  $P_e = \int P_b(\gamma) \cdot f_\Gamma(\gamma) d\gamma$ , where  $P_b(\gamma)$  denotes the BER corresponding to a received SIR per bit  $\gamma$ . For the BPSK modulation, the BER function is the well-known Gaussian  $Q$  function and  $P_b(\gamma) = Q(2\gamma)$ .

The outage probability, denoted by  $P_{out}$ , is here defined, according to the feasibility of the ensemble average received power  $\mathbf{Y}$  and the ensemble average bit error rate  $P_e$ , by

$$P_{out} \triangleq 1 - \Pr(\mathbf{Y} > 0, P_e \leq P_e^*) \\ = \begin{cases} 1, & P_e > P_e^*, \\ 1 - \Pr(\mathbf{Y} > 0), & P_e \leq P_e^*, \end{cases} \quad (5.13)$$

where  $P_e^*$  is the requirement of the ensemble average BER for the communication quality,  $\Pr(\mathbf{Y} > 0)$  denotes the probability of that the ensemble average received power vector  $\mathbf{Y}$  is feasible. It is not difficult to find that  $P_e$  is a decreasing function of  $\Gamma_{TH}$ . Thus  $P_{out}$  can be rewritten as



$$P_{out} = \begin{cases} 1, & \Gamma_{TH} < \Gamma_{TH}^*, \\ 1 - \Pr(\mathbf{Y} > 0), & \Gamma_{TH} \geq \Gamma_{TH}^*, \end{cases} \quad (5.14)$$

where  $\Gamma_{TH}^*$  denotes the minimum  $\Gamma_{TH}$  required to achieve the requirement  $P_e^*$ .

### 5.3.3 System Capacity

The system capacity for a given target SIR threshold  $\Gamma_{TH}$ , denoted by  $C$ , is defined as the maximal number of MSs for each cell the system can support such that the outage probability is less than a threshold, say 1%. It is given by

$$C = \text{Max}_{N_M} \{P_{out} < 1\%\}. \quad (5.15)$$

Applying (5.14) to (5.15), the system capacity  $C$  is obtained by

$$C = \begin{cases} 0, & \Gamma_{TH} < \Gamma_{TH}^*, \\ \text{Max}_{N_M} \{\Pr(\mathbf{Y} > 0) \geq 0.99\}, & \Gamma_{TH} \geq \Gamma_{TH}^*. \end{cases} \quad (5.16)$$

It is intuitive that the system capacity  $C$  will decrease or remain the same as the target SIR threshold  $\Gamma_{TH}$  increases.

The ensemble average received power vector  $\mathbf{Y}$  can be obtained by solving the linear equations in (5.11). Thus the ensemble average power level on each uplink received at BS  $b$ ,  $Y_b$ , is obtained by

$$Y_b = \frac{n_0 \cdot \det(\mathbf{A}_{(b)})}{\det(\mathbf{A})}, \quad b = 1, 2, \dots, N_B, \quad (5.17)$$

where  $\mathbf{A}_{(b)}$  is the matrix obtained by replacing the  $b$ -th column of  $\mathbf{A}$  by 1. According to the lemmas which are given in the Appendix, it is proven that the event  $\{\mathbf{Y} > 0\}$  is equivalent to the event  $\{\det(\mathbf{A}) > 0\}$  whenever the system is not overloaded. Therefore, as  $\Gamma_{TH} \geq \Gamma_{TH}^*$ , the system capacity  $C$  given in (5.16) can be rewritten as

$$C = \text{Max}_{N_M} \{ \Pr(\det(\mathbf{A}) > 0) \geq 0.99) \}. \quad (5.18)$$

For simplicity, it is assumed that the elements of the coefficient matrix  $\mathbf{A}$  are mutual uncorrelated random variables. By employing central limit theorem, the distribution of  $\det(\mathbf{A})$  can be approximated by that of a Gaussian random variable  $\xi$  with mean  $E(\det(\mathbf{A}))$  and variance  $\text{var}(\det(\mathbf{A}))$ . Thus as  $\Gamma_{TH} \geq \Gamma_{TH}^*$ , the system capacity  $C$  can be approximated by

$$C \cong \text{Max}_{N_M} \{ \Pr(1 - F_\xi(0)) \geq 0.99) \}, \quad (5.19)$$

where  $F_\xi(\cdot)$  denotes the cumulative distribution function of the random variable  $\xi$ . Since the elements in matrix  $\mathbf{A}$  are assumed mutually uncorrelated, we have  $E(\det(\mathbf{A})) = \det(E(\mathbf{A}))$  wherein  $E(\mathbf{A}) = [E(a_{bh})]$ ,

$$E(a_{bh}) = \begin{cases} 1, & b = h, \\ \frac{\zeta \cdot \Gamma_0 \cdot \beta \cdot N_M \cdot E(I_{h,b})}{G - \zeta \cdot \Gamma_0 \cdot (N_M - 1)}, & b \neq h, \end{cases} \quad (5.20)$$

and  $I_{h,b} \triangleq (L_{mb} \cdot L_{mh}^{-1} | L_{mi} \leq L_{mh}, \forall i)$ . The  $I_{h,b}$  had been analyzed by Zorzi [22], and its mean can be numerically computed as

$$E(I_{h,b}) = \lim_{x \rightarrow \infty} \left( x - \int_0^x \Pr(I_{h,b} \leq s) \cdot ds \right) = 1 - \int_0^1 \Pr(I_{h,b} \leq s) \cdot ds, \quad (5.21)$$

and

$$\Pr(I_h \leq s) = \frac{\int \Pr(L_{mH}(\mathbf{z}) \leq sL_{mh}(\mathbf{z}), L_{mb}(\mathbf{z}) \leq L_{mh}(\mathbf{z}), \forall b) \cdot f_{\mathbf{z}_m}(\mathbf{z}) d\mathbf{z}}{\int \Pr(L_{mb}(\mathbf{z}) \leq L_{mh}(\mathbf{z}), \forall b) \cdot f_{\mathbf{z}_m}(\mathbf{z}) d\mathbf{z}} = \frac{\varphi(s)}{\varphi(1)}, \quad (5.22)$$

where  $\mathbf{z}_m$  is a complex number representing the location of MS  $m$ ,  $L_{mh}(\mathbf{z})$  is the long-term fading of MS  $m$  whose location  $\mathbf{z}_m = \mathbf{z}$ ,  $f_{\mathbf{z}_m}(\cdot)$  denotes the pdf of the random variable  $\mathbf{z}_m$ , and

$$\varphi(s) = \int \psi(s, \mathbf{z}) \cdot f_{\mathbf{z}_m}(\mathbf{z}) d\mathbf{z} \quad (5.23)$$

with

$$\begin{aligned}\psi(s, \mathbf{z}) &= \Pr(L_{mb}(\mathbf{z}) \leq sL_{mh}(\mathbf{z}), L_{mi}(\mathbf{z}) \leq L_{mh}(\mathbf{z}), \forall i) \\ &= \int_0^\infty \Pr(L_{mb}(\mathbf{z}) \leq sy) \cdot f_{L_{mh}(\mathbf{z})}(y) \cdot \prod_{i \neq h,b} \Pr(L_{mi}(\mathbf{z}) \leq y) dy,\end{aligned}\quad (5.24)$$

and  $f_{L_{mh}(\mathbf{z})}(\cdot)$  denoting the pdf of  $L_{mh}(\mathbf{z})$ , which is a random variable due to random shadow fading for a given location  $\mathbf{z}$ .

The variance  $\text{var}(\det(\mathbf{A}))$  is obtained by  $\text{var}(\det(\mathbf{A})) = E(\det(\mathbf{A})^2) - E(\det(\mathbf{A}))^2$ . It is well known that  $E(\det(\mathbf{A})^2)$  equals to  $E(\det(\mathbf{A}^2))$ , which can be computed according to the first and second moments of each element of the coefficient matrix  $\mathbf{A}$ . The first moment statistics  $\{E(a_{bh})\}$  are already given in (5.20). The second moment statistics  $\{E(a_{bh}^2)\}$  are given by

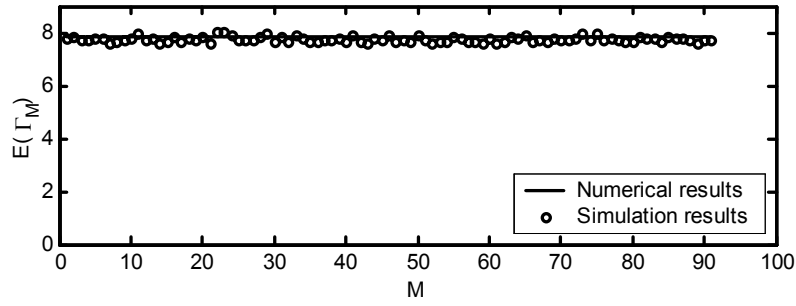
$$E(a_{bh}^2) = \begin{cases} 1, & b = h, \\ \left( \frac{\zeta \cdot \Gamma_0 \cdot \beta}{G - \zeta \cdot \Gamma_0 \cdot (N_M - 1)} \right)^2 \cdot N_M \cdot (E(I_{h,b}^2) - N_M \cdot E^2(I_{h,b})), & b \neq h, \end{cases}\quad (5.25)$$

where  $E(I_{h,b}^2)$  can be numerically computed as

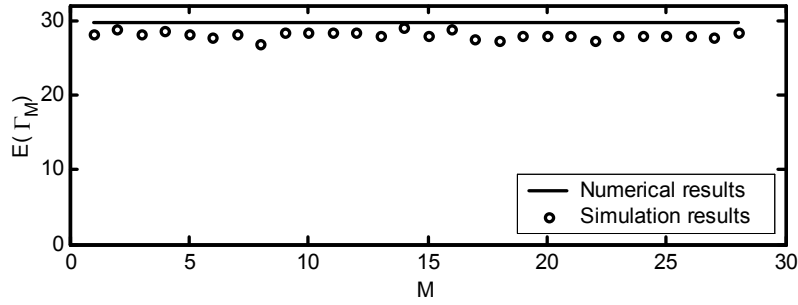
$$E(I_{h,b}^2) = \lim_{x \rightarrow \infty} \left( x^2 - 2 \int_0^x s \Pr(I_{h,b} \leq s) \cdot ds \right) = 1 - 2 \int_0^1 s \cdot \Pr(I_{h,b} \leq s) \cdot ds. \quad (5.26)$$

## 5.4 Numerical Results

The DS/CDMA cellular system is assumed to have the number of cells  $N_B = 7$  in a hexagonal-grid configuration, the propagation loss  $\eta = 3.5$ , the log-normal shadow fading standard deviation  $\sigma_x = 8$ , the resolvable path number  $K = 2$ , the processing gain  $G = 128$ , the factor  $\zeta = 2/3$  for the case of rectangular chip waveform, and the minimum ensemble average BER  $P_e^* = 10^{-3}$ . The antenna height of MS (BS) is simply set to be 0.003 (0.01) times the BS radius to avoid the case of 'zero-distance' between the MS and BS. The Rayleigh fading random processes are generated according to a simulation model with correct statistical properties



(a)  $V = 20$  km/hr,  $\tilde{\Gamma}_{TH} = 8.7$  dB,  $N_M = 13$



(b)  $V = 100$  km/hr,  $\tilde{\Gamma}_{TH} = 13.8$  dB,  $N_M = 4$

Figure 5.1: Ensemble average received SIR per bit  $E(\Gamma_M)$  versus MS index  $M$  in the system

proposed by [81] with central frequency of 2 GHz. The set of  $\{L_{mb}, \forall(m,b)\}$  is randomly generated according to the channel model and the MS locations are uniformly distributed. Furthermore, the step size of power adaptation  $\Delta_p = 1$  dB, the power control period  $T_p = 2/3$  ms, and the power control command loop delay  $T_d = 1 \cdot T_p$  are assumed for the imperfect SIR-based power control scheme. While simulating the imperfect SIR-based power control, the outage probability is calculated according to the feasibility of the ensemble average received power vector  $\mathbf{Y}$  and the ensemble average BER  $P_e$  on each uplink by considering 1000 sets of  $\{L_{mb}, \forall(m,b)\}$ . Each uplink's  $P_e$  is obtained by averaging the instantaneous BER over 500 power control cycles. Note that, the effect of the MS movement on the outage probability has been taken into account by investigating many random sets of  $\{L_{mb}, \forall(m,b)\}$  in the simulations.

Figure 5.1 plots the ensemble average SIR per bit  $E(\Gamma_M)$  versus MS index  $M$  in the system for two exemplary cases: (a) MS velocity  $V = 20$  km/hr, target SIR threshold  $\tilde{\Gamma}_{TH} = 8.7$  dB,  $N_M = 13$  MSs/cell; (b) MS velocity  $V = 100$  km/hr, target SIR threshold  $\tilde{\Gamma}_{TH} = 13.8$  dB,  $N_M = 4$  MSs/cell. The numerical results of  $\{E(\Gamma_M), 1 \leq M \leq N_B \cdot N_M\}$  are computed according to (5.4) with  $\text{var}(\tilde{\Gamma}_M) = 2.2$  and  $8.1$  for case (a) and (b), respectively. They deviate from the simulation results by about 1.7% and 5.8% for cases (a) and (b), respectively. The case (a) implies that *Property I* given in (5.5) is satisfactorily acceptable when the MS velocity  $V$  is as low as 20 km/hr. That is, the assumption that the received SIR per bit  $\Gamma_M$  is uncorrelated with the term  $(\zeta \cdot I_M + N_0)$  is quite reasonable. As the MS velocity increases, the  $\text{var}(\tilde{\Gamma}_M)$  increases and the received SIR per bit  $\Gamma_M$  becomes less uncorrelated with the term  $(\zeta \cdot I_M + N_0)$ . However, even the MS velocity  $V$  is as high as 100 km/hr, it is found that the *Property I* given in (5.5) is still acceptable since the *Lemma I* that depends on the *Property I* holds well for  $V=100$  km/hr, as shown in the next figure.

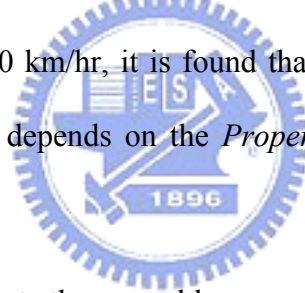


Figure 3.1(a) and 3.1(b) illustrate the ensemble average received power  $E(Q_M)$  versus MS index  $M$  for cases: (a) MS velocity  $V = 20$  km/hr, target SIR threshold  $\tilde{\Gamma}_{TH} = 8.7$  dB,  $N_M = 13$  MSs/cell,  $\text{var}(\tilde{\Gamma}_M) = 2.2$ , and the parameter  $\beta$  in (5.8) is set to 1.685; and (b) MS velocity  $V = 100$  km/hr, target SIR threshold  $\tilde{\Gamma}_{TH} = 13.8$  dB,  $\text{var}(\tilde{\Gamma}_M) = 8.1$ ,  $N_M = 4$  MSs/cell, and the  $\beta = 0.93$ , respectively. Here the MS index  $M \in \{1, 2, \dots, N_B \cdot N_M\}$  has been appropriately indexed such that  $MS^{(H)} = \{1 + (H-1) \cdot N_M, 2 + (H-1) \cdot N_M, \dots, H \cdot N_M\}$  with  $H \in \{1, 2, \dots, N_B\}$  being the index of the home BS of the MS  $M$ . From the simulation results shown in Fig. 3.1, the ensemble average received power levels on the uplinks in the same cell are substantially equal to each other, as described in *Lemma I*. The analytical ensemble average received power  $\mathbf{Y}$  derived by (5.11) is well consistent with the simulation results. They imply the suitability of *Property II*.

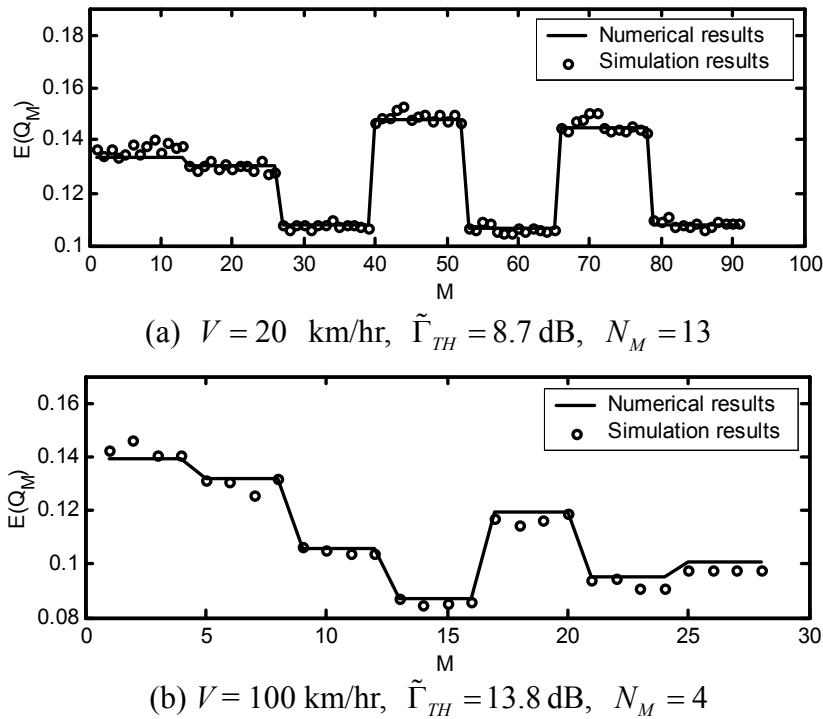


Figure 5.2: Ensemble average received power  $E(Q_M)$  versus MS index  $M$  in the system

From Fig. 5.1 and Fig. 3.1, it is shown that *Properties I* and *II* and *Lemma I* hold no matter the MS velocity is as low as 20 km/hr or as high as 100 km/hr.

Figure 5.3 plots the numerical results of the system capacity  $C$  of an imperfect SIR-based power control system versus the target SIR threshold  $\Gamma_{TH}$  for MS velocity  $V=20$  km/hr. The parameters  $(\zeta, \beta, \text{var}(\tilde{\Gamma}_M), 10 \cdot \log_{10}(\Gamma_{TH}^*))$  are set to  $(2/3, 1.685, 2.2, 8.7)$ . The maximal capacity is found to be 13. Simulation results are also shown for validating the numerical results. Results show that numerical results and the simulation results are substantially matched, which implies the novel analytical method is quite accurate. Intuitively, the system capacity would be decreased when the target SIR threshold is increased. Such a tendency is supported by both the numerical and simulation results. The system capacity shown in Fig. 5.3 seems somewhat small. One of the major reasons is regarding to the chip waveform used in the spreading code. It had

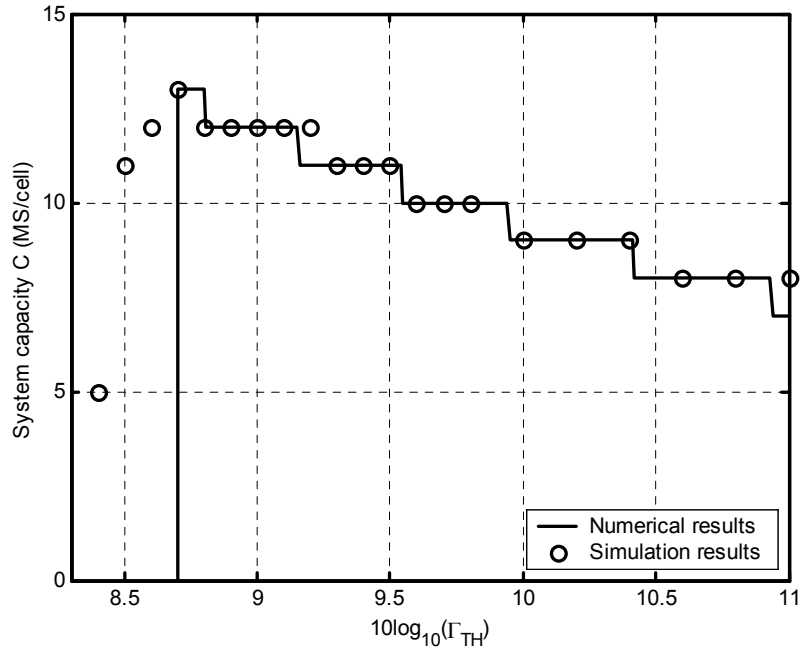


Figure 5.3: System capacity  $C$  versus the target SIR threshold  $\Gamma_{TH}$

been reported that a sinc waveform is the optimal one that can minimize the interference and improve the system capacity quite a lot [82]. By appropriately choosing the chip waveform, the parameter  $\zeta$ , which represents the correlation between the code channels, will be reduced, and the system capacity can be enhanced accordingly.

Figure 5.4 plots the numerical results of the system capacity  $C$  of an imperfect SIR-based power control system versus the target SIR threshold  $\Gamma_{TH}$  in two cases (a)  $\zeta = 2/3$ , and (b)  $\zeta = 2/9$ . The parameters  $(V, \beta, \text{var}(\tilde{\Gamma}_M), 10 \cdot \log_{10}(\Gamma_{TH}^*))$  are set to  $(100, 0.93, 8.1, 13.6)$ , respectively. The maximal capacities of the case (a) and case (b) are found to be 4 and 14, respectively. As can be seen, due to the reduction of the parameter  $\zeta$ , the factor relating on the PN chip waveform and the cross-correlation property of the PN codes, the system capacity  $C$  is increased accordingly. Compared with the results in Fig. 5.3(b), the  $\zeta$  is reduced to one-third of the original, and the system capacity is increased to about three times of the original. From Fig. 5.4, it implies that the proposed analytical method is still quite accurate for different  $\zeta$ .

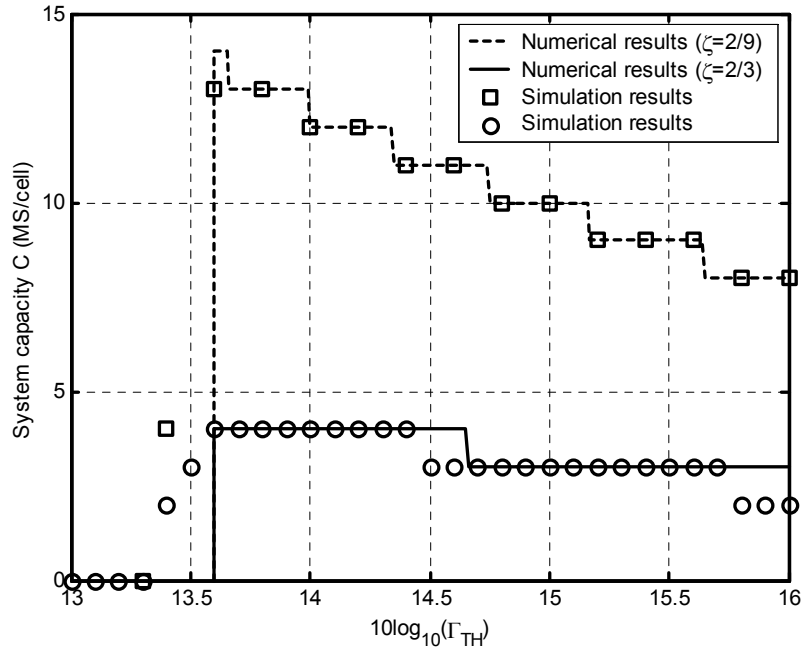


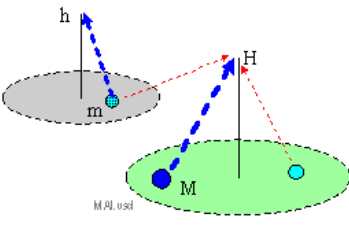
Figure 5.4: System capacity  $C$  versus the target SIR threshold  $\Gamma_{TH}$  for various  $\zeta$

## 5.5. Concluding Remarks

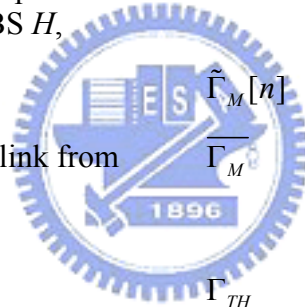
In this chapter, the system capacity of an imperfect SIR-based power control for uplinks in DS/CDMA cellular system is successfully analyzed. A novel analytical method is proposed. It firstly investigates properties of the ensemble average received SIR per bit under the imperfect SIR-based power control scheme. Based on the properties that the ensemble average received SIR per bit is approximately uncorrelated with the interference power and the interference power from an interfering MS is approximately proportional to the received power of the interfering MS at its home BS, a set of linear equations is derived to obtain the ensemble average received power on each uplink. The system capacity is then obtained according to the feasibility of the ensemble average received powers and the corresponding ensemble average bit error rates. A closed-form solution for system capacity is successfully derived. This novel analytical method is quite accurate such that the numerical results and the simulation results are substantially matched.



## 5.6 Notation List

Notation	Description	Notation	Description
$b$	Index of an arbitrary BS $b$ , $b \in \{1, 2, \dots, N_B\}$	$\mathcal{G}_{MH} \triangleq \sum_{p=1}^K \mathcal{G}_{MH,p}$	
$m$	Index of an arbitrary <b>m</b> obile station, $m \in \{1, 2, \dots, N_B \cdot N_M\}$	$g_{mH}$	Channel gain of the interference link from MS $m$ to BS $H$ , $g_{mH} \triangleq \sum_{p=1}^K g_{mH,p}$
$M$	Index of a specific MS, $M \in \{1, 2, \dots, N_B \cdot N_M\}$	$I_{h,b}$	$I_{h,b} \triangleq (L_{mb} \cdot L_{mh}^{-1} \mid L_{mi} \leq L_{mh}, \forall i)$
$H$	Index of the BS that is the home BS of the specific MS $M$	$I_M[n]$	Interference power seen by the MS $M$ at the $n$ -th data symbol period
$h$	Index of the BS that is the home BS of MS $m$	$K$	Number of resolvable paths on a link
		$L_{mb}$	Long-term fading on the link from MS $m$ to BS $b$
$\mathbf{A}$	Coefficient matrix, $\mathbf{A} = [a_{bh}]_{(N_B \times N_B)}$	$L_{MH}$	Long-term fading on the uplink from MS $M$ to its home BS $H$
$a_{bh}$	Element of coefficient matrix	$L_{mH}$	Long-term fading on the link from MS $m$ to BS $H$ , $m \neq M$
$C$	System capacity	$L_{mh}(\mathbf{z})$	Long-term fading of MS $m$ whose location $\mathbf{z}_m = \mathbf{z}$
$CMD$	Power control command	$MS^{(h)}$	Index set of those MSs communicating with BS $h$
$E(\cdot)$	Expectation function	$n$	Index of data symbol period
$f_{\Gamma}(\cdot)$	Probability density function of the received SIR per bit on each uplink	$N_B$	<b>N</b> umber of <b>b</b> ase stations in the cellular system. I.e. cell number
$f_{\mathbf{z}_m}(\cdot)$	Probability density function of the random variable $\mathbf{z}_m$	$N_M$	<b>N</b> umber of <b>m</b> obile stations in each cell of the cellular system
$f_{L_{mh}(\mathbf{z})}(\cdot)$	Probability density function of $L_{mh}(\mathbf{z})$	$N_0$	Background noise contained in the total spread bandwidth
$F_{\xi}(\cdot)$	Cumulative distribution function of the random variable $\xi$	$\mathbf{N}$	$\mathbf{N} = [n_0]_{(N_B \times 1)}$ $n_0 = (\Gamma_0 \cdot N_0) / (G - \zeta \cdot \Gamma_0 \cdot (N_M - 1))$
$G$	Processing gain. $G \triangleq T / T_c$	$p$	Index of resolvable path on an uplink
$g_{mb,p}$	Power gain of the resolvable path $p$ on a link from an arbitrary MS $m$ to an arbitrary BS $b$	$P_b(\gamma)$	Bit error rate corresponding to a SIR per bit $\gamma$
$g_{MH}$	Channel gain of the uplink from MS $M$ to BS $H$ ,	$P_e$	Ensemble average bit error rate
		$P_e^*$	Requirement of the ensemble average BER for the communication quality

Notation	Description
$P_M[n]$	Transmission power of the specific MS $M$ at the $n$ -th data symbol
$P_m[n]$	Transmission power of MS $m$ at the $n$ -th data symbol
$P_{out}$	Outage probability
$Q(\cdot)$	Gaussian $Q$ function
$Q_M[n]$	Received signal power at the $n$ -th data symbol period of MS $M$
$S_{mb,p}$	Short-term fading of the $p$ -th resolvable path on the link from MS $m$ to BS $b$
$S_{mb}$	Short-term fading on the link from MS $m$ to BS $b$ ,
	$S_{mb} \triangleq \sum_{p=1}^K S_{mb,p}$
$S_{MH}$	Short-term fading on the uplink from MS $M$ to its home BS $H$ ,
	$S_{MH} \triangleq \sum_{p=1}^K S_{MH,p}$
$S_{mH}$	Short-term fading on the link from MS $m$ to BS $H$ ,
	$S_{mH} \triangleq \sum_{p=1}^K S_{mH,p}$
$T_d$	Power control command loop delay
$T_p$	Power control period
$V$	MS velocity
$\text{var}(\cdot)$	Variance function
$Y_H$	Common ensemble average received power levels in cell $H$ , $1 \leq H \leq N_B$
$\mathbf{Y}$	Ensemble average received power vector $\mathbf{Y} = [Y_1, Y_2, \dots, Y_{N_B}]_{(N_B \times 1)}$
$\mathbf{z}_m$	Complex number representing the location of MS $m$



Notation	Description
$\beta$	A quantity defined in (5.8)
$\kappa$	$\kappa \triangleq \ln(10)/10$ ,
$\zeta$	Factor depending on the PN chip waveform and the cross-correlation property of the PN codes
$\xi$	A Gaussian random variable $\xi$ used to approximate the distribution of $\det(\mathbf{A})$
$\sigma_x$	Log-normal shadow fading standard deviation
$\Delta_p$	Step size for power adaptation
$\Gamma_0$	Common ensemble average SIR per bit
$\Gamma_M[n]$	SIR per bit at the output of RAKE receiver during the $n$ -th data symbol period of the specific MS $M$
$\tilde{\Gamma}_M[n]$	$\tilde{\Gamma}_M[n] \triangleq 10 \cdot \log_{10}(\Gamma_M[n])$ ,
$\bar{\Gamma}_M$	An average value obtained by averaging $\Gamma_M[n]$ over a power control period
$\Gamma_{TH}$	Target SIR threshold
$\Gamma_{TH}^*$	Minimum $\Gamma_{TH}$ required to achieve the requirement $P_e^*$
$\varphi(s)$	Defined in (5.23)
$\psi(s, \mathbf{z})$	Defined in (5.24)

Notation	Description
$\eta$	Propagation exponent

# Chapter 6

## Conclusions and Future Works

---

In this dissertation, performance of the power control schemes in DS/CDMA cellular systems are analyzed, including the ideal truncated closed-loop power control (TCPC) scheme, the realistic TCPC scheme, and the imperfect (realistic) SIR-based power control scheme. A method for approximating the distribution of interference statistics, which is important while analyzing a strength-based power control scheme, is also proposed.

The TCPC scheme for uplinks in DS/CDMA cellular systems over frequency-selective fading channels is analyzed. Closed-form formulae for five performance measures are successfully obtained, including system capacity, average system transmission rate, MS average transmission rate, MS average transmission energy per bit, and MS average suspension delay. For a practical system, the TCPC scheme under realistic conditions of power control error is further analyzed. Closed-form formulae are also derived. The analysis is quite accurate according to the analytical and simulation results. In fact, the analysis method presented in this chapter is a general one that can be applied to the category of strength-based closed power control scheme, including an ideal or realistic one, in either circuit-switched or packet-switched CDMA systems. For example, by setting the cutoff threshold to zero, the TCPC scheme becomes the traditional strength-based power control scheme, and the presented analysis results are still valid.

An approximation method by characteristic function (AM-CF) method is proposed to approximate the distribution of interference in DS/CDMA cellular systems. This method can be applied for a system having the effects of frequency-selective multipath fading, the perfect power

control and using a rectangular/sinc chip waveform. Typically, the traditional way is to employ the Gaussian approximation method. The proposed AM-CF method provides another way to handle such a complicated environment and yields results that fit the Monte Carlo simulation results more accurately than the conventional standard Gaussian approximation method. Therefore, the proposed AM-CF method can be used to improve the accuracy while conducting the performance analysis.

Another important kind of power control scheme, the SIR-based power control scheme, is analyzed. Some interesting and important properties of an imperfect power control scheme are revealed. Based on these properties, the behavior of a SIR-based power controlled system can be described by a set of linear equation, from which the received signal power vector is obtained. The outage-based system capacity is defined according to the feasibility of the received signal power vector and the average bit error rate. The closed-form solution for the system capacity is finally derived, which needs only the first and second order statistics of each element in the coefficient matrix of the linear equations. The proposed method can successfully analyze the SIR-based power control scheme. Good analysis accuracy is also proved by the analytical and simulation results.

From the performance analysis of these power control schemes, we have investigated the characteristics of the power control schemes, including the strength-based and the SIR-based power control scheme. Although the strength-based power control scheme is found achieving less capacity than the SIR-based power control scheme. As shown in the dissertation, the truncated closed-loop power control scheme itself indicates a way to improve the system capacity by suspending the transmission when the channel fading is lower than a threshold.

Although the traditional strength-based power control scheme is known to have less capacity as compared with other power control schemes, e.g. the SIR-based power control scheme, this kind of strength-based power control scheme, TCPC scheme, seems provide another way to

achieve the capacity enhancement. Take the well-known perfect strength-based power control scheme as an example, the two major issues that degrade the system capacity is: 1) The target threshold for received power is the same for each uplink in the system. This will make the uplink in a boundary cell have a higher, in an average manner, received SIR than that in a central cell. Since the DS/CDMA system is an interference-limited system. The unnecessarily high received SIR implies the unnecessary high transmission power, which in turn produces unnecessary high interference to the whole system. As a result, the system capacity is affected. 2) An MS under the perfect strength-based power control will inherently produce much interference to other MSs. Under the perfect strength-based power control, the MS transmission power is the inverse of the short-term fading. A deep fading makes a high MS transmission power. Again, such a situation produces high interference to the whole system. As a result, the system capacity is affected. As an extreme case, if the short-term fading is a Rayleigh one, the average interference power is theoretically infinite, which make no system capacity at all.

The reason that the TCPC can improve the system capacity is that it mitigates the impact of the second issue. The analytical results clearly reveal that a large MS transmission power can benefit only one MS, but affect all the other MSs. From this point of view, it is clear that this is not a wise thing to do. Therefore, it would have a gain if we sacrifice the MS going to have a high transmission power temporarily, while benefit all the other MSs. However, the TCPC scheme still suffers the impact of the first issue. On the other hand, it is obvious that the SIR-based power control scheme can mitigate the impact of the first issue. However, the SIR-based power control scheme does not take the second issue into account. In view of this, one question would be: is there a power control scheme that can mitigate the impact of these two issues? We think it would be an interesting research topic to find such a power control, analyze it, and then compare the performance, especially the capacity with the TCPC and SIR-based power control schemes.

## Appendices

### A. Proof the Equivalence Between the Event $\{\mathbf{Y}>0\}$ and $\{\det(\mathbf{A})>0\}$

*Lemma II:* Let  $\mathbf{L}$  and  $\mathbf{U}$  be the lower and upper triangular matrices of the LU decomposition [83] of a square matrix  $\mathbf{A}=[a_{bh}]_{(N_B \times N_B)}$  given in (5.12). If the diagonal elements of the matrix  $\mathbf{U}$  contain only one negative number, then the cellular system is overloaded.

*Proof:* As well known, a square matrix  $\mathbf{A}=[a_{bh}]_{(N_B \times N_B)}$  has an LU decomposition into lower and upper triangular matrices  $\mathbf{L}$  and  $\mathbf{U}$ , i.e.  $\mathbf{A}=\mathbf{L} \cdot \mathbf{U}$ . From [83, p. 192], the matrix  $\mathbf{U}$  is just the outcome of Gauss elimination, and  $\mathbf{L}$  satisfies that  $\det(\mathbf{L})=1$ . Thus  $\det(\mathbf{A})=\det(\mathbf{L}) \cdot \det(\mathbf{U})=\det(\mathbf{U})=\prod_{i=1}^{N_B} u_i < 0$ , where  $u_i$  denotes the  $i$ -th diagonal element of the matrix  $\mathbf{U}$ . Without loss generality, let  $u_{N_B} < 0$ , and  $u_i > 0, i=1, \dots, N_B-1$ . Let  $\mathbf{A}_{(N_B)}$  be the matrix obtained by replacing the  $N_B$ -th column of  $\mathbf{A}$  by 1. Let the LU decomposition of  $\mathbf{A}_{(N_B)}$  be  $\mathbf{A}_{(N_B)}=\mathbf{L}' \cdot \mathbf{U}'$ , and  $\{u'_1, u'_2, \dots, u'_{N_B}\}$  be the diagonal elements of  $\mathbf{U}'$ . From Gauss elimination procedure of  $\mathbf{A}_{(N_B)}$ , it can be found that  $u'_i=u_i > 0, i=1, \dots, N_B-1$ , and  $u'_{N_B} > 0$ . Therefore,  $\det(\mathbf{A}_{(N_B)})=\det(\mathbf{U}')=\prod_{i=1}^{N_B} u'_i > 0$ . From (5.17), the corresponding ensemble average received power vector  $\mathbf{Y}$  is not feasible since  $Y_{N_B} < 0$ . In other words, the cellular system is overloaded. ■

*Lemma III:* Let  $\mathbf{L}$  and  $\mathbf{U}$  be the lower and upper triangular matrices of the LU

decomposition of a square matrix  $\mathbf{A} = [a_{bh}]_{(N_B \times N_B)}$  given in (5.12). If the system is not overloaded, then the diagonal elements of the matrix  $\mathbf{U}$  are all positive.

*Proof:* Let's assume the opposite: if the system is not overloaded, the  $\{u_1, u_2, \dots, u_{N_B}\}$  contain  $N$  negative numbers where  $N > 0$ . For the case of  $N = 1$ , *Lemma II* has shown that the cellular system would be overloaded — it contradicts our initial assumption.

Consider  $N > 1$ . Without loss generality, let  $u_i > 0, i = 1, \dots, N_B - N$ , and  $u_i < 0, i = N_B - N + 1, \dots, N_B$ . Now let's consider a reduced cellular system by removing the  $(N_B - N + 2)$ -th to  $(N_B)$ -th cells out from the present cellular system. Correspondingly the  $(N_B - N + 2)$ -th to  $(N_B)$ -th rows and the  $(N_B - N + 2)$ -th to  $(N_B)$ -th column of the coefficient matrix  $\mathbf{A}$  are removed. Let  $\mathbf{A}'$  denote the coefficient matrix of the reduced cellular system. The LU decomposition of  $\mathbf{A}'$  is given by  $\mathbf{A}' = \mathbf{L}' \cdot \mathbf{U}'$ , and  $\{u'_1, u'_2, \dots, u'_{N_B - N + 1}\}$  are the diagonal elements of  $\mathbf{U}'$ . It is obviously that  $u'_i = u_i > 0, i = 1, \dots, N_B - N$ , and  $u'_i = u_i < 0, i = N_B - N + 1$ . From *Lemma II*, we know that the reduced cellular system would be overloaded. — it contradicts our initial assumption. Since, without any doubt, a cellular system being not overloaded will remain not overloaded by removing any number of cells. Overall, we conclude that the *Lemma III* must be true. ■

From *Lemma III* and the fact  $\det(\mathbf{A}) = \det(\mathbf{U})$ , it is also true that if the system is not overloaded, then the  $\det(\mathbf{A})$  would be positive.

*Lemma IV:* The determinant of matrix  $\mathbf{A} = [a_{bh}]_{(N_B \times N_B)}$ , which is given in (5.12), decreases as the mobile number per cell  $N_M$  increases, whenever the system is not overloaded.

*Proof:* Consider  $N_M = N$ , the corresponding matrix given in (5.12) is denoted by

$\mathbf{A} = [a_{bh}]_{(N_B \times N_B)}$ . Let  $\{u_1, u_2, \dots, u_{N_B}\}$  represent the diagonal elements of the matrix  $\mathbf{U}$ , which is obtained by applying Gauss elimination to the coefficient matrix  $\mathbf{A}$ . Since the system is assumed not overloaded, from *Lemma III* we know that  $u_i > 0, i = 1, \dots, N_B$ .

Consider  $N_M = N + 1$ , the corresponding matrix given in (5.12) is denoted by  $\mathbf{A}' = [a'_{bh}]_{(N_B \times N_B)}$ . Let  $\{u'_1, u'_2, \dots, u'_{N_B}\}$  represent the diagonal elements of the matrix  $\mathbf{U}'$ , which is obtained by applying Gauss elimination to the matrix  $\mathbf{A}'$ . Since the system is assumed not overloaded, from *Lemma III* we know that  $u'_i > 0, i = 1, \dots, N_B$ . From (5.12), it is found that  $a'_{bh} < a_{bh}, \forall b \neq h$ . By comparing the Gauss elimination of the coefficient matrices  $\mathbf{A}$  and  $\mathbf{A}'$ , it can be found that  $u'_1 = u_1 = 1$ , and  $u'_i < u_i, i = 2, \dots, N_B$ . Consequently,

$$\det(\mathbf{A}') = \prod_{i=1}^{N_B} u'_i < \det(\mathbf{A}) = \prod_{i=1}^{N_B} u_i \quad \blacksquare$$

From the *Lemma IV*, we realize that when the  $N_M$  increases, the  $\det(\mathbf{A})$  will decrease. Eventually the  $\det(\mathbf{A})$  will become negative, which implies, according to *Lemma III*, that the system is now overloaded, i.e. the event  $\{\mathbf{Y} > 0\}$  does not hold. Therefore, whenever the system is not overloaded, the event  $\{\det(\mathbf{A}) > 0\}$  is equivalent to the event  $\{\mathbf{Y} > 0\}$ .



## B. Abbreviations and Acronyms

<b>1G</b>	First generation	<b>IS-136</b>	EIA Interim Standard 136
<b>2G</b>	Second generation	<b>iid</b>	Independently and identically distributed
<b>2.5G</b>	Second and a half-generation generation	<b>lcr</b>	Level crossing rate
<b>3G</b>	Third generation	<b>MAI</b>	Multiple access interference
<b>4G</b>	Fourth generation	<b>MIP</b>	Multiple intensity profile
<b>AM-CF</b>	Approximation method by characteristic function	<b>MS</b>	Mobile station
<b>AMPS</b>	Advanced Mobile Phone Service	<b>MSC</b>	Mobile switching center
<b>AWGN</b>	Additive white Gaussian noise	<b>NMT</b>	Nordic Mobile Telephone
<b>BER</b>	Bit error rate	<b>NTT</b>	Nippon telephone and Telegraph
<b>BPSK</b>	Binary phase shift keying	<b>PCCU</b>	Power control command unit
<b>BS</b>	Base station	<b>PCE</b>	Power control error
<b>cdf</b>	Cumulative distribution function	<b>PCM</b>	Pulse code modulation
<b>CDMA</b>	Code division multiple access	<b>PDC</b>	Personal Digital Cellular
<b>CIR</b>	Carrier-to-interference	<b>pdf</b>	Probability density function
<b>DAMPS</b>	Digital AMPS	<b>PN</b>	Pseudonoise
<b>DPCCH</b>	Dedicated physical control channel	<b>QoS</b>	Quality of Service
<b>DPCH</b>	Dedicated physical channel	<b>RV</b>	Random variable
<b>DPDCH</b>	Dedicated physical data channel	<b>SGA</b>	Standard Gaussian approximation
<b>DS/CDMA</b>	Direct sequence/code division multiple access	<b>SIR</b>	Signal-to-interference ratio
<b>FDMA</b>	Frequency division multiple access	<b>TACS</b>	Total Access Communication System
<b>GSM</b>	Global Standard for Mobile Communications	<b>TAPC</b>	Truncated average power control
<b>IGA</b>	Improved Gaussian approximation	<b>TCPC</b>	Truncated closed-loop power control
<b>IS-95</b>	EIA Interim Standard for U.S. Code Division Multiple Access	<b>TCU</b>	Transmission control unit
		<b>TDMA</b>	Time division multiple access
		<b>TD-SCDMA</b>	Time-division synchronous CDMA
		<b>UMTS</b>	Universal Mobile Telecommunications System

# Bibliography

- [1] A. J. Viterbi, "When not to spread spectrum - A sequel," *IEEE Commun. Mag.*, vol. 23, pp. 12-17, Apr. 1985.
- [2] K. S. Gilhousen, I. M. Jacobs, R. Padovani, and L. A. Weaver, "Increased capacity using CDMA for mobile satellite communication," *IEEE J. Select. Areas Commun.*, vol. 8, no. 4, pp. 503-514, May 1990.
- [3] K. S. Gilhousen, I. M. Jacobs, R. Padovani, A. J. Viterbi, L. A. Weaver, Jr., and C. E. Wheatley, III, "On the capacity of a cellular CDMA system," *IEEE Trans. Veh. Technol.*, vol. 40, no. 2, pp. 303-312, May 1991.
- [4] J. M. Aein, "Power Balancing in Systems Employing Frequency Reuse," *COMSAT Tech. Rev.*, vol. 3, no. 2, pp. 277-300, Sep. 1973.
- [5] R. W. Nettleton, "Traffic theory and interference management for a spread spectrum cellular radio system," *Proc. IEEE Int. Conf. Commun.*, pp. 24.5.1-24.5.5, 1980.
- [6] R. W. Nettleton, and H. Alavi, "Downstream power control for a spread spectrum cellular mobile radio system," *Proc. IEEE GLOBECOM*, pp. 84-88, 1982.
- [7] R. W. Nettleton, and H. Alavi, "Power Control for Spread-Spectrum Cellular Mobile Radio System," *Proc. IEEE Veh. Technol. Conf.*, pp. 242-246, Jan. 1983.
- [8] J. Zander, "Performance of optimum transmitter power control in cellular radio systems," *IEEE Trans. Veh. Technol.*, vol. 41, no. 1, pp. 57-62, Feb. 1992.
- [9] J. Zander, "Distributed cochannel interference control in cellular radio systems," *IEEE Trans. Veh. Technol.*, vol. 41, no. 3, pp. 305-311, Aug. 1992.
- [10] J. G. Proakis, *Digital communications*, 3rd ed. New York:McGraw-Hill, 1995.
- [11] R. Prasad and M. Jansen, "Near-far-effects on performance of DS/SS CDMA systems for personal communication networks," *IEEE VTC'93*, pp. 710-713, May 1993.
- [12] S. Ariyavisitakul and L. F. Chang, "Simulation of CDMA system performance with feedback power control," *Electronics Letters*, vol. 27, no. 23, pp. 2127-2128, Nov. 1991.
- [13] A. J. Goldsmith and P. P. Varaiya, "Capacity of fading channels with channel side

information," *IEEE Trans. Inform. Theory*, vol. 43, no. 6, pp. 1986-1990, Nov. 1997.

- [14] A. J. Goldsmith and S. G. Chua, "Variable rate variable-power MQAM for fading channels," *IEEE Trans. Commun.* vol. 45, no. 10, pp. 1218-1230, Oct. 1997.
- [15] B. Hashem and E. Sousa, "A combined power/rate control scheme for data transmission over a DS/CDMA system," *IEEE VTC'98*, vol. 2, pp. 1096 –1100, May 1998.
- [16] S. W. Kim and A. J. Goldsmith, "Truncated power control in code-division multiple-access communications," *IEEE Trans. Veh. Technol.*, vol. 49, no. 3, pp. 965-972, May 2000.
- [17] N. Kong and L. B. Milstein, "Error probability of multicell CDMA over frequency selective fading channels with power control error," *IEEE Trans. Commun.*, vol. 47, no. 4, pp. 608-617, Apr. 1999.
- [18] R. K. Morrow and J. S. Lehnert, "Bit-to-bit error dependence in slotted DS/SSMA packet systems with random signature sequences," *IEEE Trans. Commun.*, vol. 37, no. 10, pp. 1052-1061, Oct. 1989.
- [19] J. M. Holtzman, "A simple, accurate method to calculate spread-spectrum multiple-access error probabilities," *IEEE Trans. Commun.*, vol. 40, no. 3, pp. 461-464, Mar. 1992.
- [20] E. A. Geraniotis and M. B. Pursley, "Error probability for Direct-Sequence Spread-Spectrum Multiple-Access Communications - Part II: Approximation," *IEEE Trans. Commun.*, vol. COM-30, no. 5, pp. 985-995, May 1982.
- [21] S. Ariyavisitakul , "Signal and Interference statistics of a CDMA system with feedback power control – Part II," *IEEE Trans. Commun.*, vol. 42, pp. 597-605, Feb./Mar./Apr. 1994.
- [22] M. Zorzi, "On the Analytical Computation of the Interference Statistics with Applications to the Performance Evaluation of Mobile Radio Systems," *IEEE Trans. Commun.*, vol. 45, pp. 103-109, Jan. 1997.
- [23] D. K. Kim and D. K. Sung, "Capacity estimation for an SIR-based power-controlled CDMA system supporting ON-OFF traffic," *IEEE Trans. Veh. Technol.*, vol. 49, no. 4, pp. 1094-1101, Jul. 2000.
- [24] B. Hashem, and E. S. Sousa, "Reverse link capacity and interference statistics of a fixed-step power-controlled DS/CDMA system under slow multipath fading," *IEEE Trans.*

*Commun.*, vol. 47, no. 12, pp. 1905-1912, Dec. 1999.

- [25] D. K. Kim and D. K. Sung, "Capacity estimation for a multicode CDMA system with SIR-based power control," *IEEE Trans. Veh. Technol.*, vol. 50, no. 3, pp. 701-710, May 2001.
- [26] D. K. Kim and F. Adachi, "Theoretical analysis of reverse link capacity for an SIR-based power-controlled cellular CDMA system in a multipath fading environment," *IEEE Trans. Veh. Technol.*, vol. 50, no. 2, pp. 452-464, Mar. 2001.
- [27] S. Ariyavisitakul, "SIR-based power control in a CDMA system," *Conf. Rec. IEEE GLOBECOM 92*, pp. 868-873, Dec. 1992.
- [28] F. C. M. Lau and W. M. Tam, "Novel SIR-estimation-based power control in a CDMA mobile radio system under multipath environment," *IEEE Trans. Veh. Technol.*, vol. 50, no. 1, pp. 314-320, Jan. 2001.
- [29] F. C. M. Lau and W. M. Tam, "Achievable-SIR-based predictive closed-loop power control in a CDMA mobile system," *IEEE Trans. Veh. Technol.*, vol. 51, no. 4, pp. 720-728, Jul. 2002.
- [30] D. M. Novakovic, and M. L. Dukic, "Evolution of the Power Control Techniques for DS-CDMA Toward 3G Wireless Communication Systems," *IEEE Commun. Surveys*, <http://www.comsoc.org/pubs/surveys>, vol. 3, no. 4, pp. 2-15, Dec. 2000.
- [31] S. A. Grandhi, R. Vijayan, D. J. Goodman, and J. Zander, "Centralized power control in cellular radio systems," *IEEE Trans. Veh. Technol.*, vol. 42, no. 4, pp. 466-468, Nov. 1993.
- [32] Q. Wu, "Performance of optimum transmitter power control in CDMA cellular mobile systems," *IEEE Trans. Veh. Technol.*, vol. 48, no. 2, pp. 571-575, Mar. 1999.
- [33] S. A. Grandhi, and J. Zander, "Constrained power control in cellular radio systems," *Proc. IEEE Veh. Technol. Conf.*, vol. 2, pp. 824-828, Jun. 1994.
- [34] D. Kim, K.-N. Chang, and S. Kim, "Efficient distributed power control for cellular mobile systems," *IEEE Trans. Veh. Technol.*, vol. 46, no. 2, pp. 313-319, May 1997.
- [35] T.-H. Lee, and J.-C. Lin, "A fully distributed power control algorithm for cellular mobile systems," *IEEE J. Select. Areas Commun.*, vol. 14, no. 4, pp. 692-697, May 1996.
- [36] A. M. Monk, and L. B. Milstein, "Open-loop power control error in a land mobile satellite system," *IEEE J. Select. Areas Commun.*, vol. 13, no. 2, pp. 205-212, Feb. 1995.

- [37] A. M. Monk, A. Chockalingam, and L. B. Milstein, "Open-loop power control error on a frequency selective CDMA channel," *Proc. IEEE GLOBECOM*, pp. 29-33, Nov. 1994.
- [38] F. D. Prisolli, and F. Sestini, "Effects of imperfect power control and user mobility on a CDMA cellular network," *IEEE J. Select. Areas Commun.*, vol. 14, no. 9, pp. 1809-1817, Dec. 1996.
- [39] R. A. Attar, and E. Esteves, "A reverse link outer-loop power control algorithm for cdma2000 1xEV systems," *Proc. IEEE Int. Conf. Commun.*, vol. 1, pp. 573-578, Apr. 2002.
- [40] A. Sampath, P. Sarath Kumar, and J. M. Holtzman, "On setting reverse link target SIR in a CDMA system," *Proc. IEEE Veh. Technol. Conf.*, vol. 2, pp. 929-933, May 1997.
- [41] S. H. Won, W. W. Kim, Y. I. Oh, and I. M. Jeong, "An analytic approach for finding optimum parameter in controlling target SIR in a CDMA system," *IEEE International Conference on Personal Wireless Communication*, pp. 219-222, Dec. 1997.
- [42] C. W. Sung, K. K. Leung, and W. S. Wong, "A quality-based fixed-step power control algorithm with adaptive target threshold," *IEEE Trans. Veh. Technol.*, vol. 49, no. 4, pp. 1430-1439, Jul. 2000.
- [43] H. Kawai, H. Suda, and F. Adachi, "Outer-loop control of target SIR for fast transmit power control in turbo-coded W-CDMA mobile radio," *Electron. Lett.*, vol. 35, no. 9, pp. 699-701, Apr. 1999.
- [44] Z. J. Haas, J. H. Winter, and D. S. Johnson, "Simulation results of the capacity of cellular systems," *IEEE Trans. Veh. Technol.*, vol. 46, no. 4, pp. 805-817, Nov. 1997.
- [45] S. Ariyavisitakul and L. F. Chang, "Signal and Interference statistics of a CDMA system with feedback power control," *IEEE Trans. Commun.*, vol. 41, pp. 1626-1634, Nov. 1993.
- [46] S. H. Won, W. W. Kim, Y. I. Oh, and I. M. Jeong, "An analytic approach for finding optimum parameter in controlling target SIR in a CDMA system," *IEEE International Conference on Personal Wireless Communication*, pp. 219-222, Dec. 1997.
- [47] Y.-J. Yang, and J.-F. Chang, "A strength-and-SIR-combined adaptive power control for CDMA mobile radio channels," *IEEE Trans. Veh. Technol.*, vol. 48, no. 6, pp. 1996-2004, Nov. 1999.
- [48] D. Zhang, Q. T. Zhang, and C. C. Ko, "A novel joint strength and SIR based CDMA

reverse link power control with variable target SIR," *Proc. IEEE Int. Conf. Commun.*, no. 3, pp. 1502-1505, Jun. 2000.

- [49] Z. Liu, and M. El Zarki, "SIR-based call admission control for DS-CDMA cellular systems," *IEEE J. Select. Areas Commun.*, vol. 12, no. 4, pp. 638-644, May 1994.
- [50] C. W. Sung, and W. S. Wong, "A distributed fixed-step power control algorithm with quantization and active link quality protection ," *IEEE Trans. Veh. Technol.*, vol. 48, no. 2, pp. 553-562, Mar. 1999.
- [51] J. D. Herdtner, and E. K. P. Chsng, "Analysis of a class of distributed asynchronous power control algorithms for cellular wireless systems ," *IEEE J. Select. Areas Commun.*, vol. 18, no.3, pp. 436-446, Mar. 2000.
- [52] M. Saquib, R. D. Yates, and A. Ganti, "Power control for an asynchronous multirate decorrelator ," *IEEE Trans. Commun.*, vol. 48, no. 5, pp. 804-812, May 2000.
- [53] A. M. Viterbi and A. J. Viterbi, "Erlang capacity of a power controlled CDMA system," *IEEE J. Select. Areas Commun.*, vol. 11, pp. 892-900, Aug. 1993.
- [54] A. J. Viterbi, A. M. Viterbi, and E. Zehavi, "Performance of power-controlled wideband terrestrial digital communication," *IEEE Trans. Commun.*, vol. 41, no. 4, pp. 559-569, Apr. 1993.
- [55] G. E. Corazza, G. De Maio, and F. Vatalaro, "CDMA cellular systems performance with fading, shadowing, and imperfect power control," *IEEE Trans. Veh. Technol.*, vol. 47, no.2, pp. 450-459, May 1998.
- [56] T. T. Tjhung, and C. C. Chai, "Distribution of SIR and performance of DS-CDMA systems in lognormally shadowed Rician channels ," *IEEE Trans. Veh. Technol.*, vol. 49, no. 4, pp. 1110-1125, Jul. 2000.
- [57] Y.-D. Yao, and A. U. H. Sheikh, "Investigations into cochannel interference in microcellular mobile radio systems," *IEEE Trans. Veh. Technol.*, vol. 41 , No. 2, pp. 114-123, May 1992.
- [58] J. M. Romero-Jerez, C. T  llez-Lavao, and A. Diaz-Estrella, "Effect of power control imperfections on the reverse link of cellular CDMA networks under multipath fading," *IEEE Trans. Veh. Technol.*, vol. 53, no. 1, pp. 61-71, Jan. 2004.
- [59] T. Shu and Z. Niu, "Uplink capacity optimization by power allocation for multimedia

CDMA networks with imperfect power control," *IEEE J. Select. Areas Commun.*, vol. 21, pp. 1585-1594, Dec. 2003.

- [60] R. Prasad, A. Kegel, and M. G. Jansen, "Effect of imperfect power control on cellular code division multiple access system," *Electron. Lett.*, vol. 28, no. 9, pp. 848-849, Apr. 1992.
- [61] J.-C. Lin, Y.-C. Lin, T.-H. Lee, and Y. T. Su, "The effect of imperfect power control on outage probability in a cellular mobile system," *Proc. IEEE Veh. Technol. Conf.*, vol. 2, pp. 574-578, Jul. 1995.
- [62] C.-J. Chang, J.-H. Lee, and F.-C. Ren, "Design of power control mechanisms with PCM realization for the uplink of a DS-CDMA cellular mobile radio system," *IEEE Trans. Veh. Technol.*, vol. 45, no. 3, pp. 522-530, Aug. 1996.
- [63] C.-H. Lee and C.-J. Chang, "Performance analysis of a truncated closed-loop power-control scheme," *IEEE Trans. Veh. Technol.*, vol. 53, no. 4, pp. 1149-1159, July. 2004.
- [64] M. L. Sim, E. Gunawan, C. B. Soh, and B. H. Soong, "Characteristics of closed loop power control algorithms for a cellular DS/CDMA system," *Proc. Inst. Elect. Eng. Commun.*, vol. 145, no.5, pp. 355-362, Oct. 1998.
- [65] J. M. A. Tanskanen, J. Mattila, M. Hall, T. Korhonen, and S. J. Ovaska, "Predictive closed loop power control for mobile CDMA systems," *Proc. IEEE Veh. Technol. Conf.*, no. 2, pp. 934-938, May 1997.
- [66] M. L. Sim, E. Gunawan, B.-H. Soong, and C.-B. Soh, "Performance study of close-loop power control algorithms for a cellular CDMA system ," *IEEE Trans. Veh. Technol.*, vol. 48, no. 3, pp. 911-921, May 1999.
- [67] F. Gunnarsson, F. Gustafsson, and J. Blom, "Dynamical effects of time delays and time delay compensation in power controlled DS-CDMA," *IEEE J. Select. Areas Commun.*, vol. 19, no. 1, pp. 141-151, Jan. 2001.
- [68] S. W. Kim, and Y. H. Lee, "Combined rate and power adaptation in DS/CDMA communications over Nakagami fading channels," *IEEE Trans. Commun.*, vol. 48, no. 1, pp. 162-168, Jan. 2000.
- [69] D. Kim, "Rate-regulated power control for supporting flexible transmission in future CDMA mobile networks," *IEEE J. Select. Areas Commun.*, vol. 17, no. 5, pp. 968-977, May 1999.

- [70] J. K. Cavers, "Variable-rate transmission for Rayleigh fading channels," *IEEE Trans. Commun.*, vol. COM-20, pp. 15-22, Feb. 1972.
- [71] S. Abeta, S. Sampei, and N. Morinaga, "Channel activation with adaptive coding rate and processing gain control for cellular DS/CDMA systems," *Proc. IEEE Veh. Technol. Conf.*, no. 2, pp. 1115-1119, Apr. 1996.
- [72] A. Baier, U.-C. Fiebig, W. Granzow, W. Koch, P. Teder, and J. Thielecke, "Design study for a CDMA-based third-generation mobile radio system," *IEEE J. Select. Areas Commun.*, vol. 12, no.4, pp. 733-743, May 1994.
- [73] A. H. Aghvami, "Future CDMA cellular mobile systems supporting multi-service operation," *Proc. IEEE Int. Symp. on Personal, Indoor, and Mobile Radio Commun.*, no. 4, pp. 1276-1279, Sep. 1994.
- [74] T. S. Rappaport, *Wireless communications principles and practice*, New Jersey: Prentice-Hall, 1996.
- [75] William C. Y. Lee, *Mobile communications engineering*, McGraw-Hill, 1982.
- [76] M. D. Yacoub, J. E. V. Bautista, and L. G. de R. Guedes, " $n$  higher order statistics of the Nakagami- $m$  distribution," *IEEE Trans. Veh. Technol.*, vol. 40, no. 3, pp. 790-794, May 1999.
- [77] 3GPP TS25.211: "Physical channels and mapping of transport channels onto physical channels (FDD)," V3.1.1, Dec, 1999.
- [78] C. H. Lee and C. J. Chang, "An Equal-Strength/Power-Suspended Power Control Scheme for a Cellular DS/CDMA System," *Proc. IEEE Veh. Technol. Conf.*, vol. 2, pp. 550-556, Sep. 2000.
- [79] M. B. Pursley, "Performance evaluation for phase-coded spread spectrum multiple-access communication—part I: System analysis," *IEEE Trans. Commun.*, vol. COM-25, pp. 795-799, Aug. 1977.
- [80] A. J. Viterbi, *CDMA: Principles of Spread Spectrum Communication*. Reading, MA: Addison-Wesley, 1995.
- [81] Y. R. Zheng and C. Xiao, "Simulation models with correct statistical properties for Rayleigh fading channels," *IEEE Trans. Commun.*, vol. 51, no. 6, pp. 920-928, Jun. 2003.
- [82] A. J. Viterbi, *CDMA: Principles of Spread Spectrum Communication*. Reading, MA:



Addison-Wesley, 1995.

- [83] B. Noble and J. W. Daniel, *Applied Linear Algebra*. 2nd Edition, Prentice-Hall, 1977.



## Vita

Chieh-Ho Lee was born in Taiwan, ROC, on Nov. 24, 1969. He received the B.E. and M.E. degrees in department of communication engineering from National Chiao Tung University, Hsinchu, Taiwan, in 1991 and 1993, respectively. From 1995 to 1997, he was an engineer in a communication equipment company, where he was involved in the digital signal process programming of the modem. Currently, he is a candidate for the Ph. D. in the Institute of communication engineering in National Chiao Tung University, Hsinchu, Taiwan. His research interests include power control in cellular systems.

